Recombinant Expression, Purification, and Reconstitution of the Chloroplast ATP Synthase c-subunit Ring

by

Robert Michael Lawrence

A Dissertation Presented in Partial Fulfillment
of the Requirements for the Degree
Doctor of Philosophy

Approved April 2011 by the
Graduate Supervisory Committee:

Petra Fromme, Chair
Julian Chen
Neal Woodbury

ARIZONA STATE UNIVERSITY

May 2011

ABSTRACT

ATP synthase is a large multimeric protein complex responsible for generating the energy molecule adenosine triphosphate (ATP) in most organisms. The catalysis involves the rotation of a ring of c-subunits, which is driven by the transmembrane electrochemical gradient. This dissertation reports how the eukaryotic c-subunit from spinach chloroplast ATP synthase has successfully been expressed in *Escherichia coli* and purified in mg quantities by incorporating a unique combination of methods. Expression was accomplished using a codon optimized gene for the c-subunit, and it was expressed as an attachment to the larger, more soluble, native maltose binding protein (MBP-c_1). The fusion protein MBP-c_1 was purified on an affinity column, and the c_1 subunit was subsequently severed by protease cleavage in the presence of detergent. Final purification of the monomeric c_1 subunit was accomplished using reversed phase column chromatography with ethanol as an eluent. Circular dichroism spectroscopy data showed clear evidence that the purified c-subunit is folded with the native alpha-helical secondary structure. Recent experiments appear to indicate that this monomeric recombinant c-subunit forms an oligomeric ring that is similar to its native tetradecameric form when reconstituted in liposomes. The F-type ATP synthase c-subunit stoichiometry is currently known to vary from 8 to 15 subunits among different organisms. This has a direct influence on the metabolic requirements of the corresponding organism because each c-subunit binds and transports one H^+ across the membrane as the ring makes a complete rotation. The c-ring rotation drives rotation of the γ-subunit, which in turn drives the

synthesis of 3 ATP for every complete rotation. The availability of a recombinantly produced c-ring will lead to new experiments which can be designed to investigate the possible factors that determine the variable c-ring stoichiometry and structure.

DEDICATION

Thank you Mom and Dad for the support, encouragement, and many childhood trips to the pet store and library. Dedicated also to Zoe.

ACKNOWLEDGMENTS

This work would not be possible without the essential guidance and support of my advisor Dr. Petra Fromme. Dr. Fromme's experience in photosynthesis and in particular with the ATP synthase enzyme was imperative for the conception and completion of this project.

Dr. Benjamin Varco-Merth provided initial instruction related to the purification and crystallography of the native ATP synthase c_{14} ring. Dr. Ingo Grotjohann also lended additional advice related to ATP synthase. The inception of this project was made possible by Dr. Julian Chen and Dr. Christopher Bley. They provided useful advice relating to the molecular biology techniques used, and supplied the essential pMAL-c2x plasmid which was used by their recommendation. They also allowed access to equipment in their laboratory that was needed during the initial stages of this project.

Dr. Joanna Porankiewicz-Asplund of Agrisera Antibodies facilitated the collaboration between the author and Agrisera that resulted in the production of the c-subunit antibody. The pOFXT7KJE3 plasmid was used with permission graciously granted by Dr. Olivier Fayet at Université Paul Sabatier, in France. And finally, the National Institutes of Health must be acknowledged for providing the generous funding via grant R01 GM081490-01, which made all of this research possible

TABLE OF CONTENTS

Page

Page

Page

Page

Page

LIST OF TABLES

LIST OF FIGURES

Page

Page

LIST OF SYMBOLS AND ABBREVIATIONS

Symbol/Abbreviation

Å ..... angstrom

A_{215} ..... 215 nm absorbance

A_{280} ..... 280 nm absorbance

A_{454} ..... 454 nm absorbance

A_{460} ..... 460 nm absorbance

A_{600} ..... 600 nm absorbance

A_{665} ..... 665 nm absorbance

AFM ..... atomic force microscopy

$AgNO_3$ ..... silver nitrate

ASU ..... Arizona State University

ATP ..... adenosine triphosphate

ADP ..... adenosine diphosphate

bp ..... base pair(s)

BSA ..... bovine serum albumin

°C ..... degrees Celsius

c_1 ..... monomeric c-subunit

c_{14} ..... tetradecameric c-subunit ring

$CaCl_2$ ..... calcium chloride

Chl ..... chlorophyll

Chl-a ..... chlorophyll-a

CBB ..... Coomassie Brilliant Blue

Symbol/Abbreviation

CCD ..... charge-coupled device

CD ..... circular dichroism

cDNA ..... complementary DNA

c_n ..... oligomeric c-subunit ring

CF_0F_1 ..... chloroplast ATP synthase

CMC ..... critical micelle concentration

Cyt. b_6f ..... cytochrome b_6f

DNA ..... deoxyribonucleic acid

DGDG ..... digalactosyl-diacyl-glycerol

dNTP ..... deoxynucleotide triphosphate

DTT ..... dithiothreitol

e^- ..... electron

EDTA ..... ethylene-diamine-tetra-acetic acid

F_0F_1 ..... ATP synthase

F_X, F_A, F_B ..... 4Fe4S cluster

Fd ..... ferrodoxin

Fl ..... flavodoxin

FNR ..... Ferrodoxin-$NADP^+$-Reductase

x g RCF ..... g-force relative centrifugal force

g ..... gram(s)

GST ..... glutathione S-transferase

H^+ ..... proton

Symbol/Abbreviation

H_2O ..... water

HCl ..... hydrochloric acid

HPLC ..... high pressure liquid chromatography

HR ..... high-resolution

HRP ..... horse radish peroxidase

hv ..... photon energy

IPTG isopropyl-β-D-1-thiogalactopyranoside

IgG ..... immunoglobulin G

kDa ..... kilo Dalton(s)

Kb ..... kilo base(s)

L ..... liter

LB ..... lysogeny broth

M ..... molar

MAD ..... multi-wavelength anomalous dispersion

MBP ..... maltose binding protein

MBP-c_1 ..... maltose binding protein-c-subunit fusion protein

MCS ..... multiple cloning sites

$MgCl_2$ ..... magnesium chloride

MGDG ..... monogalactosyl diacyl glycerol

mL ..... milliliter(s)

mM ..... millimolar

mm ..... millimeter(s)

Symbol/Abbreviation

mRNA ..... messenger RNA

N_2 ..... nitrogen gas

Na^+ ..... sodium ion

Na-cholate ..... sodium cholate

NaCl ..... sodium chloride

Na-deoxycholate ..... sodium deoxycholate

NADP+ ..... nicotinamide adenine dinucleotide phosphate

NADPH ..... reduced nicotinamide adenine dinucleotide phosphate

ng ..... nanogram(s)

nm ..... nanometer(s)

NMR ..... nuclear magnetic resonance

NRMSD ..... normalized root mean square deviation

O_2 ..... oxygen gas

O.D. ..... optical density

OEC ..... oxygen evolving complex

P ..... Promoter

PAGE ..... polyacrylamide gel electrophoresis

PC ..... plastocyanin

PCR ..... polymerase chain reaction

PG ..... phosphatidyl-glycerol

Pheo ..... pheophytin

Phy ..... phylloquinione

Symbol/Abbreviation

Pi ..... inorganic phosphate

PL ..... proteoliposome

pmol ..... picomols

PQ ..... phylloquinone

PQH ..... reduced phylloquinone

PQH2 ..... doubly reduced phylloquinone

PSI ..... Photosystem I

PSII ..... Photosystem II

PVDF ..... polyvinylidene fluoride

Q-cycle ..... quinone cycle

RC ..... reaction center

RE ..... restriction endonuclease

Recomb. ..... recombinant

RNA ..... ribonucleic acid

RPC ..... reversed phase column

RPM ..... revolutions per minute

SDS ..... sodium dodecyl-sulfate

SQDG ..... sulfoquinovosyldiacyl-glycerol

SUMO ..... small ubiquitin-like modifier

T ..... Terminator

TAE ..... Tris, Acetic Acid, EDTA

TFA ..... trifluoro acetic acid

Symbol/Abbreviation

tRNA ..... transfer RNA

TTBS ..... tween tris buffered saline

UV ..... ultra violet

V ..... volt(s)

v/v ..... volume to volume ratio

W ..... watt(s)

w/v ..... weight to volume ratio

β-car ..... beta-carotene

βDDM ..... n-β-dodecyl-D-maltoside

βOG ..... β-octyl-D-glucopyranoside

ΔpH ..... pH potential

Δε ..... molar CD

$\Delta\mu H^+$ ..... electrochemical potential

Δψ ..... electrical potential

ε_M ..... molar extinction coefficient

[θ] ..... ellipticity

μL ..... microliter

μg ..... microgram

% ..... percent

Chapter 1

INTRODUCTION

1.1 Oxygenic photosynthesis

The photosynthetic process carried out by plants, algae, and cyanobacteria to produce biochemical energy from water and sunlight provides the energetic foundation for nearly every living ecosystem on the planet. This elegant process is the sum of a series of multiple electron transfer steps, each carried out by large protein-cofactor complexes. These include Photosystems I and II, and the Cytochrome b_6f complex as shown in Figure 1A. In this figure, these complexes are represented as models that were determined from x-ray crystallography structures, with their locations relative to the thylakoid membrane also shown. Figure 1B shows how these complexes are in involved in the process of electron transport, as described below.

Photosystems I and II are both large protein-pigment complexes that catalyze light induced charge separation across the thylakoid membrane. In Photosystem II (PSII) this occurs as a pair of chlorophyll molecules designated as P680 performs the primary charge separation , which forms (P680*) upon the transfer of excitation energy from the chlorophylls in the antenna complex generated by photons (*hv*) of light. In this excited state, P680* will then donate one electron to another chlorophyll designated as Chl_{D1}, the next in a long series of electron acceptors. This electron transfer step results in an oxidized $P680^+$, which has a

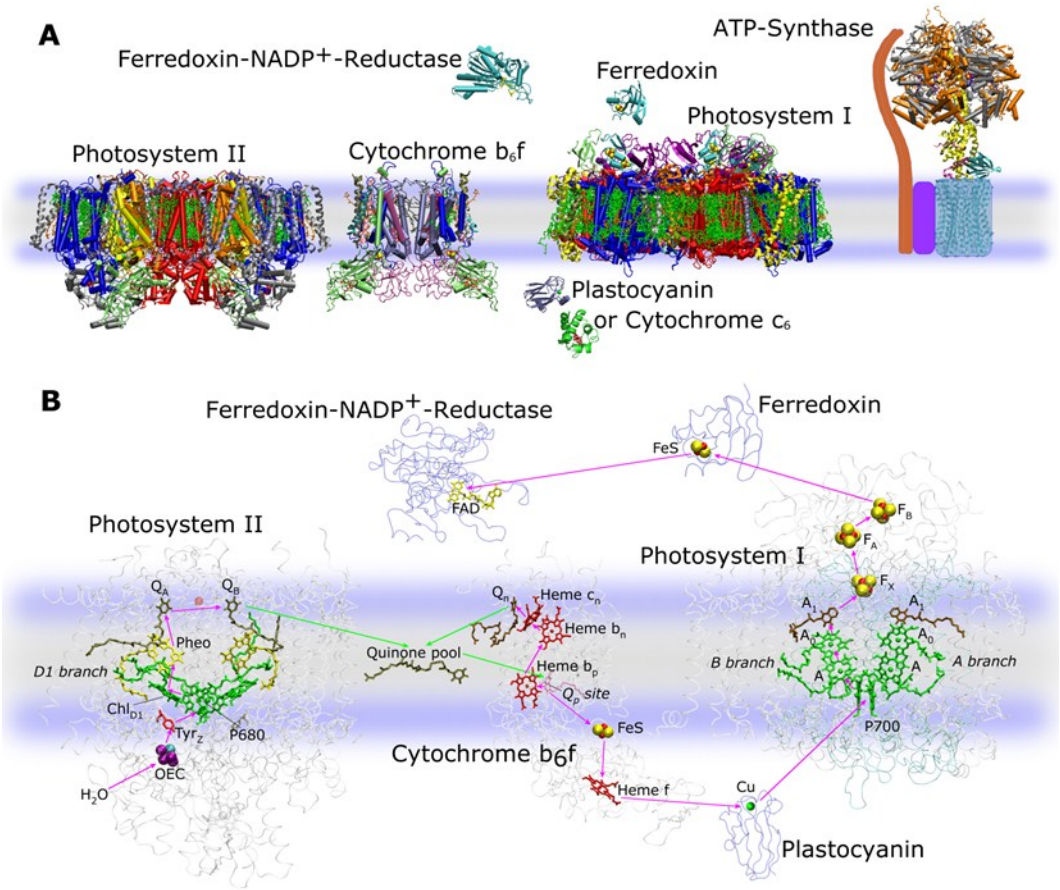

Figure 1. A. The proteins responsible for electron transport in photosynthesis are shown with their respective position relative to the thylakoid membrane (stroma above, and lumen below). Each is represented by the determined 3-dimensional structure features, wherever possible. Also included is the ATP synthase, which is not involved in electron transport, but is involved in the transport of protons generated through the electron transport process. **B.** Detailed representations of the protein cofactors and their contribution to the electron transport process. Electrons are represented by magenta arrows, and electron transport coupled to protons is represented by green arrows. Image borrowed from text edited by Fromme [1], used with editor's permission.

very positive redox potential of 1.1 V. This high redox potential enables $P680^+$ to extract an electron from the Mn_4Ca cluster in the oxygen evolving complex (OEC) in PSII via a redox active tyrosine. The Mn_4Ca cluster binds four electrons after oxidizing 2 water molecules (2 H_2O) to produce O_2 and 4 protons (4 H^+) in the lumen. This splitting of water requires 4 photons of energy to induce 4 sequential charge separations by P680.

Returning to the electron transported from P680* to Chl_{D1} at the PSII acceptor site, the electron is next passed to a pheophytin molecule (Pheo) and then to the first phylloquinone (PQ_A), both bound by PSII. Next, the electron is passed to another phylloquinone (PQ_B), and PQ_B releases from PSII in the form of PQH_2 once it has been doubly reduced by two electrons (resulting from two photon-induced P680 charge separations), and two protons originating from the stroma. PQH_2 thus can act as an acceptor of two electrons, and is replaced by another phylloquinone from the PQ-pool after release from PSII. The PQH_2 is shuttled through the membrane to the cytochrome b_6f complex (Cyt b_6f), where it then serves as a donor of the two electrons, releasing 2 H^+ into the lumen in the process.

Directly, one of the two electrons is transferred from PQH_2 to a 2Fe2S cluster in the Cyt b_6f. The other electron must then follow an indirect route known as the 'Q-cycle', where it first proceeds to a series of heme molecules in cytochrome (heme b_p, heme b_n, then heme c_n), followed by transfer to another phylloquinone

(PQ_n). This reduced PQH can then transfer electrons directly to the 2Fe2S cluster. The electron then is transferred to another heme designated as f. Whether it be through the direct or indirect route, the transfer of an electron from a reduced phylloquinone to the 2Fe2S cluster results in the additional release of protons to the lumen, and returns the phylloquinone to its oxidized state (PQ).

In the lumen, an oxidized plastocyanin (PC) protein (or Cytochrome c_6 in some cyanobacteria) will dock to Cyt b_6f, where the single electron is transferred from the heme f. From there, PC migrates to Photosystem I (PSI). Photons of light are absorbed in the core antenna complex, and the excitation energy is transferred to a pair of chlorophylls (a and a') named P700. P700 in its excited state (P700*) donates one electron to a chlorophyll-a (Chl-a A), and $P700^+$ is formed. $P700^+$ will then accept the electron from the reduced PC. From chlorophyll-a (Chl-a A), the electron then transfers to another chlorophyll-a (A0), and then to phylloquinone (Phy A1). PSI has two branches (A and B) whereby these (Chl-a A) → (Chl-a A0) → (Phy A1) steps take place. Both branch A and B are usually functional, although in some cases one may be preferred. Phy A1 then transfers the electron to a series of three 4Fe4S clusters (F_X, F_A and F_B). The single electron pathway through PSI ends at F_B, and Ferrodoxin (Fd) (or Flavodoxin (Fl)) docks on the stromal side, to which the electron then transfers as it leaves PSI.

In the stroma, the Fd (or Fl) will then transfer the single electron to the Ferrodoxin-$NADP^+$-Reductase (FNR). FNR must be reduced twice by Fd or Fl for the final step to occur. This photosynthetic electron transport chain concludes as 2 electrons are transferred from FNR to an oxidized $NADP^+$ molecule and coupled with a stromal H^+ to form the final biochemical energy product, NADPH. This path of oxygenic photosynthesis electron transport is illustrated in the flow diagram in Figure 2, where each step is associated with a color corresponding to the location where it takes places [1].

1.2. The electrochemical gradient

The process of electron transport in photosynthesis produces a gradient of both protons (ΔpH) and electrical charge (Δψ) across the thylakoid membrane. The proton gradient is influenced at four points by the electron transport process. First, the splitting of H_2O by the OEC releases H^+ in the lumen. Then the PSII associated phylloquinone (PQ_B) and the Cytochrome b_6f associated phylloquinone (PQ_n) both draw H^+ from the stroma, and release it also to the lumen. And at the conclusion of the process, $NADP^+$ binds free H^+ in the stroma when it becomes reduced as NADPH. Each of these events contributes to the ΔpH potential produced by an increase of H^+ in the lumen and a decrease of H^+ in the stroma. The Δψ gradient is formed by the electron transfer from H_2O in the lumen to $NADP^+$ in the stroma. This makes the membrane positively charged at the luminal side, and negatively charged at the stromal side. The ΔpH and Δψ electrochemical gradient is the essential driving force behind the production of

another biochemical energy source: the adenosine triphosphate (ATP) produced by the enzyme ATP synthase [2].

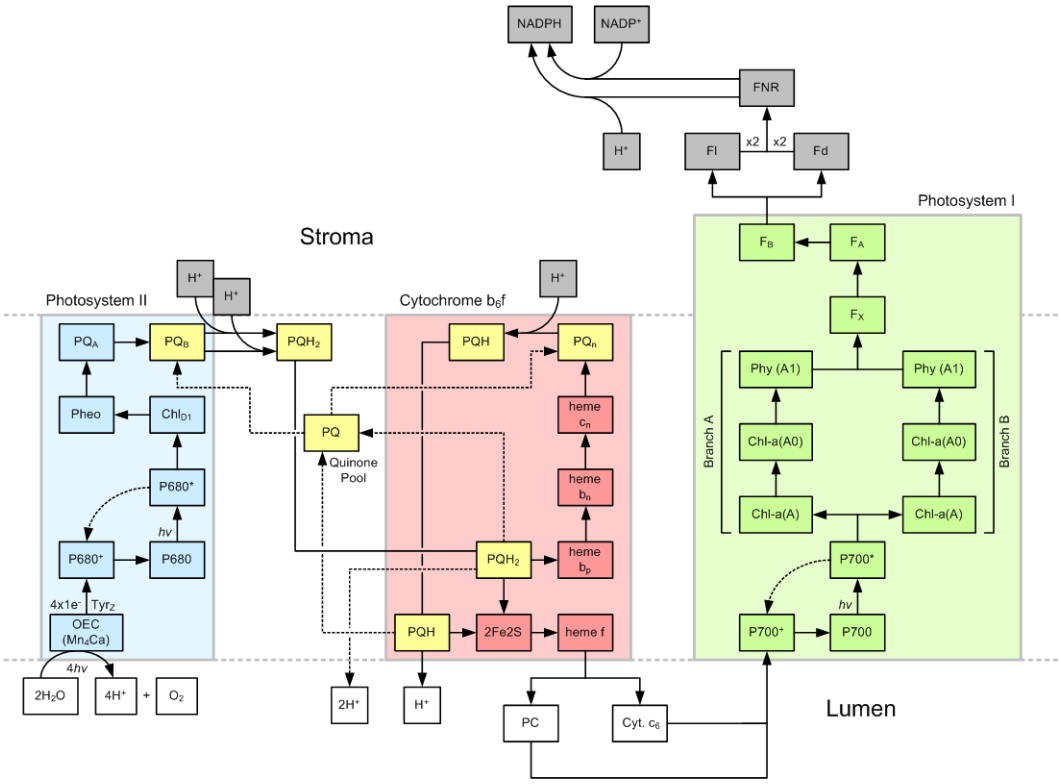

Figure 2. A schematic flow diagram of the photosynthetic electron transport chain, which produces an electrochemical gradient. Cofactors involved in the process are colored according to their locale. Each arrow denotes the transfer of one electron.

1.3. The ATP synthase enzyme

Multiple subunits comprise the ATP synthase, functioning together to form a unique rotary mechanism rarely seen among enzymes. Although there are several types of ATP synthase, the basic subunit arrangement of the enzyme is conserved among species, with some minor variations in the subunit composition. Shown in Figure 3 is the F-type ATP synthase scheme. The primary function of ATP

synthesis (or hydrolysis) for which the enzyme is named is conserved for all types of the enzyme, although the related process of ion transport varies in terms of ion type and reversibility. The ATP synthase is a membrane protein, and in chloroplasts it is located in the thylakoid membranes. In mitochondria, it resides in the inner mitochondrial membrane. And in bacteria, the ATP synthase is found in the plasma membrane [3].

1.4. ATP synthase structure and functional activity

In chloroplasts, the ATP synthase structure consists of a membrane extrinsic 'head' region designated as 'F_1', and a membrane intrinsic region designated as 'F_0' (Figure 3). Hence, the chloroplast ATP synthase is often synonymously denoted as CF_0F_1. The F_1 region includes the stromal subunits α_3, β_3, γ, δ, and ε. Subunits a, b, b' and c_n comprise the F_0 region. The two regions are connected by a rotational central γ-stalk and a stationary b/b'-stalk, and thus mechanically coupled. In the chloroplast F_0 region, single protons from the lumen are directed to a Glutamate residue on c_1 (monomeric) subunits through a putative half-channel provided by the adjacent a-subunit. As (*n*) protons enter from the lumen and bind to (*n*) c-subunits, a complete 360° stepwise rotation of the c_n (multimeric) ring takes place that allows the bound protons to be released individually at each step, and directed into the stroma via another putative half-channel provided by the a-subunit [4]. Thus, the number of protons transported per rotation is equal to the number of c-subunits (*n*). The rotation of the c_n ring is coupled to the rotation of the γ-stalk in the F_1 region, where subunit γ functions as

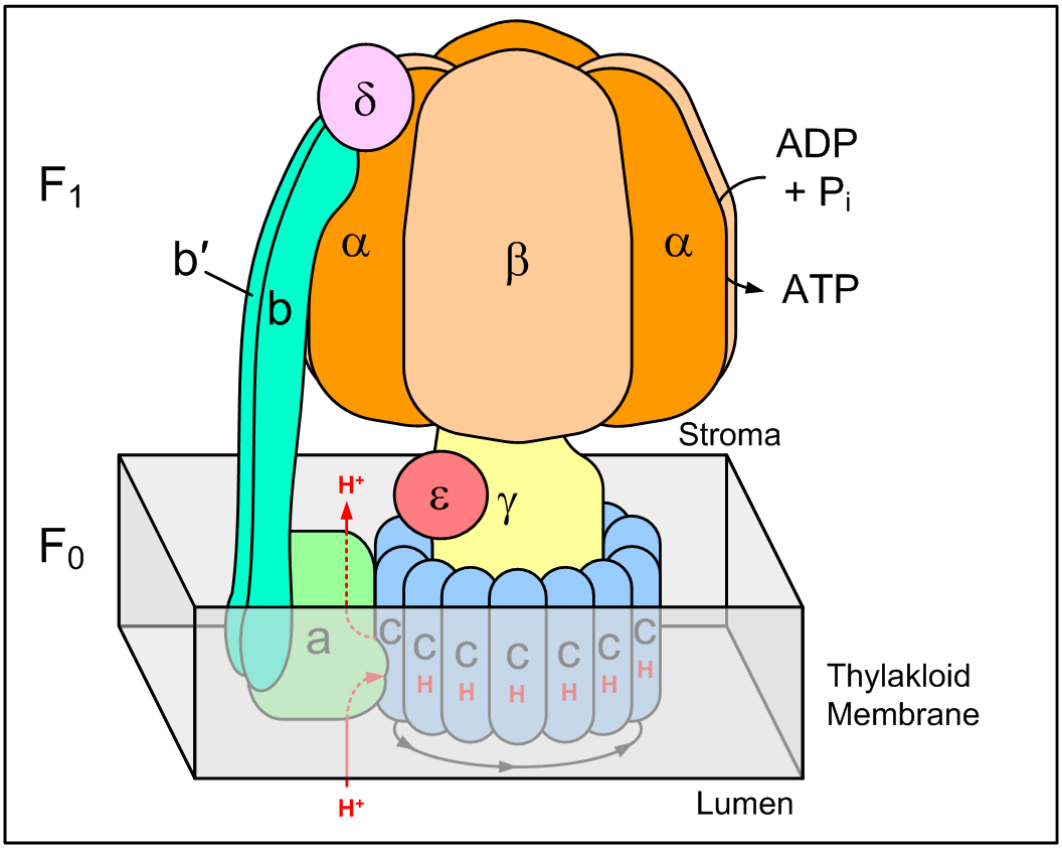

Figure 3. General subunit arrangement of the F-type ATP synthase. Latin characters are used for the F_0 membrane bound subunits, and Greek characters are used for the F_1 membrane exterior subunits. In chloroplasts these subunits have traditionally been denoted as IV(a), I(b), II(b'), and $III_n(c_n)$. However, the a, b, b', c_n notation is used here in order to facilitate comparison with other ATP synthases. During catalytic activity, the rotational portion of the enzyme is comprised of subunits c_n, γ, and ε; while the other subunits form the stationary component.

a shaft inside the $\alpha_3\beta_3$ head. The γ-rotation drives the catalysis of the ADP + P_i → ATP reaction that occurs at each of the three α-β subunit interfaces in F_1 [3]. This cyclical sequence of rotation, translocation and catalysis produces 3 ATP molecules for every (*n*) value of protons that pass from the lumen to the stroma

[3, 5, 6]. This process is reversible in the chloroplast ATP synthase and it is classified as an F-type enzyme. Archaeal (A-type) ATP synthases are also reversible, while vacuolar (V-type) ATP-ases function only as proton or ion pumps driven by ATP hydrolysis. Naturally, the F-type ATP synthase associated with photosynthesis transports H^+; however in some non-photosynthetic organisms such as *Ilyobacter tartaricus* the ion transported may be Na^+ [7, 8].

1.5. Stoichiometry of the c-subunit ring and coupling ratio

The stoichiometry of F-type ATP synthase c_n rings is currently known to range from c_8 to c_{15} among the slowly expanding list of organisms for which it has been determined in recent years (Table 1). Estimations of c_{13} have been made for *C. reinhardtii* [9], and $c_{13\text{-}15}$ among 8 different cyanobacterial species [10], based on gel electrophoresis comparisons. As noted, each individual c-subunit may bind a single proton from the lumen and mediate transport of that proton to the stroma following a complete rotation of the c-subunit ring. And so, because the number of c subunits per ring (*n*) is organism dependent, the ratio of ions transported to ATP generated ranges from 2.7 to 5.0 among these organisms [11-13]. This ratio is known as the 'coupling ratio', and is entirely dependent on the variable (*n*) since the number of ATP generated per c_n rotation is constantly held at 3 in all known ATP synthases [14]. Chapter 2 is devoted to a discussion on the variable ring stoichiometries and coupling ratios.

1.6. Sequence alignments

For the sake of comparison, the 81 amino acid sequence of the spinach chloroplast c-subunit is shown in alignment with the sequences of nine other F-type c-subunits for which the stoichiometry is known, or estimated in the case *C. reinhardtii*. Individual alignments are shown in Figure 4, and a multiple sequence alignment is shown in Figure 5. The percentage of identical resides (PID_2) was calculated by dividing the total number of residues that are identical by the total number of amino acids (including gaps), for both strands compared. Positions where sequence identity is not observed often do have sequence similarity. The percentage of similar residues was similarly calculated by dividing the total number of residues that are identical or similar, by the total number of amino acids (including gaps). Similar residues were defined as G/A, V/L, L/I, I/V, S/T, Q/N, and D/E. The resulting values are listed in Table 1. The 10 c-subunit sequences were also cross-aligned to one another, and sequence identity was calculated for comparison, as shown in the 2-dimensional table in Figure 6.

As noted, the ATP synthase is presumably conserved throughout biology, and as indicated by the sequence alignments the amino acid sequence homology of the enzyme tends to correlate with phylogenetic comparisons. For instance, the c_{11} sequences of *I. tartaricus* and *P. modestum* are nearly identical, and these two species of bacteria have been both classified in the Fusobacteria family. As might be expected, there is very little similarity between the *E. coli* c_{10} and *S. cerevisiae* c_{10} sequences, and likewise little similarity between the *B. pseudofirmus* c_{13} and *S.*

elongatus c_{13} sequences. It is interesting that these distantly related organisms have such low sequence similarity, but the same stoichiometry. These examples of convergence show that there is more than one path toward a particular ring stoichiometry, likely due to some biological constraint on the number of stoichiometries that are metabolically possible.

Organism	(*n*)	Total aa	Identical aa	% Identity	Similar aa	% Similarity
***Bos taurus* [13]**	8	75 +3	29	36	42	53
***Saccharomyces cerevisiae* [15]**	10	76 +1	21	27	37	47
***Escherichia coli* [16]**	10	79	23	29	39	49
***Ilyobacter tartaricus* [8]**	11	89 +1	46	54	54	63
***Propionigenium modestum* [17]**	11	89 +1	46	54	54	63
***Bacillus pseudofirmus* [18]**	13	69	19	25	37	49
***Synechococcus elongatus* [10]**	13	81	70	86	74	91
***Clamydomonas reinhardtii* [9]**	13?	82	69	85	72	88
***Spinacia oleracea* [19]**	14	81	81	100	81	100
***Arthrospira platensis* [20]**	15	82	71	87	75	92

Table 1. Determined stoichiometries for F-type ATP synthase c-subunit rings (*n*). Upon comparing the amino acid sequence of the spinach chloroplast c_{14} subunit to the sequences of the other c-subunits, a correlation is observed between the value of (*n*) and the percentage of identical residues (PID_2), based on optimal sequence alignments (Figure 4). PID_2 is determined by dividing the total number of identical amino acids by the total number of amino acids in the two sequences. Gaps resulting from sequence alignments are counted as additional amino acids (indicated in the 'Total aa' column as '+1', for example, where applicable).

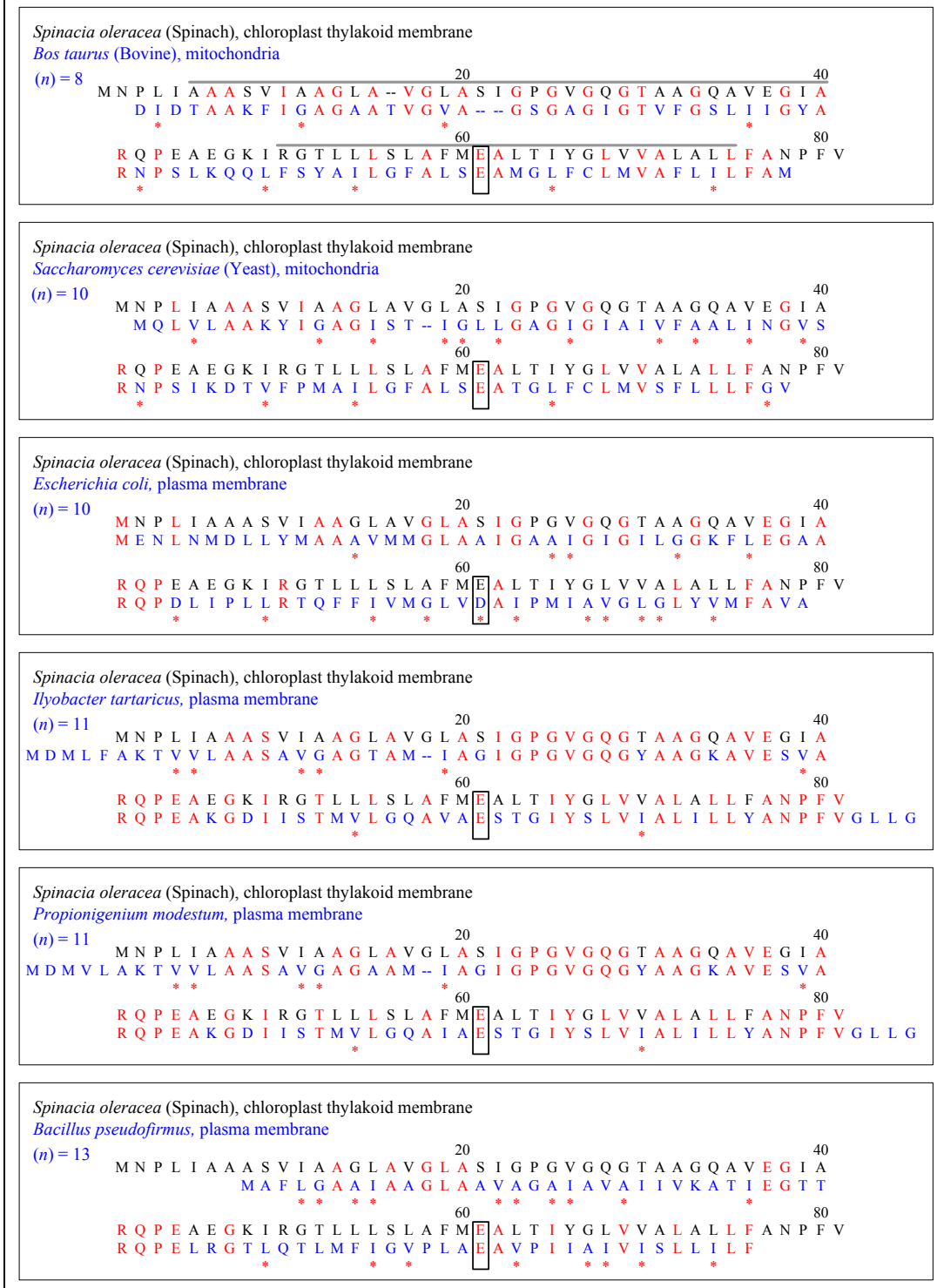

Figure 4. (continued on next page)

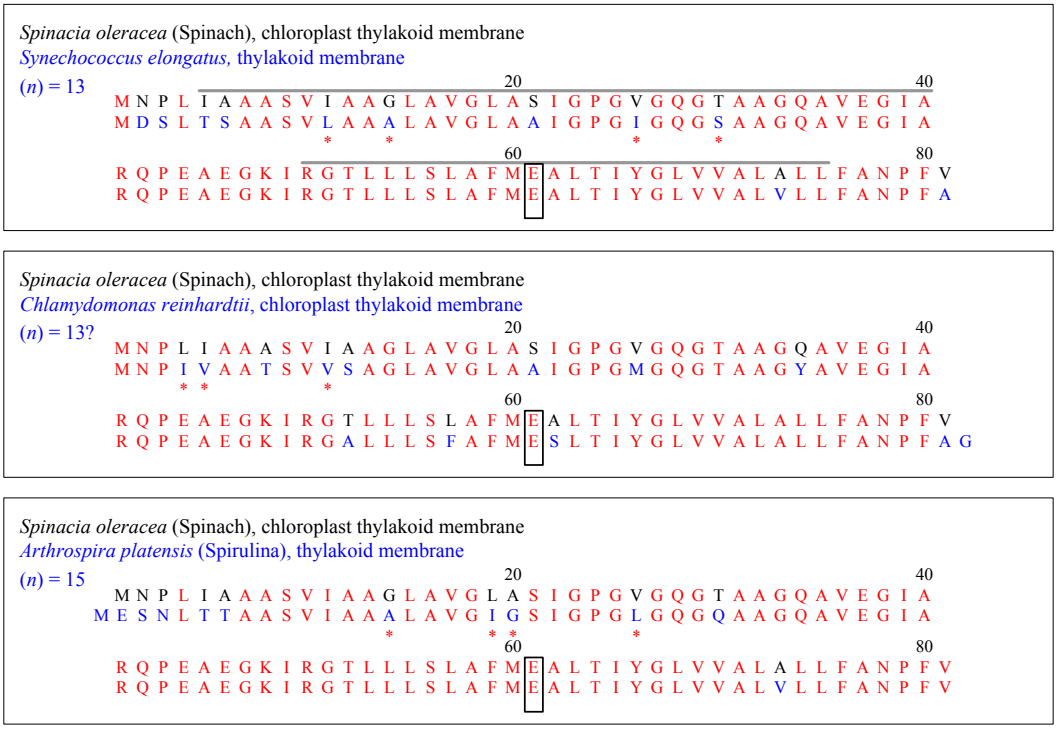

Figure 4. Alignments of amino acid sequences for F-type c-subunits of known stoichiometry (blue) to the sequence of spinach chloroplast ATP synthase c_{14} subunit (black). Identical residues are highlighted in red. Similar residues are designated by a red asterisk (*). The two putative transmembrane regions of the spinach sequence are highlighted by the gray bar shown on the *B. taurus* and *C. reinhardtii* alignments. The stoichiometry of *C. reinhardtii* is not conclusively determined, but has been suggested based on experiments [9]. In all alignments, the Glu61 residue is conserved, except in *E. coli* where it is the similar Asp61. The loop region near the middle of the sequence is somewhat conserved in some cases as well. As might be expected, the c-subunits from photosynthetic organisms (thylakoid membranes) share the greatest sequence identity.

Interesting comparisons can also be made with the cyanobacterial *S. elongatus* c_{13} and *A. platensis* c_{15} to the *S. oleracea* chloroplast c_{14} sequence. In contrast to the two c_{10} and two c_{13} examples, these sequences have high similarity, but different stoichiometries. This is also apparent when comparing the other chloroplast sequence of *C. reinhardtii*, which appears to also have a different stoichiometry

[9]. A comparison of these highly similar sequences could provide a hypothesis for which residues are critical in influencing the value of (n). Such hypotheses will be discussed in Section 6.2.

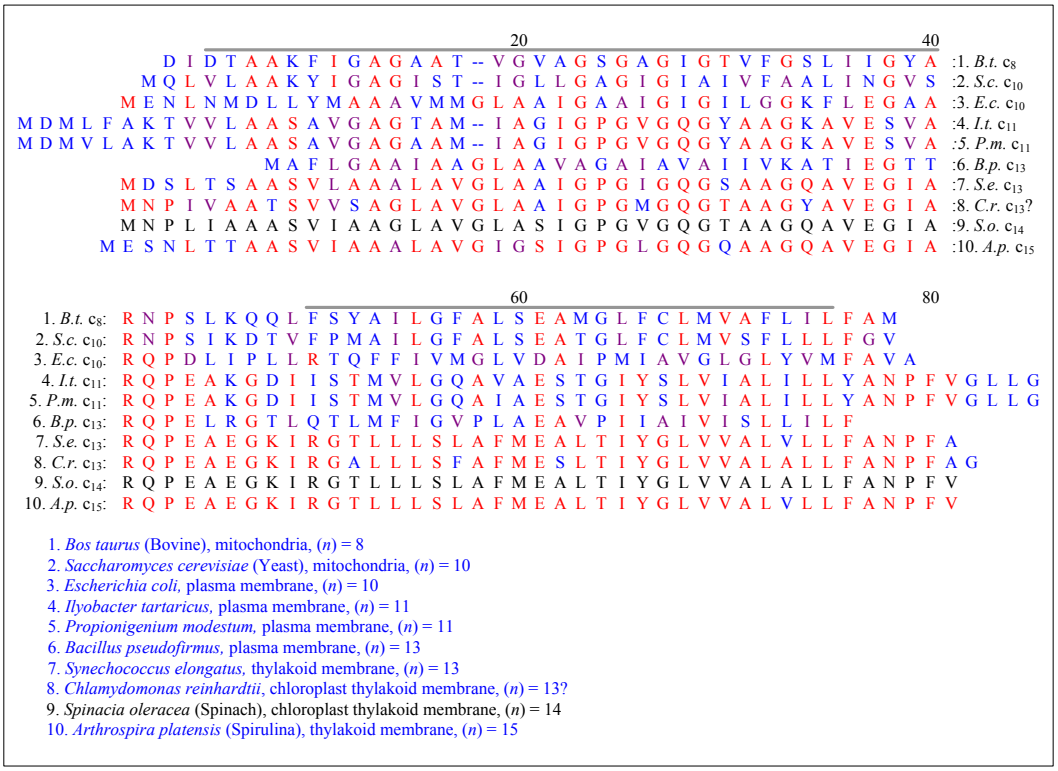

Figure 5. Multiple sequence alignment where the *S. oleracea* chloroplast c_{14} subunit (#9) is compared to the other nine c_n subunits of known stoichiometry. Identical residues are highlighted in red, similar residues are highlighted in violet. Possible trends can be observed at positions such as Ser21, where substitutions may correlate to (n).

Alignment Sequence Identity: Total # Identical aa / Total # aa + gaps (values noted as percentages)	*Bos taurus*, c_8	*Saccharomyces cerevisiae*, c_{10}	*Escherichia coli*, c_{10}	*Ilyobacter tartaricus*, c_{11}	*Propionigenium modestum*, c_{11}	*Bacillus pseudofirmus*, c_{13}	*Synechococcus elongatus*, c_{13}	*Chlamydomonas reinhardtii*, c_{13}?	*Spinacia oleracea*, c_{14}	*Arthrospira platensis*, c_{15}
Bos taurus, c_8	--	60	26	30	32	29	34	35	36	32
Saccharomyces cerevisiae, c_{10}	60	--	18	29	29	27	20	26	29	26
Escherichia coli, c_{10}	26	18	--	17	17	23	33	25	26	27
Ilyobacter tartaricus, c_{11}	30	29	17	--	96	26	55	53	54	51
Propionigenium modestum, c_{11}	32	29	17	96	--	19	45	53	54	44
Bacillus pseudofirmus, c_{13}	29	27	23	26	19	--	19	25	25	17
Synechococcus elongatus, c_{13}	34	20	33	55	45	19	--	65	86	85
Chlamydomonas reinhardtii, c_{13}?	35	26	25	53	53	25	65	--	85	72
Spinacia oleracea, c_{14}	36	29	26	54	54	25	86	85	--	72
Arthrospira platensis, c_{15}	32	26	27	51	44	17	85	72	72	--

Figure 6. A sequence cross-alignment 2-D table for the 10 F-type ATP synthase c-subunits of known stoichiometry. Sequence identity percentage values (PID_2) are shown, and were calculated as noted on the table. Alignments were carried out using the BLOSUM62 comparison matrix [21].

1.7. Recombinant protein expression

The technique of using plasmid DNA as a shuttle vector for genetically transforming the bacterium *Escherichia coli* was developed in the early 1970's [22], and began to be used routinely during the following decade [23, 24]. Since

that time, thousands of proteins have been successfully produced in recombinant expression systems which often facilitate subsequent isolation and purification steps [25]. Typically, a chosen gene is ligated into a carefully designed plasmid vector, and a given cell type is induced to uptake the vector, and thus transformed genetically. Certain cell types are more amenable to this genetic transformation than others, usually with some modifications. Strains of *Escherichia coli* have been developed for this purpose and have proven to be particularly capable of expressing various genes from other organisms, making *E. coli* the most common host for recombinant protein expression. Because this bacterium is so commonly used, a broad assortment of genetic strains, compatible vectors, growth techniques, and extraction/purification methods are available from commercial and/or academic sources [25, 26].

Among the thousands of proteins that have successfully been recombinantly expressed in *E. coli*, few of them are membrane proteins, even fewer are eukaryotic, and yet even fewer are eukaryotic membrane proteins. The expression of recombinant membrane proteins in *E. coli* can often be toxic, a result of the direct effect of the foreign membrane protein on the physiology of the bacterium. The prokaryotic *E. coli* bacterium lacks the necessary chaperones that may assist in the synthesis, folding, and channeling of an expressed eukaryotic protein. And so in the unlikely event that it is not toxic, the expressed eukaryotic membrane protein will likely not be stable, and is either quickly degraded or inclined to form inclusion bodies (aggregates of unfolded protein).

Such proteins that have been expressed usually need to be extracted as inclusion bodies, followed by attempts to refold the protein, which often fail [27]. And, in the unlikely event that recombinant membrane protein expression is successful, the amount will be much limited by the minimal bacterial membrane space available for incorporation. In consideration of these barriers, one can understand why so few eukaryotic membrane proteins have been isolated in *E. coli*, in spite of their physiological importance that makes them valued in therapeutic studies. And so in recent years, alternate approaches have been developed with moderate success. Such approaches include the use of various fusion tags [28], the directed evolution of more tolerant *E. coli* mutant cell lines [29], or in vitro expression systems [30].

1.8. History of c-subunit expression in E. coli

Naturally, proteins from other prokaryotes tend to be more likely to express in *E. coli* [26]. And naturally, soluble proteins tend to be much easier to purify and express in *E. coli* [31]. The c_1 subunit of the ATP synthase from the chloroplast of spinach is neither prokaryotic in origin nor soluble in nature. Therefore, expressing it in *E. coli* is an expected challenge. It was reported to have been expressed on one occasion in 1990 [32]. In this case, an *E. coli* knock-out strain lacking the *uncE* gene was transformed with an *atpH*-bearing plasmid. In *E. coli* and spinach chloroplast, the ATP synthase subunit c is coded for by *uncE* and *atpH*, respectively – so this was an attempt to produce a hybrid ATP synthase complex by swapping genes. Reportedly, the desired hybrid complex did not

form, but c-subunit was expressed, and expression was directed mostly to the membrane regions of the cell. This report was somewhat lacking in details. There was no discussion of how the *uncE* lacking bacterium was cultured without a complete ATP synthase. It did not include any protocol for the purification of the expressed protein, and did not indicate the quantity of protein produced, or if it formed inclusion bodies. No follow up experiments were reported, so there is some doubt as to the whether the experiment had any practical applications, assuming that it was reproducible. Given this assessment of the reported experiment, it was decided that an alternate strategy for recombinant expression of the chloroplast c-subunit would be a preferable means of achieving the stated objectives described in Chapter 3.

Recombinant expression of bacterial c-subunits in *E. coli* has been reported as well. The c_{11} ring of *P. modestum* and the very similar c_{11} ring of *I. tartaricus* were both expressed in standard *E. coli* BL21(DE3) cells [33], [34]. In both cases, the yield was low, and expression was directed to the cell membrane fractions. These results have reportedly been repeated for other applications [34]. There is little sequence similarity between these c_{11} subunits and that of the spinach chloroplast; and since these were prokaryotic proteins expressed in a prokaryotic system, there is little implicated by this report with regard to the less straightforward recombinant expression of the eukaryotic spinach chloroplast c-subunit.

Chapter 2

RING STOICHIOMETRY: HYPOTHESES AND DISCUSSION

2.1. The value of (n)

The observation that the number of subunits in a c-ring (*n*) varies among organisms has recently led to the plausible hypothesis that (*n*) is evolutionarily determined to fulfill the metabolic needs of the corresponding organism [12]. Indeed, one of the most fascinating aspects of biology is the diversity of conditions under which an organism can thrive; and this is a manifestation of the diversity of means by which organisms are able to metabolize the energy sources that are available. The metabolic nature of an organism influences the rate of cellular ATP consumption, as well as the electrochemical potential across the membrane [35]. Because the rate of ATP consumption must be maintained consistent with the rate of ATP synthesis, the value of (*n*) is critical.

An ATP synthase with a higher value of (*n*) will have a higher coupling ratio, and this has several implications for the electrochemical potential as well. A higher coupling ratio connotes that more H^+ can be transported in the generation of 3 ATP. For comparison, the *A. platensis* c_{15} ring transports 1/3 more H^+ than the *S. cerevisiae* c_{10} ring per 3 ATP generated. And so given an equivalent proton gradient, *S. cerevisiae* would produce 1/3 more ATP than *A. platensis*. Although the overall proton-motive electrochemical driving force ($\Delta\mu H^+$) is a function of both ΔpH and $\Delta\psi$, in thylakoid membranes the ΔpH is the greater force

component. This is in contrast to mitochondrial and some bacterial membranes where $\Delta\psi$ is of greater influence [7, 12]. Torque generation in general has been shown to be driven more so by $\Delta\psi$ than ΔpH [2, 36]. Although $\Delta\psi$ is not high in chloroplast membranes, it has been hypothesized that the larger c_n rings are able to acquire sufficient torque as a consequence of smaller rotation steps that result from having more subunits [7]. And so it is conceivable that larger c_n rings in plants and cyanobacteria are preferred, given the low $\Delta\psi$ in the thylakoids, and lower average rates required for ATP synthesis in low light conditions or during periods of slow growth.

2.2. Factors of possible influence

Although it is apparent that the purpose of c_n ring stoichiometric variations is metabolically related, it is less obvious which factors govern the stoichiometric variation. A number of hypotheses have been presented, however, the molecular basis for the c_n stoichiometric regulation has not yet been defined, and this has led to much discussion on the matter [9, 10, 12, 13]. It is reasonable to assume that stoichiometry may be influenced by factors such as the amino acid sequence and post-translational modifications, lipid membrane environment, the presence of molecular co-factors, or the steric forces of adjacent subunits. Some of these factors will be discussed in examples provided by different organisms in the following sections.

2.3. The fixed c_n ring of C. reinhardtii

Tittingdorf, et al. reported a purification procedure for the chloroplast c_n ring from the unicellular green alga, *Chlamydomonas reinhardtii* [9]. In this report, the c_n ring was extracted from the organism after growth under a range of varied conditions, including differences in light intensity, carbon source, pH, and CO_2 concentration. The purified c_n ring was then run on a gradient SDS polyacrylamide gel and immunoblotted, and migration was compared to the purified c-rings from organisms of known stoichiometries as standards, including the *S. oleracea* chloroplast c_{14} and *I. tartaricus* c_{11}. There appeared to be no variance in the stoichiometry of the *C. reinhardtii* chloroplast c_n ring, regardless of the growth parameters for the organism. The stoichiometry of the *C. reinhardtii* c_n ring is not conclusively determined, but the authors suggest that it may be c_{13} based on comparison to the *S. oleracea* c_{14} and *I. tartaricus* c_{11} standards.

It should be acknowledged that no other chloroplast c_n stoichiometry has yet been determined besides the spinach chloroplast c_{14}. And so if the *C. reinhardtii* chloroplast c_{13} can be confirmed by more reliable physical characterization methods, it would imply that although c_n may be fixed in some plants, it may still be somewhat variable among plant species.

2.4. The E. coli c_{10} ring

Early ATP synthase studies were often directed toward the *Escherichia coli* enzyme, where it was sometimes reported that the ring stoichiometry was (*n*)=12 [37, 38], among other values. This c_{12} assertion supported the hypothesis that the value of (*n*) would need to be a multiple of 3 in order to correspond to the ratio of 1 ATP generated per 120° stepwise rotation. But as it has turned out, the *E. coli* ring was later determined to be preferably (*n*)=10 based on more reliable cross-linking data [16, 39], and as of yet no organism has been found to have a fixed c_{12} stoichiometry.

It has been reported that although c_{10} is preferred in *E. coli*, other stoichiometries may also be present [16]. In that report, the *E. coli* c-subunit was expressed as cysteine-substituted genetically fused c_3 and/or c_4 oligomers, the resulting rings were formed in vivo, and then cross linked. Of all the combinations of c_3 and c_4 possible, it was observed that c_{10} was preferred, but others also existed. Among other minor stoichiometries observed, it was reported that c_8 and c_9 could still form functional complexes. And so although the *E. coli* c_{10} appears to be preferred under normal physiological conditions, this study provided some of the first evidence that it was at least possible for a variation in stoichiometry that is not dependent on amino acid sequence.

2.5. The recombinant I. tartaricus and P. modestum c_{11} ring

The nearly identical bacterial c_{11} rings from *I. tartaricus* and *P. modestum* were reportedly expressed recombinantly in the bacterium *E. coli*, strain BL21(DE3). The sequence identity of *I. tartaricus* and *P. modestum* with *E. coli* surprisingly is very low, only 17% for both species. Nevertheless, both reportedly expressed in *E. coli*, and low amounts of the native c_{11} ring was observed. It was also reported that other stoichiometries resulted as well. Closer examination with AFM revealed that rings of stoichiometries less than 11 had no change in diameter, and incidentally had an open spot where the missing monomers otherwise would have been. Interestingly, c_{12} rings also showed no change in diameter, with the additional subunit bound to the exterior of the ring. These results provide further support for the hypothesis that ring stoichiometry is primarily influenced by the amino acid sequence. In this case, the sequence appeared to influence the angle at which proximal c_1 monomers were associated in the ring formation. The results also cast some doubt on the validity of the observed alternate stoichiometries reported in *E. coli* [40], assuming that it is the result of a similar phenomenon.

2.6. Hypothetical summary

The examples discussed in this chapter provide strong evidence for the hypothesis that the value of (n) is determined by the amino acid sequence. This hypothesis has been applied to the c_8 sequence from *B. taurus* (bovine) mitochondria, where it has been proposed that all mammals (including humans) and invertebrates may also have a c_8 stoichiometry based on the observation that several representative

sequences are identical (or nearly identical) to the bovine c_8 [13]. This hypothesis can be supported by examination of the sequence alignments discussed in Section 1.6. As noted in Table 1, the sequence of the cyanobacterial *S. elongatus* c_{13} and *A. platensis* c_{15} have respectively 86% and 87% sequence identity with the *S. oleracea* chloroplast c_{14} sequence. In consideration of the endosymbiotic theory relating cyanobacteria to chloroplasts, and the fact that all three organisms are photosynthetic, the high sequence homology and high (*n*)-determined coupling ratios are probably not coincidental. Conversely, this is also supported by the low sequence identity of the bacterial and mitochondrial c-subunits with the chloroplast c_{14}. As expected, there is high sequence identity in the two chloroplast sequences shown, the *S. oleracea* c_{14} and the *C. reinhardtii* c_n. High sequence identity is also observed between the related organisms *I. tartaricus* and *P. modestum*. When considering these alignments, there is support for the hypothesis that the divergence that exists in F-type c-subunit sequence homologies among species correlates with the divergence in respective stoichiometries [11].

Although there appears to be a strong correlation between amino acid sequence and ring stoichiometry, it does not necessarily exclude the possibility that other factors may have an influence as well. In the purification of the native spinach chloroplast ATP synthase c_{14} ring, it has been observed in the Fromme lab at ASU that carotenoids, chlorophyll, and possibly pheophytin co-purify with the ring and also co-crystalize [41]. An electron density map generated in the Fromme lab

from the crystal structure of this native spinach chloroplast c_{14} ring (currently unpublished) shows electron densities inside the ring and near the loop region of the ring which may correspond to a carotene and a chlorophyll, respectively (Figure 7). It is possible that the association of the pigments is simply an artifact of purification, however the alternate possibility that the pigments may play an important role in the stability or the stoichiometry of the ring should not be ignored [41].

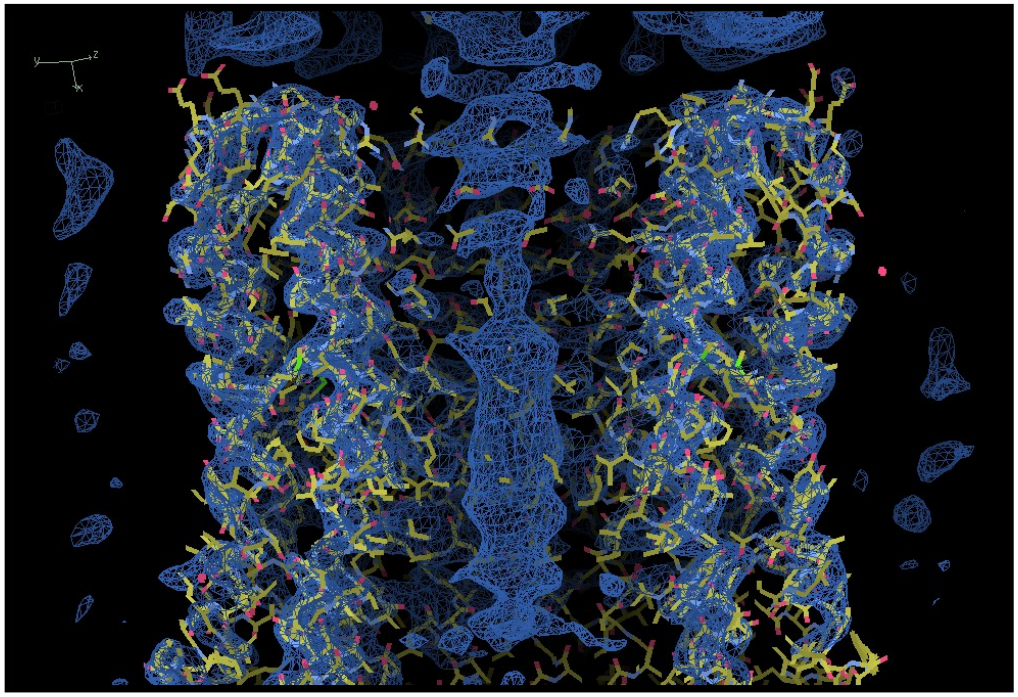

Figure 7. Electron density map of the native spinach chloroplast c_{14} ring. The ring is shown as a cross section to reveal electron densities in the center of the ring, and near the top as well. These densities may be evidence of pigments associating with the native ring.

Other factors may also have some influence on the stoichiometry. The membranes of chloroplasts, mitochondria and bacteria each have unique lipid compositions, and this composition can vary depending on environmental conditions. For example, the chloroplast membrane harbors unique lipids known as galactolipids. And it has been shown that the proportion of galactolipids in spinach chloroplast membranes can vary depending on environmental conditions [42]. In addition to investigating the influence of amino acid residues, the influence of the lipid membrane and cofactors should also be investigated in order to gain a comprehensive understanding of how the c-ring stoichiometry is regulated throughout biology. In the case that more conclusive data emerges showing that variable ring stoichiometries are possible under different environmental conditions, it is likely that these factors may be the means of regulation. In time, additional c-subunit ring stoichiometries from other organisms not yet known will be determined and this will likely assist stoichiometric studies by enabling broader comparisons to be made.

Chapter 3

OBJECTIVES AND CHALLENGES

3.1. Overview

The overarching goal of the work described in this dissertation has been to produce a recombinant chloroplast ATP synthase c-subunit ring. Leading to this end is a progressive series of multiple steps, which in many cases have been experimentally developed and optimized. These steps are described in detail in Chapter 4, and can be categorized as components of a subset of three objectives which are outlined in this chapter below.

3.2. Recombinant expression of the c-subunit

The first objective of this project was to develop a system in which the c-subunit of spinach chloroplast ATP synthase could be produced via genetic recombination in the bacterial host *Escherichia coli*. As noted, the expression of this protein is expected to be considerably difficult due to its hydrophobic nature and eukaryotic origin [26, 31]. Although methods are established for the native extraction and purification of c_{14} from spinach leaves [6, 41], the availability of a recombinant expression system offers several possible advantages. Primarily, in most cases the amount of recombinant protein extracted from *E. coli* can be far greater than what can be obtained from a native source. The subsequent isolation and purification of the expressed protein is usually facilitated as well because affinity tags can be attached to the expressed protein of interest, and *E. coli* cells are

easily lysed. Because recombinant expression begins at the genetic level, this also allows for genetic manipulations which can be engineered to alter the amino acid sequence of a given protein as desired. This is essential for experiments that could be designed to investigate which amino acids may be determinant for the value of (*n*). Another advantage is the enabled use of heavy atom labeling techniques that are very useful, if not sometimes indispensable for determining the phases when processing x-ray crystallographic data. These advantages are all relevant to the c-subunit, and currently there is a demand for a recombinant c-subunit expression system that will enable in vitro investigations of the factors that influence the stoichiometric variation of the intact ring [10]. This, and other applications will likely be benefited by the availability of this recombinant technique.

3.3. Isolation and purification of the expressed c-subunit

Following successful expression, the second objective was to isolate and purify the recombinant c-subunit in its monomeric form. Protein purification typically employs assorted techniques which must artfully be combined in order to isolate the protein of interest from the thousands of other proteins present in a cell. Proteins can be separated based on unique physical properties such as solubility, non-covalent bonding interactions, and hydrophobicity. This process is usually carried out in part by using columns packed with a medium chosen according to the preferred binding properties. Protein is passed through the column, and fractions are collected as proteins begin to elute. Ideally there is some separation

in their elution times, allowing for a purified product to be contained in a particular fraction. This is often carried out under high pressures in combination with chromatographic techniques that detect when protein is being eluted (HPLC, high pressure liquid chromatography). The purification method for the recombinant c_1 monomer was developed through systematic refinement of such techniques designed to exploit chosen properties of the protein. Completing this second objective of producing a highly purified cleaved c_1 is a notable prerequisite for the third objective: successful reconstitution of the monomer into its oligomeric form.

3.4. Reconstitution of an oligomeric recombinant c-ring

Once expressed and purified, the final objective was to reconstitute the monomeric c_1 into its oligomeric form. Membrane proteins are routinely inserted into liposomes and used for further applications. The hydrophobicity of membrane proteins leads them to interact readily with phospholipids and detergents. As detergents are removed, the phospholipids and membrane proteins are drawn together and thus induced to form proteoliposomes. Application of this principle was investigated with the monomeric recombinant chloroplast c-subunit. Successful reconstitution of this ring, whatever the stoichiometry, will ultimately lead to some very interesting experiments that can be designed to investigate which factors may have an influence on the oligomeric state the chloroplast c-ring, both in terms of stoichiometry as well as stability.

3.5. Other challenges related to objectives

Being a very hydrophobic eukaryotic membrane protein makes subunit c not only difficult to express and purify, but also difficult to detect using standard analytical lab techniques. Detection with polyacrylamide gel electrophoresis is difficult because the c-subunit does not resolve well. This is due in part to its hydrophobic nature, and also in part to its small size (8 kDa). As a consequence, immunoblotting or silver staining is used in place of the less sensitive and less difficult Coomassie Blue staining method. Analytical difficulties are also compounded by the fact that the 81 amino acid sequence contains no tryptophan residues, and only one tyrosine. This is problematic because these residues (particularly the absent tryptophan) contribute to the standard absorbance of proteins at 280 nm during routine determinations of protein concentration, including the application of this principle during HPLC purification methods. Because of this, spectrophotometric concentration determination methods needed to be substituted with a more time-intensive modified Lowry assay technique. Another challenge for detection of the c_1 subunit during purification steps was the lack of a commercial antibody, which is required for immunoblotting procedures. And so because it was not available, this antibody was produced by the author in collaboration with Agrisera, a company specializing in the production of plant related antibodies. In order to accomplish the defined expression and purification objectives, the related steps were engineered to obviate these challenges and are therefore not entirely conventional.

Chapter 4

METHODS

4.1. Expression

The development of an *E. coli* expression system that is capable of producing significant quantities of spinach chloroplast ATP synthase c-subunit required a comparative approach with a variety of methods. This is evident in the following subsections, which describe the methods used to produce the gene and express the corresponding c-subunit protein. Some reasoning and background for the methods chosen is also provided.

4.1.1. Optimized atpH gene design

The plastid genome sequence of spinach (*Spinacia oleracea*) is mapped and sequenced, with the gene *atpH* coding for the c-subunit of ATP synthase [43, 44]. The *atpH* gene is 243 bp in length and codes for 81 amino acids (UniProtKB accession number: P69447). A synthetic *atpH* gene was designed with a sequence of alternative codons that were optimally selected to match the most prevalent *E. coli* tRNAs (Figure 8). This is an important modification, particularly when expressing an eukaryotic protein in a bacterium [26, 45]. Another consideration in designing the gene was to avoid the use of repeated codons in tandem, wherever practical. As such, the synthetic *atpH* gene does not have the same base pair sequence as is found in the native spinach chloroplast, but

the translated amino acid sequence does not vary (Figure 9). The design was engineered with the use of Gene Designer software by DNA2.0 [46].

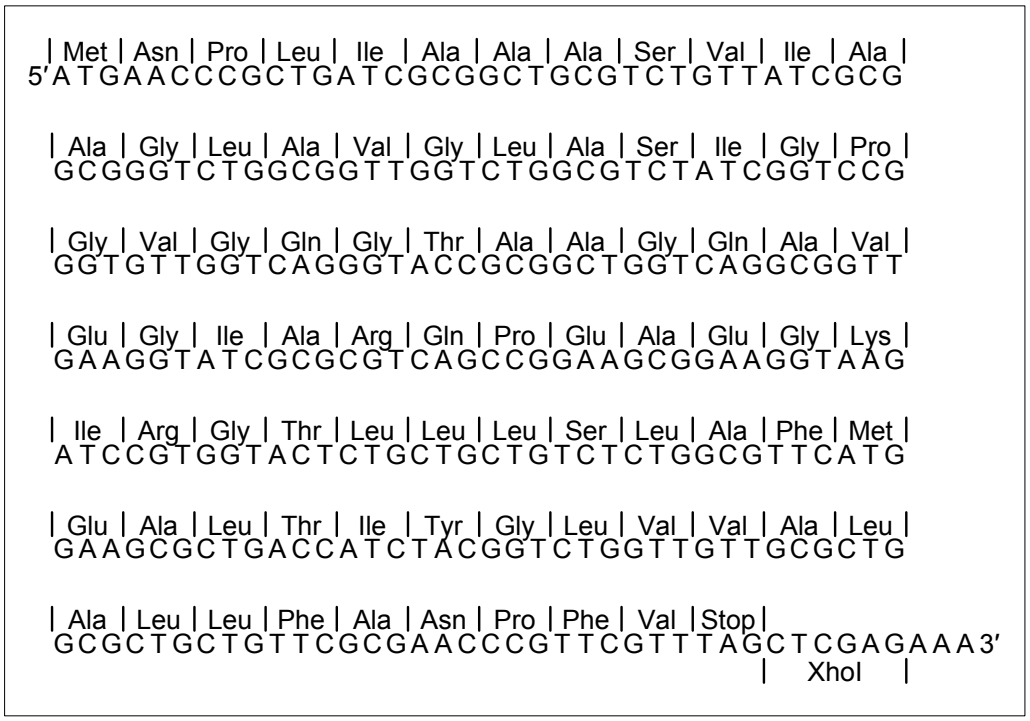

Figure 8. The *atpH* gene for spinach chloroplast ATP synthase subunit c, codon optimized for expression in *E. coli*. This construct of the gene was designed for the production of the plasmid pMAL-c2x-malE/atpH, with a blunt 5' end and a XhoI 3' end.

4.1.2. Synthesis of recombinant atpH gene

The recombinant *atpH* gene was synthesized by annealing and ligating overlapping oligonucleotide fragments to form the whole gene. The base pair sequence of the designed *atpH* gene (both the sense and antisense strands) was divided into 14 oligonucleotides ranging from 24 to 46 bp in length (Figure 10), and these oligonucleotides were commercially produced using in vitro methods by Integrated DNA Technologies. Prior to annealing the matching coding and non-

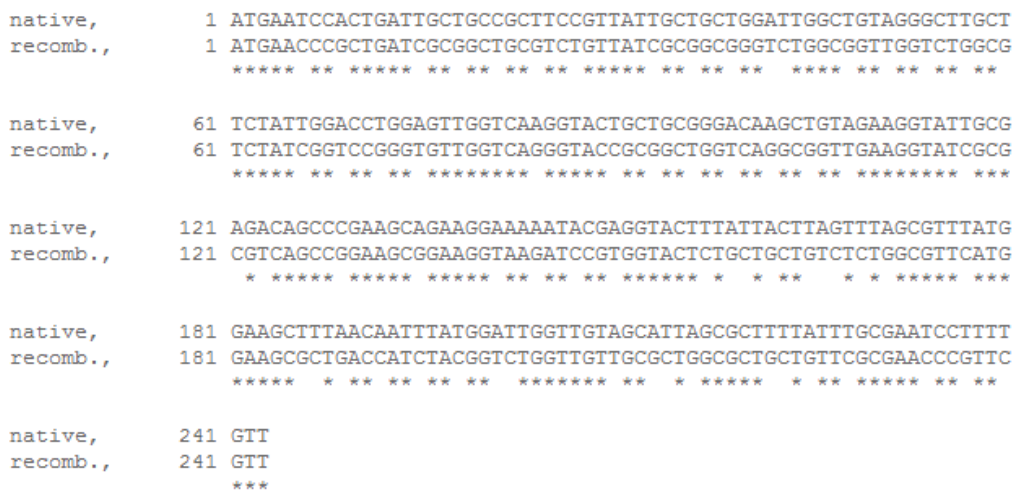

Figure 9. An alignment comparison of the native *S. oleracea* plastid gene sequence for *atpH* (above) compared to the codon optimized *atpH* sequence designed for recombinant *E. coli* expression (below). The two sequences are 72.4% identical. Alignment performed by ExPASy SIM Alignment Tool.

coding fragments, phosphates were added to the 5' end of all individual oligonucleotides (minus the two 5' terminus oligonucleotides) in 10 µL reactions by mixing 100 pmol of each oligonucleotide with 1 mM ATP, 1X T4 Polynucleotide Kinase Buffer A (Appendix A), and 0.1 units T4 Polynucleotide Kinase (Fermentas, EK0031). This kinase reaction was incubated for 30 minutes at 37°C, followed by a 5 minute inactivation period at 70°C. A 5 µL volume of each oligonucleotide in this solution was mixed with 5 µL of its corresponding annealing partner, heated to 80°C, and cooled to 20°C over a 60 minute period in order to produce 7 annealed duplex DNA fragments.

Oligo 1: 29-mer
5’ – ATGAACCCGCTGATCGCGGCTGCGTCTGT

Oligo 2: 18-mer
3’ – TACTTGGGCGACTAGCGC

Oligo 3: 42-mer
TATCGCGGCGGGTCTGGCGGTTGGTCTGGCGTCTATCGGTCC

Oligo 4: 41-mer
CGACGCAGACAATAGCGCCGCCCAGACCGCCAACCAGACCG

Oligo 5: 43-mer
GGGTGTTGGTCAGGGTACCGCGGCTGGTCAGGCGGTTGAAGGT

Oligo 6: 43-mer
CAGATAGCCAGGCCCACAACCAGTCCCATGGCGCCGACCAGTC

Oligo 7: 44-mer
ATCGCGCGTCAGCCGGAAGCGGAAGGTAAGATCCGTGGTACTCT

Oligo 8: 46-mer
CGCCAACTTCCATAGCGCGCAGTCGGCCTTCGCCTTCCATTCTAGG

Oligo 9: 37-mer
GCTGCTGTCTCTGGCGTTCATGGAAGCGCTGACCATC

Oligo 10: 37-mer
CACCATGAGACGACGACAGAGACCGCAAGTACCTTCG

Oligo 11: 40-mer
TACGGTCTGGTTGTTGCGCTGGCGCTGCTGTTCGCGAACC

Oligo 12: 39-mer
CGACTGGTAGATGCCAGACCAACAACGCGACCGCGACGA

Oligo 13: 20-mer
CGTTCGTTTAGCTCGAGAAA – 3’

Oligo 14: 31-mer
CAAGCGCTTGGGCAAGCAAATCGAGCTCTTT – 5’

Figure 10. The nucleotide sequences and sizes of the 14 synthesized oligonucleotides from which *atpH* was synthesized. Oligos 1 and 14 shown here are designed so that the complete ligated gene can be inserted into the pMAL-c2x vector at the XnmI and XhoI restriction sites.

The annealed duplex fragments were ligated together in sequence to form the complete *atpH* gene in a two-step ligation process. First, 1.5 µL of four proximal duplexes from the previous annealing reaction were mixed with DNA Ligase Reaction Buffer (Appendix A) at 1X concentration in a 20 µL volume. The same reaction was prepared for the other three proximal duplex DNA fragments, and both reaction mixtures were heated to 50°C then cooled to 20°C over a 60 minute period, followed by an additional 2 hour incubation period at room temperature with 0.5 units of T4 DNA Ligase (Invitrogen, 15224-017) in each reaction. The resulting ligated fragments were separated on a 3% agarose gel (Section 4.4.1). Successfully ligated DNA was excised from the gel and purified using the Promega Wizard SV Gel and PCR Clean-Up Kit (Promega, A9281) according to product instructions (Appendix B). The two purified fragments were mixed together in equimolar amounts with 1X Ligase Buffer in a 10 uL volume. The reaction was heated to 50°C and cooled to 20°C over a 60 minute period, followed by the 2 hour incubation period at room temperature with 0.5 units of T4 DNA Ligase. The resulting DNA was again separated on a 3% agarose gel (Figure 18), and the ligated *atpH* fragment was excised from the gel, and purified in the same way as described in the previous step. The process of annealing and ligating these oligonucleotides to form the complete gene is outlined schematically in Figure 11.

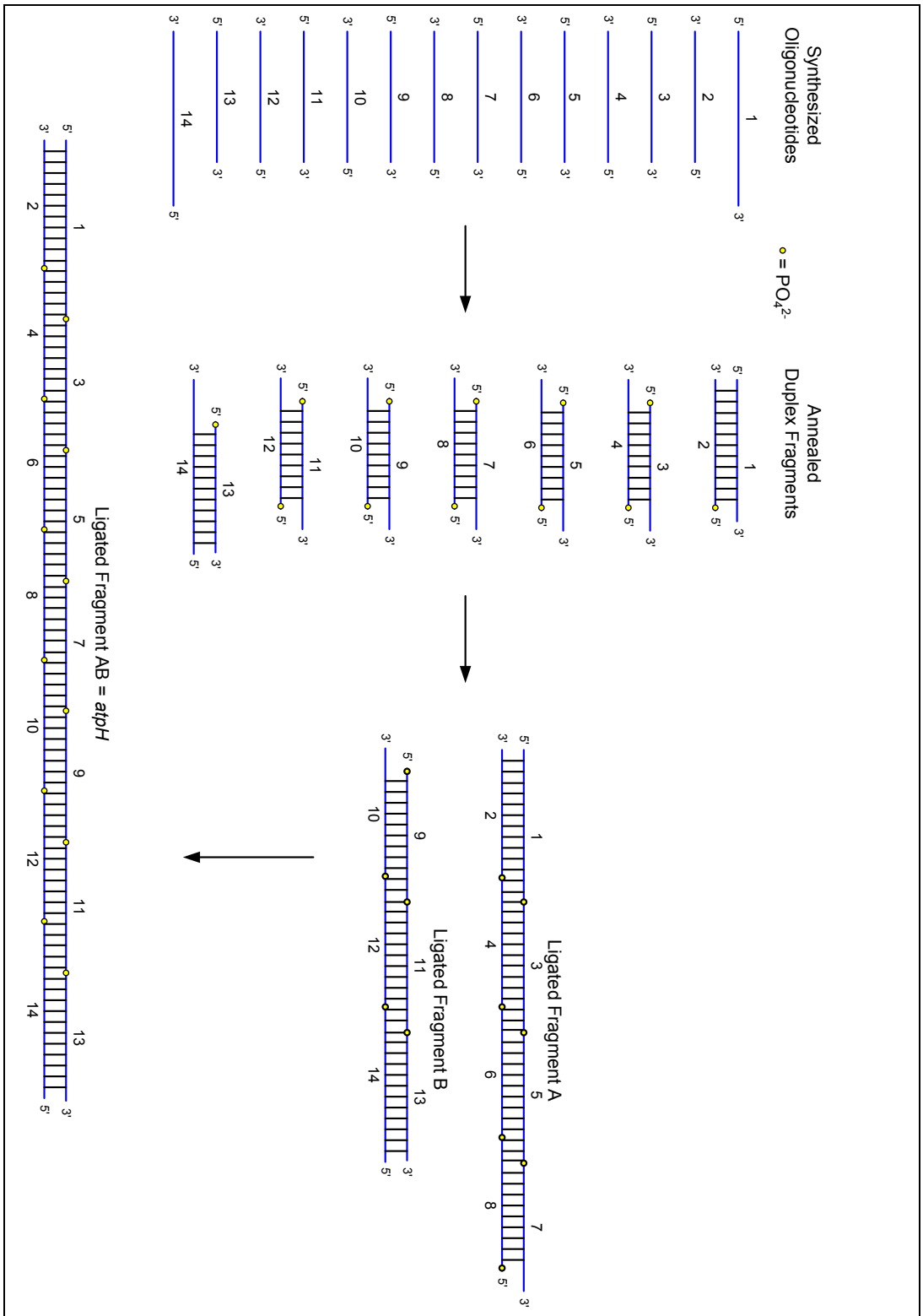

Figure 11. A schematic outline of the process of synthesizing *atpH* from 14 oligonucleotide fragments.

4.1.3. Plasmid vectors tested

A multitude of plasmid vectors are available commercially, each with distinct features designed to alter the mode of expression of an inserted target gene. The DNA sequences of most plasmids are engineered with some general elements. Most vectors contain a gene which confers antibiotic resistance to the host, providing a convenient positive selection marker when transformed cells are grown in the presence of that antibiotic. All vectors used in this work include the gene *bla* for β-lactamase, which provides resistance to the penicillin family of antibiotics such as ampicillin and carbenicillin. Plasmid vectors also contain a promoter sequence, recognized by a corresponding RNA polymerase. Immediately following the promoter is an operator sequence, with a ribosome binding site downstream. The vectors used in this work all contained *lac* operators, which activate transcription in the presence of allolactose, or its homolog isopropyl β-D-1-thiogalactopyranoside (IPTG). The ribosome binding site (Shine-Delgarno sequence) used in these vectors is a consensus A-G-G-A nucleotide sequence specific for the *lac* operator, located 8-9 bp before the first start codon that follows the promoter. A little further downstream are the multiple cloning sites (MCS), which are a series of common restriction endonuclease sites intended for the insertion of the desired gene. Some plasmids will have sequences for fusion tags placed somewhere in the middle of the MCS for the optional purpose of attaching a carrier such as 6X-Histidine to the N or C-terminus of the expressed protein, depending on exactly where the gene is inserted. And of

course, beyond the MCS is a transcription terminator sequence that corresponds with the upstream promoter. For the expression of *atpH*, three different plasmids were tested.

First tested was the Novagen plasmid pET-32a(+) (Novagen, 69015-3), which is a fairly standard 5900 bp plasmid. Versions -32b(+) and -32c(+) are also available, which have a 1 bp and 2 bp frameshift in the MCS, which can be useful for gene inserts that would otherwise be out of the reading frame. It uses a T7 promoter which has become common in *E. coli* recombinant expression for several reasons. The origin of this promoter and the corresponding T7 RNA polymerase is the T7 bacteriophage. *E. coli* cells designated as λ(DE3) are normally used for *E. coli* cell expression and are lysogenic (phage carrying) for this polymerase [47]. Because T7 polymerase is not native to *E. coli* and highly specific for the T7 promoter, no basal-level expression of genes under control of this promoter should occur. Furthermore, the T7 RNA polymerase transcribes at a rate approximately 5-times faster than native *E. coli* polymerases [48], and this is what makes the difference between 'expression' and 'over-expression' of recombinant proteins. In other words, an abundant amount of the product expressed under control of T7 is usually expected compared to other native proteins that are inherently expressed in *E. coli*. This can be distinctly observed by analysis of a total cell lysate run on a stained polyacrylamide gel. Plasmid pET-32a(+) also codes for several fusion tags, however none were used with *atpH* as it was intended to be expressed as a stand-alone protein in this vector.

The vector pFLAG-MAC is manufactured by Sigma-Aldrich (E8033). It is a 5071 bp plasmid designed for expression of the target protein with an N-terminus FLAG fusion tag. FLAG is a small tag with sequence of seven amino acids (MDYKDDK), amounting to a total molecular weight of 0.914 kDa. In this vector, the FLAG-tag is cleavable with enterokinase. It can be purified using a corresponding commercial affinity agarose media, and it can be detected with a corresponding commercial antibody. In this vector the P*tacI* promoter is included. P*tacI* is a hybrid promoter constructed in part from the sequence of the *trp* promoter and in part from *lac* UV5 promoter, both of which originate from *E. coli* (although the latter is a mutation of *lac*). Transcription with P*tacI* occurs more efficiently than with either of its constituent promoters – approximately 3 times more efficiently than with *trp*, and 11 times more so than with *lac* UV5 [49]. And so as with T7, the end result is 'over-expression' of the gene that follows. The gene *atpH* was inserted so that the FLAG sequence would be expressed on the N-terminus of the c-subunit. The purpose of this design was to test the possibility that stand-alone expression of c_1 is inhibited by the mRNA sequence secondary structure near the ribosome binding site [26].

The plasmid pMAL-c2x was once produced by New England Biolabs (N8076), and has since been replaced by newer versions, the most current of which is pMAL-c5x (New England Biolabs, N8108S) . The 6646 bp version of this plasmid used was obtained from the Chen Lab at Arizona State University, where

it was previously modified with a 6X-Histidine tag downstream from the MCS (although this modification was not relevant to any work done with this plasmid). Like the pFLAG-MAC vector, pMAL-c2x uses a P*tacI* promoter. As discussed, P*tacI* is transcriptionally inducible at a highly efficient rate with IPTG [49]. Because it is recognized by native *E. coli* RNA polymerase rather than a foreign phage RNA polymerase like T7, there is no requirement nor disadvantage to using λ(DE3) *E. coli* cells for transformation and expression. The most notable feature of pMAL-c2x is the sequence coding for the maltose binding protein (MBP) fusion tag. MBP is a highly soluble periplasmic *E. coli* protein [50]. When fused in tandem to less soluble proteins, it has proven to be quite capable at conferring soluble and stable expression, where inclusion bodies, aggregation, or degradation would otherwise result [51, 52]. As it is expressed in pMAL-c2x, it is a 42 kDa protein capable of complete cleavage with Factor Xa protease. Two versions of this plasmid were created with *atpH*: one designed to express c_1 N-terminally fused to MBP, and one designed to express c_1 alone. A plasmid map for pMAL-c2x is shown in Figure 12, with the relative locations of these various features illustrated including the restriction sites used to generate the two *atpH* versions of the plasmid.

It is known that various factors can influence the expression of a protein [53]. Such factors include the rate at which a gene is transcribed under control of a given promoter, as well as the placement of different fusion tags. This insertion

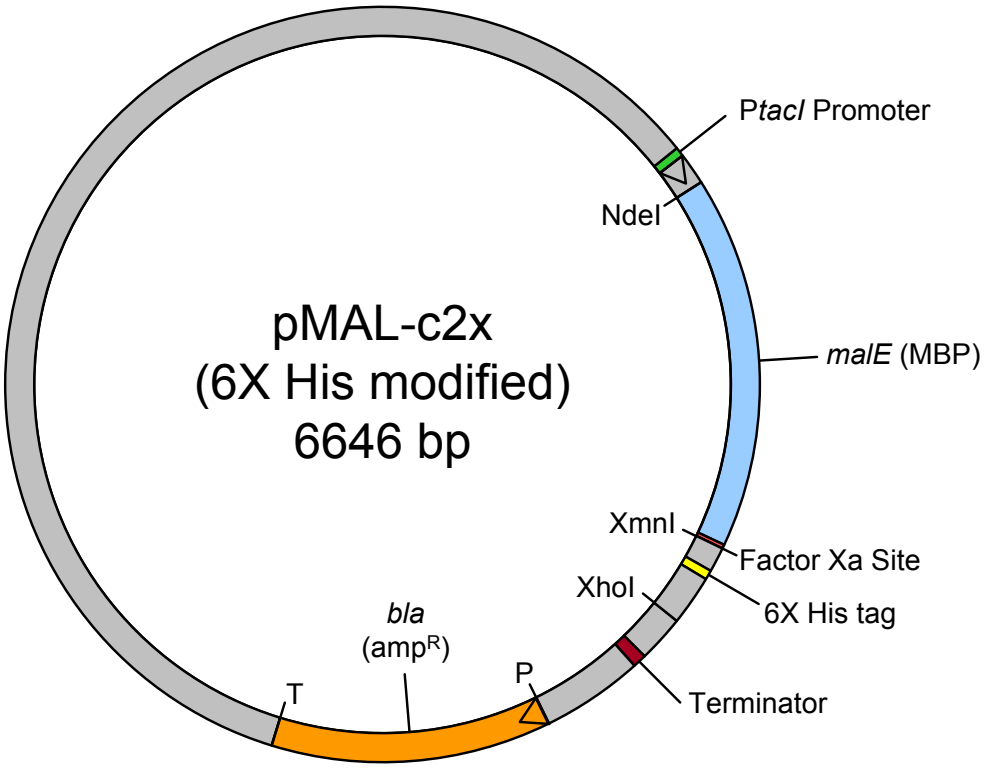

Figure 12. The plasmid map of vector pMAL-c2x. Features are shown with relative locations, including the promoter, the maltose binding protein gene (*malE*), the Factor Xa recognition site gene, the 6X His tag (not used), the ampicillin resistance gene (*bla*), and the restriction endonuclease sites used (NdeI, XmnI, and XhoI). As indicated, the *bla* gene uses its own promoter and terminator.

Plasmid	Promoter	Fusion tag	Product
pET-32a(+)-atpH	T7	--	c_1
pFLAG-atpH	P*tacI*	FLAG	FLAG-c_1
pMAL-c2x-atpH	P*tacI*	--	c_1
pMAL-c2x-malE/atpH	P*tacI*	MBP	MBP-c_1

Table 2. A comparison of the expression vectors produced for testing different expression modes of *atpH*.

of *atpH* into these assorted plasmids enabled the comparison of stand-alone c_1 expression under two different promoters (T7 and P*tacI*). And it also enabled a comparison of the expression of c_1 with two different N-terminal fusion tags (FLAG and MBP). This is summarized in Table 2.

4.1.4. Cloning of atpH into various vectors

The synthetic *atpH* gene was inserted into the described vectors pMAL-c2x, pET-32a(+), and pFLAG-MAC for the purpose of comparing alternate modes of c-subunit expression. Prior to inserting into each vector, the freshly ligated synthetic *atpH* gene was amplified by using high-fidelity PCR with the Phusion Polymerase (New England Biolabs F-530S), according to product instructions (Appendix C). The thermocycler profile used is shown in Figure 13, with temperature and time periods illustrated.

A synthetic *atpH* gene was produced with a 5' blunt end and 3' XhoI restriction site for insertion into the pMAL-c2x vector at the XmnI and XhoI restriction sites to produce the plasmid pMAL-c2x-*malE/atpH*. Similarly, an *atpH* gene was produced with 5' NdeI and 3' XhoI terminal restriction sites, and inserted into the pMAL-c2x vector at the corresponding sites to create pMAL-c2x-*atpH*. The same *atpH* insert was also inserted into the pET-32a(+) vector at the NdeI and XhoI restriction sites to create pET-32a(+)-*atpH*. And, an *atpH* gene was produced with 5' HindIII and 3' XhoI terminal restriction sites and inserted into

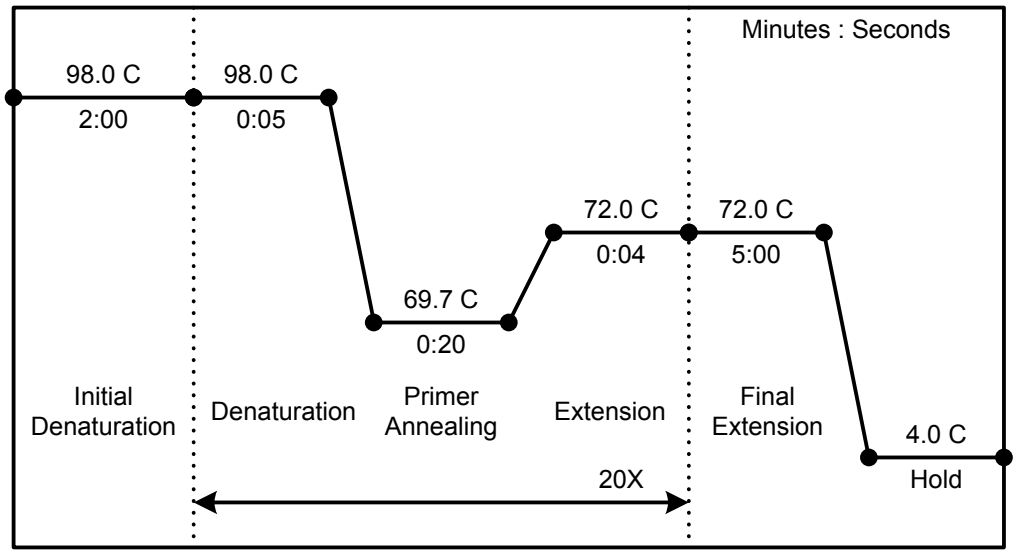

Figure 13. The thermocycle profile used for amplification of the synthesized *atpH* gene prior to insertion into plasmid DNA.

the pFLAG-MAC vector at the corresponding sites to create vector pFLAG-*atpH*. Figure 14 shows a visual representation of the design of these four vectors. Following ligation, each new vector construct was cloned by transforming DH10B *E. coli* cells (Invitrogen, 12033-015) via electroporation at 1660 V [54], according to product instructions (Appendix D). A Qiagen QIAprep Miniprep kit (Qiagen, 27104) was used according to product instructions (Appendix E) to lyse DH10B cells and harvest high concentrations of plasmid DNA from viable transformant growth cultures. The plasmid DNA was then digested by treatment with a restriction endonuclease that corresponds to known sites on the plasmid that would distinguish the presence or absence of the *atpH* gene (Figure 19). Restriction endonuclease digestion was usually carried out at 37°C for 2 hours with 2 units of the endonuclease and approximately 800 ng of plasmid DNA, in a

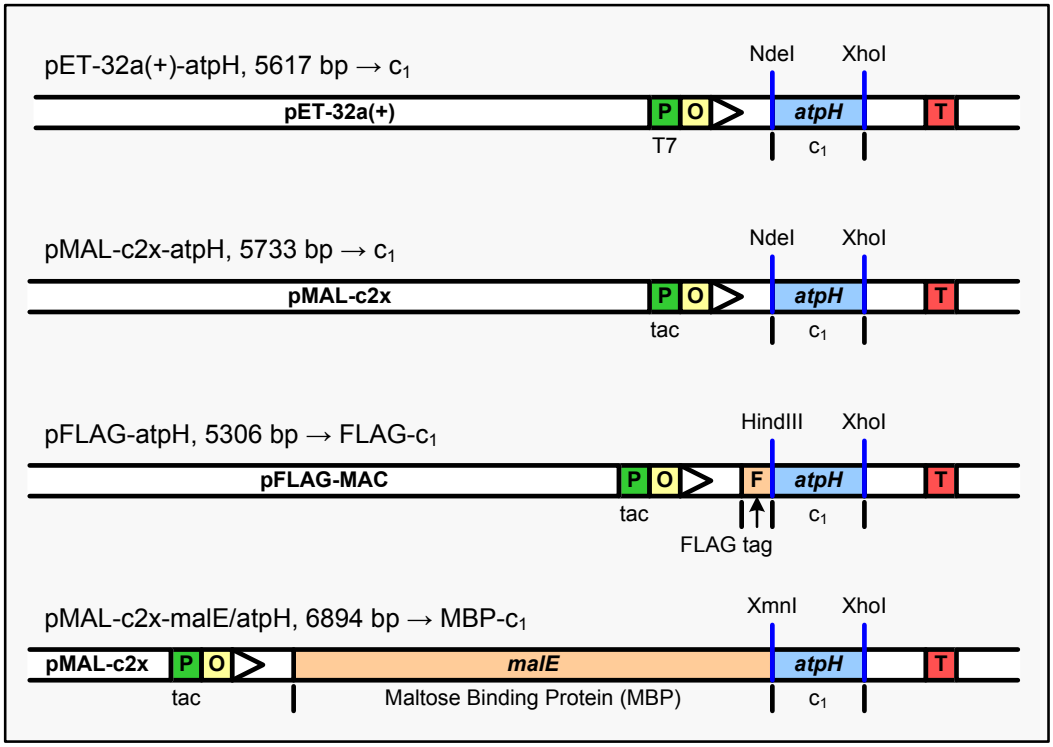

Figure 14. Genetic design of the four different expression vectors, showing the placement of *atpH* relative to promoters, operators, fusion tags, and terminators.

10 µL reaction, which also contained the corresponding endonuclease buffer. Further confirmation of successful *atpH* gene insertion into a given plasmid was provided by nucleotide sequencing, with oligonucleotide primers specific for *atpH*, or universal M13 primers specific for the regions between the promoter and terminator. This technique also confirms that all expected nucleotides are present in the gene, without insertions, deletions, or mutations. Nucleotide sequencing services were provided by the Core DNA Laboratory at Arizona State University, where automated methods are used with an Applied Biosystems 3730 capillary sequencer. Restriction endonucleases were obtained from New England Biolabs,

and were used according to product instructions. Product instructions were followed for restriction endonuclease reactions, shown in Appendix F.

BL21 derivative *E. coli* cells (T7 Express *lysY*/I^q, New England Biolabs, C3013H) were separately transformed with each vector construct. Cells were also transformed with pMAL-c2x (no *atpH*) for use as a negative control for *atpH* expression; and co-transformed with the pMAL-c2x-*malE/atpH* and pOFXT7KJE3 vectors, where the latter expresses the chaperone proteins DnaK, DnaJ, and GrpE. The co-expression of these chaperone proteins has been shown to substantially increase quantities of recombinant proteins which are toxic or otherwise difficult to produce [55]. The pOFXT7KJE3 plasmid was produced and generously provided by Castanié, et al [56]. The accompanying protocol (Appendix G) for transformation of T7 Express lysY/I^q cells was followed precisely, except with the co-transformation where 118 ng of pMAL-c2x-*malE/atpH* and 75 ng of pOFXT7KJE3 plasmid was used. Successful transformant clones were selected for on LB-agar plates with 50 µg/mL ampicillin. For the co-transformants, double antibiotic plates that also included 50 µg/mL spectinomycin were used.

4.1.5. atpH expression with different vectors

The expression levels of ATP synthase c-subunit were compared in the *E. coli* transformed with pMAL-c2x-*malE/atpH*, pMAL-c2x-*atpH*, pET-32a(+)-*atpH*, pFLAG-*atpH*, pMAL-c2x negative control, and pMAL-c2x-*malE/atpH* +

pOFXT7KJE3. 100 mL of LB-Lennox glucose expression medium (1.0% tryptone, 0.5% yeast extract, 0.4% glucose, 0.5% NaCl, 50 μg/mL ampicillin, and 50 μg/mL spectinomycin for the co-transformant) was inoculated separately with each transformant, and grown to an optical density of 0.6-0.7 at 37°C incubation and 200 RPM 1" orbital shaking. At this point, targeted expression of *atpH* as c_1, FLAG-c_1, or MBP-c_1 was induced by adding isopropyl β-D-1-thiogalactopyranoside (IPTG) to 1.0 mM concentration and incubating for an additional 30 minutes. Cell pellets were prepared by centrifugation at 6029 x g RCF for 20 minutes, and stored at -80°C. Thawed cell pellets were resuspended in 2 mL of Lysis Buffer (20 mM Tris-HCl pH 8.0, 1 mM EDTA, 2% v/v Protease Inhibitor Cocktail (Sigma, P8465). Lysozyme was added to each resuspension to 1 mg/mL, and they were incubated at 4°C for 1.5 hours prior to sonication at 50-75 W. Sonication was carried out using a micro-tip sonicator in 30 shock increments repeated three times, with 1 minute of cooling between. The micro-tip used was 5/32" diameter, stepped composed of titanium (Biologics, 0-120-0005).

A 12% polyacrylamide denaturing gel (Section 4.4.2) was prepared with 0.25 μL samples of total cell lysate from each transformant, along with 0.4 μg native spinach ATP synthase as a positive control for c-subunit, and 8 μL of Bio-Rad Western C standard. The gel was used for immunoblotting (Section 4.4.4) to confirm expression of c_1. It was determined that c_1 could only be expressed when fused to MBP by the vector pMAL-c2x-*malE/atpH* (see Section 5.1.3 and Figure 20), so this construct was chosen for further experimental application.

4.1.6. Reverse Transcriptase PCR

The lack of c_1 subunit production with vectors pET-32a(+)-atpH, pMAL-c2x-atpH, and pFLAG-atpH was investigated by using reverse transcriptase PCR methods to evaluate the mRNA produced by the respective clones during induced transcription. BL21(DE3) strain *E. coli* cells were transformed with these three vectors, as well as the MBP-c_1 expressing pMAL-c2x-malE/atpH, and vector pMAL-c2x with no gene insert for use as a negative control. A pMAL-c2x-malE/atpH + pOFXT7KJE3 co-transformant was also included in the experiment for comparison of *malE/atpH* transcription with the chaperones present. LB-Lennox medium (without glucose) cultures of 50 mL volumes were inoculated separately with clones of each transformant. Each culture was grown at 37°C and 200 RPM orbital shaking to an A_{600} optical density (O.D.) of about 0.6, at which point the cultures were induced to express *atpH* by adding IPTG to a final concentration of 1 mM. Induced growth proceeded for 30 minutes, and the A_{600} O.D. was measured for each culture (see Table 3).

Earlier experiments were performed to correlate cell count to optical density. Certain diluted volumes of *E. coli* culture with a known O.D. were plated, and the resulting colonies were counted. From the results, it was estimated that an O.D. value of 1.0 correlates to a concentration of 2.4×10^9 cells per mL of culture. From this estimation and the determined O.D. values of the individual cultures, a normalized volume containing an estimated 0.75×10^9 cells was measured from

Cloned Transformant	Induction A_{600}	Harvest A_{600}	Volume (µL)	[RNA] (ng/µL)	A_{260} : A_{280}
pMAL-c2x (control–)	0.60	0.91	347	38	2.30
pET-32a(+)-atpH	0.66	0.95	331	39	2.20
pMAL-c2x-atpH	0.63	0.95	334	44	2.22
pFLAG-atpH	0.66	0.96	330	38	2.20
pMAL-c2x-malE/atpH	0.63	0.95	334	37	2.11
pMAL-c2x-malE/atpH + pOFXT7KJE3	0.61	0.87	362	32	2.26

Table 3. Measurements taken during the Reverse Transcriptase PCR procedure.

each culture and centrifuged at 14,100 x g RCF for 75 seconds (see Table 3). The supernatant liquid was removed and the cell pellets were resuspended in 350 µL of sterile H_2O. The centrifugation was repeated, supernatant removed again, and the final separated cell pellets were used for RNA extraction.

A commercial kit was used for the purpose of extracting the total RNA from the cell pellets. The RiboPure-Bacteria kit produced by Ambion (AM1925) was used, and the included instructions were followed precisely, including the optional DNaseI step (Appendix F). The concentration and ratio of A_{260}/A_{280} for the purified RNA was measured for each resulting sample. The A_{260}/A_{280} ratios were found to be slightly above the recommended range of 1.8-2.1. (see Table 3), however the purity is sufficient for the application. This ratio provides some indication of how pure the extracted RNA is, relative to proteins and other contaminants that may absorb at 280 nm.

pET-32a(+) Reverse Transcriptase Primer

TTATTGCTCAGCGGTGGC

---

pMAL-c2x Reverse Transcriptase Primer

CCAAGCTGCCATTCGCCA

---

pFLAG Reverse Transcriptase Primer

ATTTAATCTGTATCAGGC

Forward *atpH* Polymerase Primer

ATGAACCCGCTGATCGCGGCTGCGTCTGT

Reverse *atpH* Polymerase Primer

CTAAACGAACGGGTTCGCGAAC

Figure 15. Primers used for the reverse transcriptase PCR procedure. All primers are shown in the conventional 5' to 3' orientation.

The extracted RNA was used in reverse transcriptase reactions prepared for the synthesis of cDNA from mRNA strands. In each reaction, 600 ng of RNA was mixed with 2 ng of primer for the corresponding vector used in each transformant, and compensated with a sufficient amount of sterile H_2O to bring the volume to 22.0 μL. The primer sequences are shown in Figure 15, and are specific for the 3' terminal end of an mRNA transcript corresponding to the terminator region of the

plasmid. The samples were heated to an annealing temperature of 70°C for 5 minutes, followed by 2 minutes of cooling on ice. Then further reagents were added to each reaction, including 4.0 µL of 0.1 M DTT, 5.0 µL of 10 mM dNTPs, 1.0 µL of SUPERase-IN RNase Inhibitor (Ambion, AM2694), and 8.0 µL of Thermoscript Reverse Transcriptase 5X Buffer (Appendix A). The sample volumes were then heated to 48°C for 2 minutes, at which point 0.5 µL of Thermoscript reverse transcriptase (Invitrogen, 12236-014) was added to each reaction, and incubation continued for 60 minutes at 48°C.

Individual polymerase chain reactions (PCR) were prepared using the cDNA produced by the reverse transcriptase. Each reaction included 4.0 µL of 10 mM dNTPs, 10.0 µL of 5X Phusion High Fidelity Polymerase Buffer (Appendix A) 0.5 µg of *atpH* forward primer, 0.5 µg of *atpH* reverse primer, 1 unit of Phusion High-Fidelity DNA Polymerase (New England Biolabs, F-530S), 1.5 µL of a given cDNA product, and 33.0 µL of sterile H_2O to bring the total volume to 50.0 µL. The *atpH* forward and reverse primer sequences are shown in Figure 15. The thermocycle profile included a 98.0°C denaturation, a 61.7°C annealing, and a 72.0°C extension temperature. The profile is shown with the corresponding time steps in Figure 16. The final sample was stored at 4°C. A schematic representation of the steps involved in reverse transcriptase PCR is shown in Figure 17.

The resulting reverse transcriptase PCR products were analyzed by electrophoresis using a 3% agarose gel (Section 4.4.1). 10 µL of each PCR product was mixed with 2 µL of 6X DNA loading buffer (5 mM xylene cyanol FF, 4 mM bromophenol blue, 30% glycerol). 10 µL of a 100 bp standard was also used. The gel was run at 75 V to completion, and stained by equilibration in 1 µg/mL Ethidium Bromide for 15 minutes. DNA fragments could then be visualized as bands absorbing UV light (Figure 21).

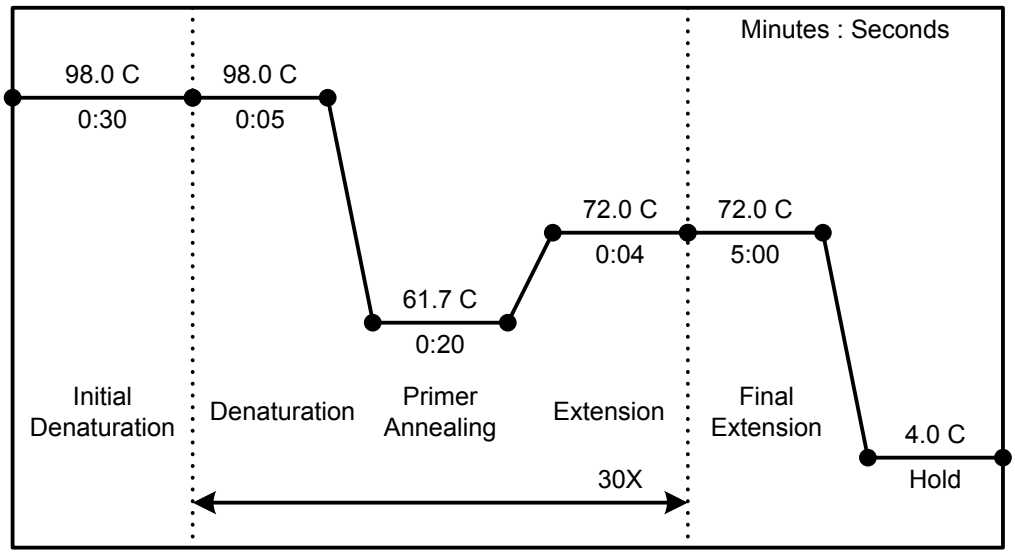

Figure 16. Thermocycle profile used for amplification of cDNA in the reverse transcriptase PCR procedure.

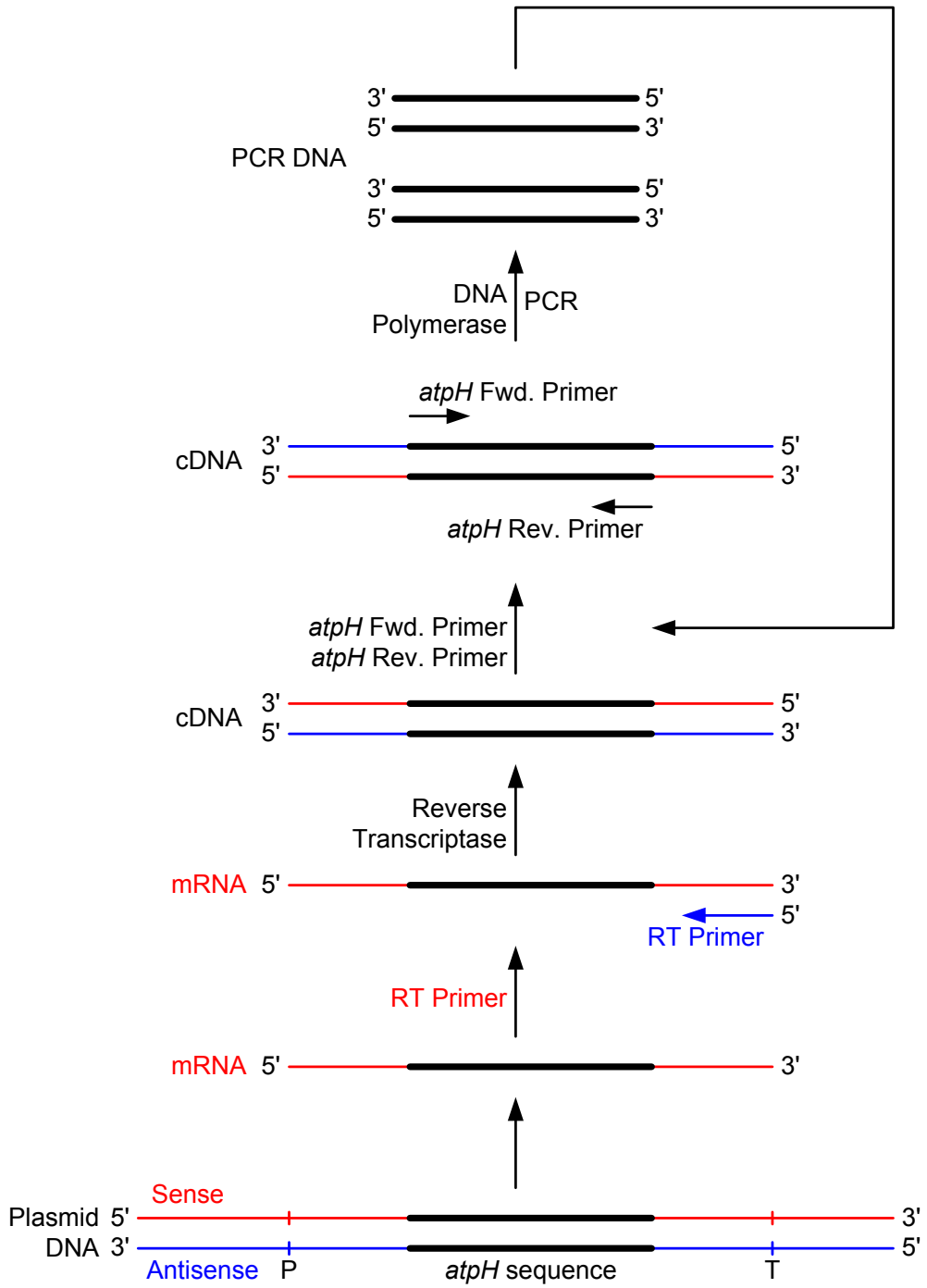

Figure 17. A schematic overview of reverse transcriptase (RT) PCR. mRNA transcribed from plasmid DNA between the promoter (P) and terminator (T) region is reverse transcribed to make cDNA of the transcript, and the *atpH* gene is amplified via PCR if it is present. RT Primers are reverse compliments of the nucleotide sequences preceding the terminator regions of corresponding plasmids.

4.1.7. Large scale expression and purification of MBP-c_1

For preparative purposes, a 1-2 L volume of cells co-transformed with pMAL-c2x-*malE/atpH* + pOFXT7KJE3 was usually cultured for the extraction of MBP-c_1. LB-Lennox culture media with glucose was used (1.0% tryptone, 0.5% yeast extract, 0.4% glucose, 0.5% NaCl, 50 μg/mL ampicillin, and 50 μg/mL spectinomycin for the pOFXT7KJE3 co-transformant). Glucose is included in the media to repress production of a native amylase in the cells that will otherwise inhibit the binding of MBP to amylose resin in the first purification step. Starter cultures were typically prepared by adding one transformant bacterial colony to 5-10 mL of the LB-Lennox culture media, and incubating at 37°C and 200 RPM 1" orbital shaking for about 16 hours. 1 mL of the starter cultures was then used to inoculate 1 L of LB-Lennox glucose growth media. Large scale cultures were usually divided into 500-750 mL of culture per 2000 mL Pyrex baffled flask (Sigma, CLS44442L). Typically after 275 minutes of continued incubation at 37°C and 200 RPM shaking, the A_{600} O.D. would reach a value of about 0.6-0.7. At this point, targeted expression of *malE/atpH* as MBP-c_1 was induced by adding IPTG to 1.0 mM concentration and incubating for an additional 2 hours. For each 1 L of culture, 3.1 g of bacterial cell pellet was routinely collected by centrifugation at 6029 x g RCF for 20 minutes. The bacterial cell pellet can be stored long term at -80°C, and used for extraction of MBP-c_1 when needed.

4.2. Protein Purification

Like the protein expression steps, the methods for protein purification also relied on comparative studies and process development. The following subsections discuss the use and reasoning behind the methods that were selected, tested, and developed for the purification steps.

4.2.1. Purification of MBP-c_1

Frozen cell pellet collected from large scale culture of *E. coli* co-transformed with the plasmids pMAL-c2x-malE/atpH and pOFXT7KJE3 was used for extraction and purification of the expressed target protein MBP-c_1. Typically, 3-4 g of the cell pellet was thawed, and resuspended in 50 mL of Lysis Buffer (20 mM Tris-HCl pH 8.0, 1 mM EDTA, 2 mM 2-mercaptoethanol, 2% v/v Protease Inhibitor Cocktail (Sigma, P8465)). Lysozyme was added to the resuspension at 1 mg/mL final concentration, and incubation proceeded at 4°C for 1-2 hours to hydrolyze bacterial cell walls. Cell lysis was completed by using a tip sonicator to sonicate the viscous resuspension at 150 W in intervals with cooling on ice in between, until it was no longer viscous (typically, 30 shocks repeated three times with 1 minute of cooling between). A titanium 3/8" tip was used with the sonicator (Biologics, 0-120-0009). The cell lysate was then centrifuged for 30 minutes at 18,677 x g RCF, and the resulting supernatant was separated from the pellet. The cell lysate supernatant was diluted to a 100 mL volume in Amylose Column Buffer 1 (20 mM Tris-HCl pH 8.0, 0.2 M NaCl, 1 mM EDTA) and passed through 7.5 mL of amylose resin (New England Biolabs, E8021L) on a 25 mm

diameter gravity column to bind the MBP-c_1 fusion protein. The flow rate was maintained at ~1 mL/min during this step. The resin was then washed of non-binding cell lysate proteins by passing through 420 mL of Amylose Column Buffer 2 (20 mM Tris-HCl pH 8.0, 0.2 M NaCl). Finally, MBP-c_1 was eluted with 50 mL Maltose Elution Buffer (20 mM Tris-HCl pH 8.0, 0.2 M NaCl, 10 mM maltose). The eluted fraction was typically concentrated ~10X to 5 mL using a Vivaspin 20 30K MWCO centrifugal concentrator with a polyethersulfone (PES) membrane (Sartorius, VS2022). Concentration was typically carried out in a series of 15 minute centrifugation steps at 3500 x g RCF. From a 3 g cell pellet, the typical yield of MBP-c_1 after amylose column purification and concentration was about 10-12 mg, according modified Lowry assay determinations (Section 4.4.6).

Samples were taken from each of the following fractions for analysis on a coomassie blue stained 12% polyacrylamide gel (Sections 4.4.2, 4.4.3): total cell lysate (3 μL), cell lysate pellet (3 μL), cell lysate supernatant (6 μL), amylose column flow through (6 μL), Amylose Column Buffer 2 wash (9 μL), and Maltose Elution Buffer wash (9 μL). Also included was 10 μL of the Bio-Rad standard. The resulting gel is shown in Figure 22.

4.2.2. Protease cleavage of c_1 from MBP

Optimal protease cleavage conditions were determined based on prior experimental comparisons using variations of temperature, incubation period, and

protease concentration. These factors are known to influence the activity of the protease Factor Xa, which preferably recognizes the sequence I-E/D-G-R and cleaves after the Arg residue [57]. The effect of detergent as a variable factor in protease cleavage was also tested because it is needed in order to prevent aggregation of the cleaved c_1 subunit product. Initial experiments were conducted with 0.01% w/v SDS, 20 mM Tris-HCl pH 8.0, and 2 mM $CaCl_2$ in the protease reaction buffer and a MBP-c_1 concentration of 550 µg/mL. Under these conditions, the concentration of Factor Xa as a variable was examined over a range of 0.3-1.82% w/w protease, incubated at room temperature for 48 hours. The incubation time period was tested over a range of 12-96 hours at room temperature, with 1.8% w/w Factor Xa protease. Temperature was examined by incubation for 48 hours with 1.0% w/w protease at 4°C, 13°C, 25°C, and 37°C. As these parameters were tested, it was observed that no variable appeared to increase the amount of cleaved c_1 product (Figure 23). And so the effect of the detergent was investigated as another variable in the reaction buffer, and this turned out to have the most significant effect on the protease cleavage reaction.

Protease Buffers were prepared with different detergents at a range of concentrations. Sodium dodecyl sulfate (SDS, 0.01%) for comparison, Na-cholate (0.01%, 0.1%, 1.0%), n-β-dodecyl-D-maltoside (βDDM, 0.001%, 0.01%, 0.1%), and β-octyl-D-glucopyranoside (βOG, 0.01%, 0.1%, 1.0%) were each added to 20 mM Tris-HCl pH 8.0, and 2 mM $CaCl_2$. 0.3 mL of MBP-c_1 (1 mg) was dialyzed against each of these Protease Buffers, and 1% w/w Factor Xa

Protease (1 mg/mL) was added. The protease reactions were incubated at 4°C for 24 hours. For analytical comparison, a 12% polyacrylamide gel was prepared for immunoblotting (Section 4.1.14) with 1.25 μL of each protease reaction product, 0.5 μg of native spinach ATP synthase as a positive control for c_1, and 8 μL of Bio-Rad Western C standard. The highest yield of c_1 product was achieved with βDDM in the Protease Buffer at 0.01% (1X critical micelle concentration (CMC)) and 0.10% (10X CMC), as discussed in Section 5.2.6 and Figure 25. The detergent concentration was further optimized to 0.05% (5X CMC) βDDM, which was used for all subsequent preparative purposes. The Factor Xa protease used in these experiments was acquired from New England Biolabs (P8010, 1 mg/mL).

In preparation for protease cleavage, the preparative MBP-c_1 fusion protein sample (~5 mL collected after purification on the amylose column and concentration (Section 4.1.7)) was dialyzed against 2 L of optimized Protease Buffer (20 mM Tris-HCl pH 8.0, 2 mM $CaCl_2$, 0.05% βDDM) for at least 12 hours at 4°C using 13K MWCO dialysis tubing. 13000 MWCO dialysis tubing was used (Sigma, D9777). 1% w/w Factor Xa Protease was then added to the dialyzed protein and the protease reaction was incubated at 4°C for about 24 hours with light stirring. The post-protease cleaved sample (MBP+c_1) was then immediately applied to the reversed phase column in the next step.

4.2.3. Reversed phase HPLC column purification of c_1

Typical reversed phase column (RPC) purification schemes include a gradient with two solvents of disparate polarities. In the case of c-subunit, the protein was bound to the column resin in the presence of a polar solvent (Eluent A), and eluted along a gradient of increasing non-polar solvent (Eluent B). Eluent A was typically pure water buffered to pH 8.0 with 20 mM Tris-HCl. Small scale trials were tested to compare the effects of different solvents as Eluent B, including methanol, ethanol, and 2-propanol. A test was also done with 0.02% βDDM added to Eluent A, used in conjunction with methanol as Eluent B. A RESOURCE RPC 3 mL column (GE Healthcare, 17-1182-01) was used for these analytical trials. In each trial, the column was equilibrated by washing with 1-2 column volumes of Eluent A, then Eluent B, then Eluent A again. About 1.7 mg of protease cleaved sample (MBP+c_1) was loaded onto the column following centrifugation to remove any precipitant. The column was run with 10 column volumes of Eluent A, followed by a gradient increasing to 100% Eluent B over a 100 minute period. The column continued to be washed with 100% Eluent B until protein no longer eluted from the column. A flow rate of 1 mL/min. was maintained. Immunoblot analysis (Section 4.4.4, Figures 26-28) was performed on fractions collected from each Eluent B trial, and those fractions which contained c_1 were further analyzed on silver stained 12% polyacrylamide gels (Sections 4.4.1, 4.4.3) to assess purity. Ethanol proved to be the most favorable Eluent B solvent tested in terms of both yield and purity (Section 5.2.7), and so this was used in subsequent larger scale preparative column runs.

A 15 mL SOURCE HR 16/10 reversed phase column manufactured by GE Healthcare (90-1002-15) was chosen for the large scale purification of c_1. This preparative column uses the same hydrophobic polystyrene/divinyl benzene bead media as the 3 mL analytical column. The Eluent A was 20 mM Tris-HCl pH 8.0 in water, and the Eluent B was 100% HPLC grade ethanol (Sigma). Both buffers were degassed thoroughly. The column was equilibrated with Eluent A, then Eluent B, then Eluent A again by washing with 1-2 column volumes of each. Immediately following the 24 hour Factor Xa protease cleavage incubation period, the ~5 mL sample of MBP+c_1 was filtered through a 0.45 µm mixed cellulose ester membrane (Millipore, SLHA033SB), and loaded onto the equilibrated reversed phase column. The amount of protein loaded was typically 15-20 mg, according to the modified Lowry assay technique (Section 4.4.6). Hydrophilic protein products were eluted with 10 column volumes of Eluent A. A gradient was produced increasing to 100% Eluent B over a 500 minute period, and washing continued with 100% Eluent B until a stable UV absorbance signal indicated that no more protein was eluting. A flow rate of 1 mL/min. was maintained throughout the process, and 10 mL fractions were collected.

To confirm the presence of c_1 in the fractions, a 12% polyacrylamide gel was prepared for immunoblotting (Section 4.4.4) with 12 µL of fractions E10, E11, E12, F1 and F2, 0.375 µL of MBP+c_1, 0.375 µL of MBP-c_1, 0.3 µg native spinach ATP synthase as a positive control for c_1, and 10 µL Bio-Rad Western C standard.

The immunoblot is shown in Figure 29B. To assess the purity of the c_1 containing fractions, a 12% polyacrylamide gel was prepared for silver staining (Section 4.4.3) with 1.25 mL (27 μg c_1) of combined fractions E11+E12, 2.5 μL (4.4 μg) of MBP+c_1, 2.5 μL (4.4 μg) of MBP-c_1, 8.25 μg native spinach ATP synthase as positive control, and 3.3 μL of Bio-Rad standard. The silver stained gel is shown in Figure 29C. The ethanol-containing RPC fractions were first evaporated, then resuspended in water and Sample Loading Buffer followed by heating at 95°C for 5 minutes prior to loading onto the polyacrylamide gels. N-terminus amino acid sequencing services were provided by the Core Proteomics and Protein Chemistry Lab at Arizona State University, where automated Edman degradation methods are used.

4.3. Reconstitution

The process of inducing monomeric c-subunits to assemble into a ring is dependent on having a properly folded and purified protein. The methods included in this section first examine the folded state of the c-subunit, then attempted to achieve ring formation by reconstituting the protein into a liposome. The reconstitution was performed in the absence, and in the presence of native pigments to test the hypothesis that pigments may have some influence in this process. Included also is the background and reasoning that influenced the choice of methods used.

4.3.1. Circular Dichroism spectroscopy

A Jasco J-710 Spectropolarimeter was used for measuring the circular dichroism (CD) spectrum of the purified recombinant c_1 subunit. The CD spectrum provides a good indication of what the secondary structure of the protein is. The purified c_1 sample was prepared for CD measurement as described for expression and purification, with the exception that a 10 mM phosphate buffer at pH 8.1 was used for Eluent A during the reversed phase column purification (Section 4.2.3). Under these conditions, c_1 eluted on the gradient at about 83% ethanol (Eluent B) and 17% Eluent A. A buffer of this composition was used for the blank reference measurement. The eluted c_1 was concentrated to approximately 0.1 mg/mL using a 5000 MWCO Vivaspin 2 concentrator with a Hydrosart membrane (Sartorius, VS02H11). The protein concentration was determined according to modified Lowry methods (Section 4.4.6). CD spectra were measured from 195-260 nm at room temperature (25°C) in a 0.1 cm quartz cuvette. Parameters were set at 0.2 nm data pitch, continuous scan mode, 50 nm/min scan speed, 4 second response, and 1 nm bandwidth. Output data was generated from an accumulation of 3 scans. Values of mean residue ellipticity ($[\theta]$) and molar CD ($\Delta\varepsilon$) were calculated as described by Greenfield [58]. The algorithm CDSSTR [59] was used with the CDPro [60] software program to estimate the secondary structure content of the sample by comparing the measured data with the data set SMP50, which contains 13 membrane proteins and 37 soluble proteins [61].

4.3.2. Reconstitution of c_n into liposomes

Self-assembly of an oligomeric c_n ring from the recombinantly expressed monomers was attempted by reconstitution into liposomes. This in vitro approach has been successfully developed for use with the native F_0 complex of *E. coli* [62], and later adapted for the bacterial F_0 complex of *P. modestum* and *I. tartaricus* where the c-subunit was expressed recombinantly in *E. coli* [33]. In these two reconstitution scenarios, the ring was reportedly formed in the F_0 complex in its native stoichiometry, and the resulting F_0 channel was functional. These reconstitution methods begin with a c-subunit (ring or monomer) isolated from the cell membrane of *E. coli* in organic solvent (chloroform : methanol, 2:1). In contrast, MBP-c_1 originates in the soluble fraction of the cell; but because c_1 is purified after cleavage from MBP in organic solvent (ethanol), it was hypothesized by the author that these reconstitution methods could also be effectively adapted for use with the recombinant chloroplast c-subunit.

The modified Lowry assay technique (Section 4.4.6) was used to estimate the concentration of recombinant c-subunit obtained following reversed phase column HPLC purification. In order to use this technique with the RPC eluted sample, the solvent was first evaporated. A volume containing 80 µg of recombinant c-subunit was mixed with 250 µL of 10% Na-cholate, and evaporated completely using a vacuum centrifuge. The evaporation produced a small solid pellet, which was re-dissolved in 70 µL of Resuspension Buffer (5 mM K_2HPO_4, 5 mM $MgCl_2$), followed by the addition of 180 µL of Sonication Buffer (10 mM Tris-

HCl pH 8.0, 50 mM NaCl, 10% glycerol, 1% Na-cholate). The sample was sealed in a glass test tube blanketed with N_2 gas, and sonicated at room temperature in a water bath sonicator for 20 minutes. Afterward, the sample was placed on ice for 1 hour.

Phospholipids were prepared from soybean phosphatidylcholine type II-S (Sigma, P5638). However, it is important to note that the purity of this particular phosphatidylcholine is specified as 14-23%, and therefore considered to be crude at best. Other phospholipids in this product include primarily phosphatidylethanolamine, and inositol phosphatides, according to product literature. 80 µg of this soybean phospholipid mixture was added to 1 mL of Phospholipid Buffer (15 mM Tricine pH 8.0, 7.5 mM DTT, 0.2 mM EDTA, 1.6% Na-cholate, 0.8% Na-deoxycholate) and mostly dissolved by vortexing for several minutes. The sample was placed on ice for 60 minutes to continue dissolving. Inside a glass test tube blanketed with N_2 gas, the dissolved phospholipids were bath sonicated in ice water for 5 minutes (using five intervals of 1 minute each with at least 1 minute of cooling in between). At this point, the phospholipid suspension was opalescent and homogeneous.

Of the prepared phospholipids, 250 µL was added to the resuspended c-subunit sample. This mixture became clear, indicating that all aggregates of phospholipids had dissociated completely. The sample was sealed in a glass vial under a N_2 gas blanket, and the 5 minute sonication period in the ice water bath

was repeated. The sample was dialyzed at 4°C in 500 mL of Dialysis Buffer (5 mM Bis-Tris Propane pH 7.4, 2.5 mM $MgCl_2$, 0.2 mM Na-EDTA pH 8.0, 0.2 mM DTT). In order to remove completely the detergent and induce maximal liposome formation, the dialysis buffer needed to be exchanged 3-4 times over a 48 hour period. This is because a 3500 MWCO dialysis cassette (Thermo Scientific, 66330) was used in order to avoid loss of the 8 kDa monomeric c-subunit. However, it should be noted that because the protein is solubilized in a βDDM detergent micelle which is 50 kDa, this step could be carried out more easily using a larger pore size.

Following dialysis, the appearance of the sample had progressed from clarity to turbity, indicating the formation of liposomes. The sample volume was then diluted with an equal volume of 5 mM Bis-Tris propane pH 7.4. Under a blanket of N_2 gas the sample was then sonicated in a bath sonicator with ice water five times, for 5 seconds with 30 seconds cooling in between. Then, the sample was flash frozen in liquid N_2, and remained so for 15 minutes. After thawing at room temperature, the sample was centrifuged at 4°C and 18,000 x g RCF for at least 60 minutes. The resulting proteoliposome pellet was separated from the supernatant, and resuspended in 100 µL of Proteoliposome Buffer (5 mM Bis-Tris propane pH 7.4, 1 mM $MgCl_2$). The ice water bath sonication step was repeated, and the samples were stored in liquid N_2 until further experimental evaluation.

For comparison to reconstituted native c_{14}-ring as a positive control, this reconstitution approach was used with a native c_{14} sample as well. Purification of native c_{14} from spinach chloroplasts was completed according to methods published by Varco-Merth, et al. [41]. A volume of purified native c_{14} containing 70 µg of protein was mixed with 250 µL of 10% Na-cholate, and evaporated in the vacuum centrifuge. During the final dialysis step, 13000 MWCO dialysis tubing (Sigma, D9777) was used and a 1 L dialysis only required about 16 hours, with one buffer exchange. Otherwise, all steps were followed in the same manner as used with the recombinant sample.

4.3.3. Reconstitution of c_n into liposomes with pigments

Because it has been observed that the native spinach chloroplast c_{14} ring co-purifies and co-crystallizes with pigments [41], it was hypothesized that inclusion of native pigments into the reconstitution of the recombinant protein may assist in the formation and/or stability of any resulting ring. Methods for the extraction of pigments from spinach leaves are well established [63]. For the purposes of this experiment, a crude extract containing a mixture of chlorophylls, carotenoids, and other supposed pigments was preferred over individually purified pigments because the effect of various pigments in a crude extract may also have an influence which is more likely to be of benefit than detriment.

To produce a pigment extract, 1 g of spinach leaves with ribs removed was cut into pieces, which were ground to liquid-paste with a mortar and pestle in 2 mL of

acetone. And additional 2 mL of acetone was used to rinse and added to the sample volume. The sample was centrifuged for 5 minutes at 3400 x g RCF and room temperature. A firm pellet was formed on the bottom, and to the supernatant 4 mL of hexane was added. The sample was thoroughly mixed, 2 mL of H_2O was added, and the centrifugation was repeated. The darker green hexane layer on top was separated from the solid pellet and acetone layer, and added to 1 mL of hexane. The centrifugation step was repeated once more, and the top layer was again separated and used as the crude pigment extract. An absorbance scan was run from 400 to 800 nm to confirm the presence of chlorophylls and carotenoids, and used for the calculated estimate of chlorophyll-a concentration. Chlorophyll-a concentration was determined using the published molar extinction coefficients (ε_M = 76790) in 80% acetone correlated to maximum absorbance at 664 nm, with background absorbance at 710 nm subtracted [64].

For reconstitution of the recombinant c-subunit, a volume of reversed phase column HPLC purified c-subunit containing 70 µg of the protein was mixed with 200 µL of 10% Na-cholate and evaporated in the vacuum centrifuge. To the evaporated sample, 21 µL of the native crude pigment extract was added, and the sample was evaporated again in the vacuum centrifuge. This volume of crude pigment extract was estimated to contain a 5:1 molar ratio of chlorophyll-a : c_{14}-ring. Beyond this addition of pigment extract, the remainder of the reconstitution steps was carried out in the same manner as the reconstitution without pigment (Section 3.2.2).

4.3.4. Mild dissolution of liposomes

In order to evaluate the oligomeric state of the reconstituted recombinant c_n-subunit using gel filtration chromatography or native gel electrophoresis, it is necessary to extract the reconstituted protein from the liposomes. This must be accomplished by dissolving the liposome under the mildest conditions possible while still preserving the intended oligomeric state of the protein, if it is indeed present. βDDM is a mild detergent used during prior and subsequent steps of the protein preparation and analysis, and so it was chosen for the purpose of liposome dissolution and tested on empty liposomes.

Empty liposomes were prepared using the same methods described for the reconstituted proteoliposomes with the c-subunit absented from the protocol. A 40 µL sample of the empty liposome was centrifuged at 18,000 x g RCF for 15 minutes, the supernatant was removed, and liposomal pellet was resuspended in 400 µL of 2% βDDM Dissolution Buffer (50 mM imidazole, 50 mM NaCl, 2 mM 6-aminohexanoic acid, 1 mM EDTA, 2% βDDM, pH 7.0). The sample was placed in a spectrophotometer at room temperature where the absorbance was measured at 20 time points over a 400 minute period. The sample was lightly mixed after each measurement. The results of this time scale measurement shown in Figure 32 were useful for providing some frame of reference for how much time would be needed to dissolve the c_n proteoliposomes, although it should be noted that proteoliposomes can in theory be more rigid than empty liposomes

4.3.5. Gel filtration analysis of proteoliposomes

Intact protein complexes can be separated according to total mass using gel filtration chromatography, which makes it a useful tool for distinguishing oligomeric states of proteins. For dissolution of the recombinant c_n and native c_{14} proteoliposomes, 75 µL of thawed proteoliposome same was added to 1.5 mL of Solubilization Buffer (50 mM imidazole, 50 mM NaCl, 2 mM 6-aminohexanoic acid, 1 mM EDTA, pH 7.0), and centrifuged at 18,000 x g RCF for 15 minutes. The supernatant was removed, and the proteoliposomal pellet was resuspended in 1.425 mL of 2% βDDM Dissolution Buffer. The samples were thus incubated at room temperature prior to loading onto the gel filtration column. The incubation time period for the recombinant sample reconstituted without pigments was 225 minutes, and 270 minutes for the corresponding native control sample. The incubation time was 240 minutes for the recombinant sample reconstituted with pigments, as well as the corresponding native control sample. Gel Filtration Buffer (10 mM HEPES pH 7.0, 50 mM NaCl, 0.02% βDDM) was eluted through the column at a flow rate of 0.4 mL/min. Fractions were collected according to peak separation. For the recombinant c_n and native c_{14} samples reconstituted in the absence of pigments, absorbance was measured at 280 nm and 215 nm. And for the recombinant c_n sample reconstituted in the presence of pigments and corresponding native c_{14} positive control sample, absorbance was measured at 280 nm, 665 nm, and 460 nm. Chlorophyll-a is detected at 665 nm, and carotenoids at the 460 nm wavelength absorbance.

For the pigment reconstituted sample and corresponding native control sample, an absorbance spectrum was measured from 200-800 nm to make a quantitative comparison of the pigments present in each sample. In order to get usable absorbance data from the pigments, the first peak fractions were combined and concentrated 6X using a Vivaspin 20 30K MWCO centrifugal concentrator with a polyethersulfone (PES) membrane (Sartorius, VS2022). Centrifugal concentration was carried out in 10 minute intervals at approximately 3500 x g RCF. The molar extinction coefficients (ε_M) for chlorophyll-a at 665 nm and β-carotene at 454 nm in 80% acetone are 76,790 $M^{-1}cm^{-1}$ [64] and 140,000 $M^{-1}cm^{-1}$ [65], respectively. Because these values are not published for the pigments in the 0.02% Gel Filtration Buffer, the known acetone values were used for a crude estimate of the molar ratio of chlorophyll-a to β-carotene, using Beer's Law.

4.3.6. Native immunoblot analysis of proteoliposomes

Like other c-rings [10, 20], the native chloroplast c_{14} ring is unusually stable in its oligomeric form, which may be further stabilized by lipids or cofactors. It has been shown to run on SDS polyacrylamide gel electrophoresis in an oligomeric state, unless heated above 60°C for several minutes [66]. However, because the c_n ring was reconstituted experimentally from recombinant monomers in vitro, it may not have the same stability as the native form. Therefore, native gel electrophoresis remains an important technique for evaluating the oligomeric state of the sample. Native gel electrophoresis is not as generally applicable as the SDS denaturing approach, and so native methods often require some experimental

development of specific conditions that are optimal for the protein of interest. Wittig, et al. published some very useful methods for high-resolution clear native electrophoresis (hrCNE) of membrane proteins [67], and these methods have been developed here for use with the c_{14} ring. As with the SDS PAGE methods used in this dissertation for the denatured gels [68], these native methods are based on the use of an anode and cathode tricine buffer system. The anode buffer is a simple 25 mM imidazole solution, buffered to pH 7.0. The cathode buffer contains 50 mM tricine, 7.5 mM imidazole, and 0.02% βDDM, with no adjustment needed to attain a near-neutral pH. The theoretical pI value for the c-subunit is 4.94, making it capable of following an electrical current toward the cathode under neutral conditions. The polyacrylamide gel was prepared with 4% acrylamide:bis 29:1 (Biorad, 161-0156**)**, 2% βDDM, 25% Native Gel Buffer (75 mM imidazole, 1.5 M 6-aminohexanoic acid, pH 7.0), with ammonium persulfate and TEMED added to polymerize. Due to the low percentage of the gel, no stacking portion was included.

Preparation of the proteoliposome samples (without pigment) for analysis with native electrophoresis involved adding 0.5 µL of the proteoliposome to 250 µL of Solubilization Buffer, centrifuging at 18,000 x g RCF for 15 minutes at 4°C, and removing the supernatant. The proteoliposome pellet was resuspended in 10 µL of 2% βDDM Dissolution Buffer and incubated at room temperature for 180 minutes. The 10 µL sample was added to 2 uL of Red Loading Buffer (50%

glycerol, 0.1% Ponceau S), prior to loading on the gel. For analysis of the sample after elution from the gel filtration column, 10 μL of the fraction from the first peak (~12.5 mL) was mixed with the 2 μL of Red Loading Buffer prior to loading. The same preparation conditions were used for the native c_{14} sample as well as the recombinant c_n sample.

For analysis of the pigment proteoliposome sample, a fraction of the sample that was loaded on the gel filtration column was used for the native gel, making the incubation period in 2% βDDM Dissolution Buffer closer to 240 minutes. A sample volume of 5 μL was used, which was added to 1 μL of the Red Loading Buffer prior to loading on the gel. After elution from the gel filtration column, the sample was prepared by adding 10 μL of the eluted peak fraction to 2 μL of the Red Loading Buffer prior to loading. Because the profile of the first peak has a shoulder (see Figure 34), two separate fractions of the peak were analyzed: a fraction which begins to elute at about 13 mL, and a fraction which begins to elute at about 14 mL. These preparation conditions were used for the native c_{14} sample as well as the recombinant c_n sample.

The gel electrophoresis was carried out at approximately 4°C, with pre-chilled anode and cathode buffers. Once samples were loaded, the gel was run at 100 V for about 30 minutes, followed by an increase to 300 V until completion. The gel was then prepared for transfer using the same immunoblotting technique that is used for SDS polyacrylamide gels (Section 4.4.4). Because the 4%

polyacrylamide native gel is more difficult to handle than a 12% polyacrylamide gel, it is useful to replace it on the surface of the glass plate after equilibrating in Tricine Transfer Buffer, and use the glass plate as a means of support while laying the gel onto the surface of the blotting filter paper. The transfer was carried out at 100 mA for 50 minutes. The results are shown in Figures 35, 36, and 38.

4.3.7. Denaturing immunoblot analysis of proteoliposomes

It is useful to compare the reconstituted recombinant c_n ring to the reconstituted native c_{14} ring, which has been shown to be somewhat stable under standard SDS denaturing polyacrylamide gel conditions.

For the reconstituted proteoliposomes without pigment, proteoliposomes were dissolved in 2% βDDM Dissolution Buffer in the same manner as in the native sample preparation, for approximately 200 minutes. A volume of 5 µL of the dissolved proteoliposome was added to 10 µL of H_2O and 5 µL of a 4X SDS Sample Loading Buffer (133 mM Tris-HCl pH 8.0, 26.7% SDS, 2.5 M 2-mercaptoethanol, 26.7% glycerol, 133 µM bromophenol blue). For the reconstituted samples eluted from the gel filtration column, 10 µL of sample was added to 5 µL H_2O and 5 µL of the 4X SDS Sample Loading Buffer. As a control, a sample of native c_{14} which was not reconstituted was also included. A volume of 0.5 µL (approximately 1.4 µg) was mixed with 14.5 µL H_2O and 5 µL of 4X SDS Sample Loading Buffer. Because a portion of the native c_{14} ring typically dissociates into its monomeric c_1 form on SDS denaturing gels, this

sample conveniently serves as a control for both the oligomeric c_{14} state as well as the monomeric c_1 state. The same preparation conditions were used for the recombinant c_n and native c_{14} sample, and the samples were not heated prior to loading on the gel.

The proteoliposome samples reconstituted with pigment were prepared similarly. However, the proteoliposomes were not dissolved in 2% βDDM Dissolution Buffer prior to preparation in order to reduce unnecessary solubilization that may further destabilize formed rings. Instead, 1 µL of proteoliposome was mixed directly with 14 µL of H_2O and 5 µL of 4X SDS Sample Loading Buffer, immediately prior to loading. The fractions of sample eluted from the gel filtration column were prepared by adding 10 µL of sample to 5 µL of H_2O and 5 µL of SDS Sample Loading Buffer. A sample of purified c_{14} ring (not reconstituted) was included as a control, and prepared in the same manner as was done for the samples reconstituted without pigment. The samples were loaded immediately after preparation, and not subjected to heating conditions. The native c_{14} and recombinant c_n samples were both prepared in this way.

For this analysis, a 12% polyacrylamide gel was used. The gel was prepared in the manner described in Section 4.4.2, and used for immunoblotting as described in Section 4.4.4. The gel was run at room temperature and the immunoblot was run at 4°C. The results are shown in Figures 37 and 39.

4.4. General Analytical Methods

The following techniques were employed for analytical purposes during various steps of the expression, purification, and reconstitution. Some of these techniques are therefore referenced in multiple subsections throughout this chapter, and also occasionally in the Chapter 5 Results. They are organized here together in this subsection for easy reference.

4.4.1. Agarose gel electrophoresis

Separation of DNA fragments during gene synthesis and cloning was executed with agarose gel electrophoresis. Typically, for larger fragments (>1000 bp) 1% agarose gels were used, and for smaller fragments (<1000 bp) 3% agarose gels were used. GenePure LE GQA Quick Dissolve agarose (ISC BioExpress, E-3109) was used for 1% gels, and MetaPhor agarose (Lonza, 50181) was used for 3% gels. All gels were prepared with and run in 1X TAE Buffer (40 mM Tris Base, 20 mM glacial acetic acid, 0.1 mM EDTA, pH 8.0). Gels were typically run at a constant voltage between 75 and 100 V. 1 kb standards or 100 bp standards were used, produced by New England Biolabs (N3232, N3231). Upon completion, the agarose gel was normally equilibrated in a solution of 1 μg/mL ethidium bromide for 15 minutes, followed by a 5 minute wash. The DNA bands could then be visualized by absorbance of the intercalated ethidium bromide under an ultra-violet lamp.

4.4.2. SDS denaturing polyacrylamide gel electrophoresis

Tricine SDS polyacrylamide gel electrophoresis techniques described by Schägger [68] were used for the qualitative analysis of various protein samples. For most purposes, adequate separation of protein bands could be obtained with a 12% polyacrylamide separating gel layered with a 1 cm 4% polyacrylamide stacking gel. A 30% solution of acrylamide and bis-acrylamide solution, 29:1 was used for the gels, purchased from Bio-Rad (161-0156). Gels were typically run at a constant voltage of 50 V during migration in the 4% stacking portion, followed by an increase to 150 V during migration in the separating gel portion. The Bio-Rad Mini-PROTEAN Tetra Cell electrophoresis system (Bio-Rad, 165-8000) was used for preparing and running gels. Precision Plus Standards (Bio-Rad, 181-0374) were used for gels which were stained, and Precision Plus WesternC Standards (Bio-Rad, 161-0376) were used for gels which were immunoblotted. Samples were prepared for loading on the gel by mixing with 4X SDS Sample Loading Buffer (26.7% sodium dodecyl sulfate, 133 mM Tris-HCl pH 8.0, 2.5 M 2-mercaptoethanol, 26.7% glycerol, 133 μM bromophenol blue). The 4X SDS Sample Loading Buffer was added to samples in a volume that corresponds to 1X final concentration of the total volume (25% v/v). Denaturation and solubilization of the samples was typically accomplished by heating samples at 95°C prior to loading. Cell lysate, cell pellet, and native ATP synthase samples required 15 minutes of heating to denature, and other samples required 1-5 minutes of heating.

4.4.3. Polyacrylamide gel staining

Protein bands on polyacrylamide gels were detected either with Coomassie Blue Staining or Silver Staining methods. Coomassie Blue Staining was done by equilibrating the polyacrylamide gel in heated Coomassie Blue Stain (0.1% Coomassie Brilliant Blue (CBB) 250, 30% methanol, 10% acetic acid) for 5 minutes, followed by equilibration in heated Destain I (50% methanol, 10% acetic acid) for 5 minutes, and final equilibration in Destain II (5% methanol, 10% acetic acid) until bands were adequately resolved. For the heating steps, the gels and solutions were heated together in a microwave (0.95 kW) for 30 seconds.

Silver Staining was done by equilibrating the polyacrylamide gel in 12.5% glutaraldehyde solution for 60 minutes, followed by a 5 minute rinse in H_2O and equilibration in a 1.0% $AgNO_3$ solution for 60 minutes, also followed with a 5 minute rinse in H_2O. The gel was then transferred to Developer Solution (0.25% formaldehyde, 6.25% Na_2CO_3) and equilibrated until bands could be distinctly resolved, at which point the gel was immediately transferred to Fixing Solution (10.0% w/v glycerol, 10% v/v acetic acid) to preserve development. All silver staining steps are carried out at room temperature.

Silver Staining has proven to be the most practical means for visualizing the hydrophobic 8 kDa c_1 subunit, while Coomassie Blue Staining is sufficient for detecting the 50 kDa MBP-c_1 fusion protein. In general, Silver Staining is about 10-fold more sensitive than Coomassie Blue Staining; and so for optimal results 1

µg of protein may be sufficient for Silver Staining while 10 µg may be needed for Coomassie Blue Staining.

4.4.4. Western immunoblotting

Protein samples separated on a 12% polyacrylamide SDS tricine gel as described in Section 4.4.1 were blotted onto a PVDF membrane (Bio-Rad, 162-0174) at 100 mA for 85 minutes in a Tricine Transfer Buffer (25 mM Tris-Base, 192 mM tricine, 20% v/v methanol). The Bio-Rad Mini Trans-Blot Module (170-3935) was used for the electrophoretic transfer. Blotted PVDF membranes were equilibrated in blocking solution (50 mM Tris-Base, 150 mM NaCl, 0.05% Tween 20, 5% w/v Non-fat Dry Milk) for 30 minutes. Then the polyclonal primary antibody against c_1 subunit (Agrisera AS05 071, Section 4.4.5) was added in a 1:1000 dilution and equilibration continued for an additional 60 minutes. Two 5 minute washes in Tween-Tris Buffered Saline (TTBS) Buffer (50 mM Tris-Base, 150 mM NaCl, 0.05% Tween 20) followed. Then the PVDF membrane was transferred to 20 mL TTBS Buffer treated with a 1:5000 dilution of goat anti-rabbit IgG-HRP conjugate (Santa Cruz Biotechnology, sc-2004) and 1:5000 StrepTactin-HRP conjugate (Bio-Rad, 161-0380) and equilibrated for 75 minutes. Two 20 minute washes of the PVDF membrane in TTBS Solution followed. Immun-Star HRP substrate (Bio-Rad, 170-5040) was used to activate secondary antibody luminescence. Chemiluminescent images of the bound conjugates were taken with a Kodak Gel Logic 440 CCD camera using a 2 minute dark exposure period.

4.4.5. Antibody production

A polyclonal antibody was produced for the native spinach chloroplast ATP synthase c_{14} by Agrisera in collaboration with the author. This antibody was needed in order to positively identify the presence of c-subunit or ring in recombinant samples using western immunoblotting techniques. The native c_{14} ring was extracted and purified from spinach leaves using methods established in the Fromme lab at Arizona State University [41] based on published techniques [6]. The purified native c_{14} ring was provided to Agrisera for use as the antigen to illicit an immune response in the serum of rabbits over a period of eight weeks. Resulting antibody samples produced from serum of six rabbits was provided to the author periodically during this period by Agrisera for comparative screening. The resulting antibody sample with the strongest and most specific signal after this screening process was chosen for commercial production (Agrisera, AS05 071), and used to produce the immunoblot results reported herein. This antibody has proven to be very sensitive and specific for the c_1 subunit and c_{14} ring of spinach chloroplast ATP synthase. The antibody has also been tested on thylakoid extracts of *Nicotiana benthamiana* and *Thermosynechococcus elongatus* and has shown a positive signal, and would likewise be expected to work with other similar cyanobacterial or chloroplast c-rings and subunits.

4.4.6. Modified Lowry assay

The most practical means of determining the concentration of c-subunit is using an assay procedure modified from methods described by Lowry, et al. [69]. The

modified Lowry assay is useful for membrane proteins because it includes a 1% SDS reagent which effectively solubilizes any membrane lipids which may otherwise interfere with the ensuing reaction. It is also highly sensitive. As noted, the c-subunit does not absorb well at 280 nm due to the lack of aromatic residues, and so this assay is a useful alternative. Although it is more consuming of both time and protein, the modified Lowry assay does provide a more accurate determination of protein concentration.

The method was carried out as follows. Standards were prepared from bovine serum albumin (BSA) in 250 µL volumes, at concentrations of 0, 20, 40, 60, 80 and 100 µg/mL in H_2O. The samples of unknown concentration that were being tested were also prepared in 250 µL volumes in triplicate if possible, and at concentrations estimated to be within the range of the BSA standards. Stock solutions of a Reagent A and Reagent B were prepared. Reagent A contains 2.0% Na_2CO_3, 0.4% NaOH, 0.16% tartaric acid and 1% SDS. Reagent B is 4% $CuSO_4$-$5H_2O$. Reagent C was prepared by mixing Reagents A and B in a 100:1 volume ratio. 750 µL of the Reagent C was then added to the 250 µL BSA and test samples. The samples were then mixed by vortexing briefly, and incubated at room temperature for 20 minutes. The purpose of this mixing and incubation period is to ensure that all protein is solubilized. Next, 75 µL of Folin-Ciocalteu phenol reagent was added to each sample in 1 minute increments. Each sample was mixed thoroughly, and allowed to incubate at room temperature for exactly 45 minutes. During this time, a light blue color will develop in the solutions,

which is proportional to protein concentration. The absorbance of each sample can then be measured at 660 nm, also in 1 minute increments. Adding the phenol reagent in 1 minute increments allows measurement also in 1 minute increments, thus ensuring that all samples are incubated equally for 45 minutes. A standard curve is then plotted to correlate the absorbance values of the BSA standards to their known concentrations. And this curve is then used to calculate the concentrations of the unknown test samples, based their absorbance.

Chapter 5

RESULTS AND DISCUSSION

5.1. Expression of MBP-c_1

The c-subunit was successfully expressed in *E. coli* as the fusion protein MBP-c_1. The completion of this objective was confirmed based on the following series of successful results.

5.1.1. Codon optimized atpH gene constructed

A synthetic *atpH* gene was successfully constructed from 14 oligonucleotide fragments. The fragments were custom synthesized and designed to produce a final gene product with codons strategically chosen for optimal translation in the bacterium *Escherichia coli*. Different versions of the *atpH* gene were constructed with alternate terminal restriction sites to allow insertion of the gene into the various vectors at the chosen locations. The size of the synthesized *atpH* gene prior to restriction cleavage was approximately 260 bp, depending on the terminal restriction sites used. Table 4 provides a list of the alternate *atpH* genes that were successfully produced, their exact size, corresponding restriction sites, and the vector for which each is intended. Successful ligation of the oligonucleotide fragments to form the complete gene was visualized by analysis on 3% agarose gels. An example is shown in Figure 18.

Intended Plasmid	5' *atpH* RE Site	3' *atpH* RE Site	*atpH* size (bp)
pET-32a(+)	NdeI	XhoI	261
pMAL-c2x	NdeI	XhoI	261
pFLAG	HindIII	XhoI	264
pMAL-c2x	Blunt end	XhoI	255

Table 4. The synthesized *atpH* genes, each with the same core coding sequence and alternate restriction endonuclease (RE) termini. The 3' and 5' terminal RE sites enable insertion of the gene into a chosen location on the intended plasmid.

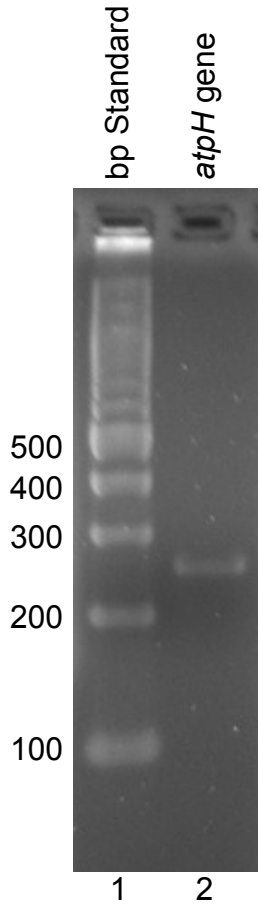

Figure 18. The synthesized *atpH* gene run on a 3% agarose gel. The signal at ~260 bp is a positive indication of successful ligation and annealing of the 14 synthesized oligonucleotides to form the complete gene. The *atpH* gene shown here was inserted into pMAL-c2x to create the vector pMAL-c2x-malE/atpH.

5.1.2. The atpH gene is inserted into various plasmids

The codon optimized *atpH* gene was inserted into vectors pET-32a(+), pFLAG, and pMAL-c2x at the intended restriction sites to produce four vectors, as previously described in Figure 14 with the intended expression products and the respective promoters. Successful growth of transformed DH10B *E. coli* colonies on antibiotic plates provided initial confirmation that the *atpH* insert was successfully ligated into a given vector. Restriction digestion of extracted plasmid DNA provided further confirmation of successful plasmid ligation by examining the size of the digested fragment(s). For example, Figure 19 shows the digestion of the pMAL-c2x-malE/atpH vector with a SacII endonuclease specific for a singular site on the inserted *atpH* gene. Nucleotide sequencing showed conclusively that the *atpH* gene was successfully inserted into all vectors and that no mutations, insertions or deletions were introduced into the *atpH* gene in the process.

5.1.3. atpH expression is enabled by maltose binding protein tag

A comparison of the expression products generated by the *E. coli* cells transformed with each of the four vectors showed clear evidence that the c-subunit will only be expressed under these conditions when it is attached to the maltose binding protein (MBP). Recombinant synthesis of the c_1 subunit as a standalone expression product of *atpH* was not observed in *E. coli* cells transformed with pET-32a(+)-atpH or pMAL-c2x-atpH, where the T7 and P*tacI* promoters were included, respectively. Likewise, c_1 expression was not observed

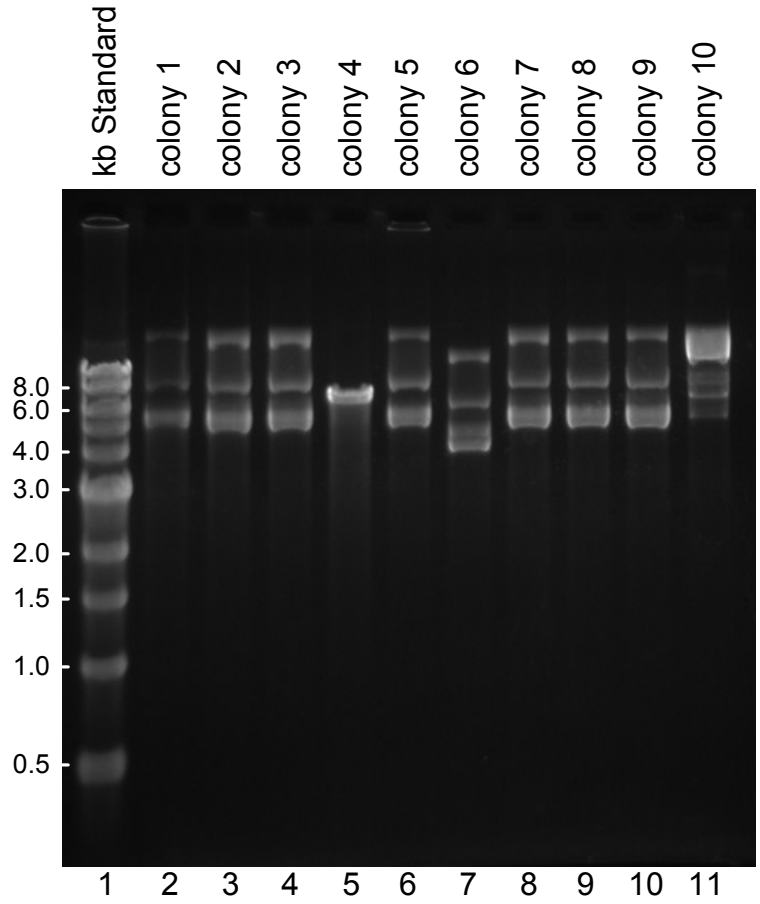

Figure 19. Plasmid DNA was extracted from ten DH10B clones transformed with ligated pMAL-c2x-malE/atpH, and digested with the restriction endonuclease SacII. This endonuclease recognizes a single site on the *atpH* gene, found nowhere else on the plasmid. Clone number 4 in lane 5 showed the expected pattern for a resulting linear strand of DNA 6894 bp in length. This is a typically reliable indication that the plasmid was successfully ligated with *atpH* inserted, and transformed into the bacterium.

with the vector pFLAG-atpH, where the 1 kDa FLAG tag would hypothetically be attached to the N-terminus of the expressed c_1 subunit. However, expression of c_1 was clearly observed in *E. coli* cells that were transformed with the pMAL-c2x-

malE/atpH vector, which is designed to express a maltose binding protein (MBP) fusion attached to the N-terminus of c_1. These results are summarized in Table 5 and demonstrated in Figure 20, where a denaturing polyacrylamide gel immunoblot only detects the 50 kDa MBP-c_1 fusion protein.

In contrast to the 1 kDa FLAG tag fusion attachment, the 42 kDa MBP is considerably larger than the 8 kDa c_1 subunit. Both FLAG and MBP are N-terminal fusion tags; however, the results have clearly shown that the size and solubility of the maltose binding protein are advantageous properties. Fusion of c_1 to the larger MBP is therefore required to influence the stability and solubility of recombinantly expressed c-subunit.

Transformant	**Expres. Product**	**Product Size**	**c_1 T-lation.?**	***atpH* T-scription?**
pET-32a(+)-atpH	c_1	8 kDa	No	Yes
pFLAG-atpH	FLAG-c_1	9 kDa	No	Yes
pMAL-c2x-atpH	c_1	8 kDa	No	Yes
pMAL-c2x-malE/atpH	MBP-c_1	50 kDa	Yes	Yes
pMAL-c2x-malE/atpH + pOFXT7KJE3	MBP-c_1	50 kDa	Yes	Yes

Table 5. A summary of the transformants tested for expression of their corresponding products, and the results observed. Although *atpH* was transcribed in all transformants, expression was only observed when the c_1 product was fused to MBP.

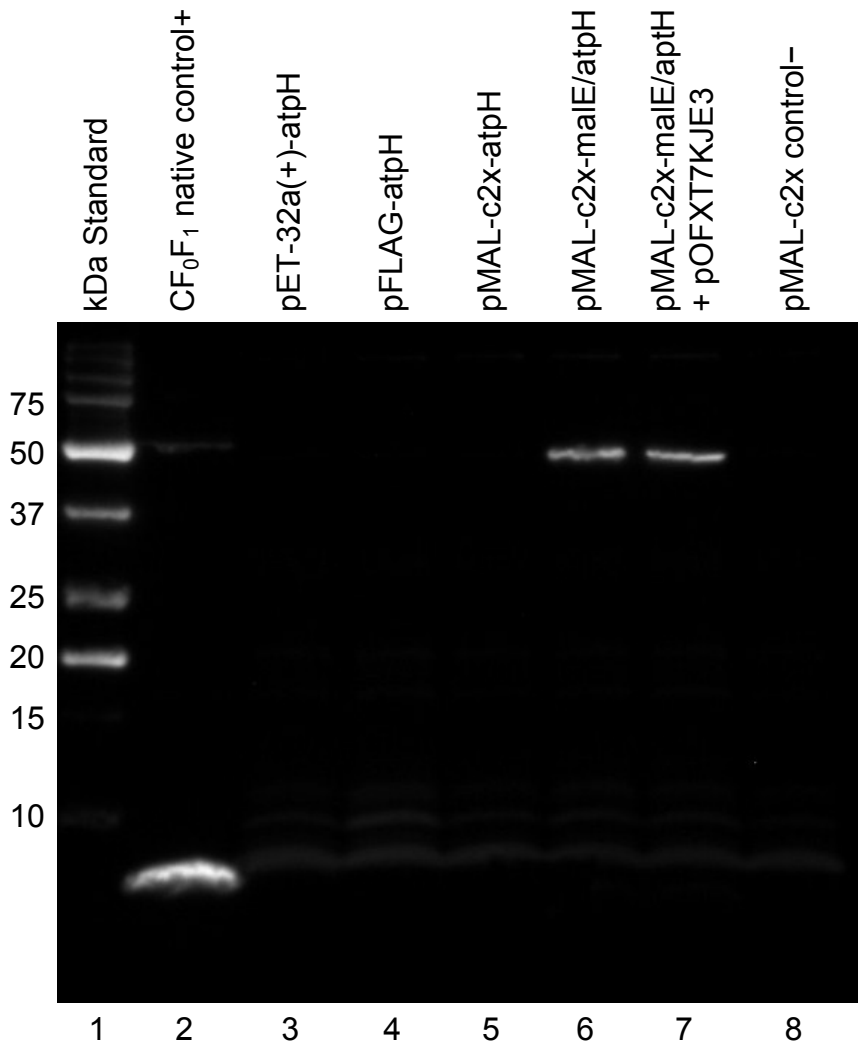

Figure 20. Immunoblot comparison of the cell lysate expression products from each transformant after 30 minutes of IPTG induction. Detection of c_1 subunit is only observed when expressed as the 50 kDa fusion protein MBP-c_1, as shown in lanes 6 and 7. The 8 kDa c_1 (lanes 3,5) or 9 kDa FLAG-c_1 (lane 4) is not detected in the other cell lysates. A native sample of spinach chloroplast ATP synthase (CF_0F_1) was included in lane 2 for use a positive control for the 8 kDa c-subunit. Cell lysate from a pMAL-c2x (no *atpH*) transformant was included in lane 8 as a negative control for spinach chloroplast c-subunit expression.

5.1.4. atpH is transcribed where it is not translated

The question arose regarding why the c-subunit could not be detected at the protein level in any of the other modes of expression which did not incorporate a MBP. Reverse transcriptase PCR was used to investigate this question, and results showed that transcription of the *atpH* gene occurs in cells that are transformed with pET-32a(+)-atpH, pMAL-c2x-atpH, and pFLAG-atpH. These results are shown in Figure 21, where the reverse transcribed and PCR amplified *atpH* from these transformants is visible on the gel. The results are also summarized also in Table 5. These data are interesting, considering that none of these transformants produced any evidence of recombinant *atpH* gene translation after 30 minutes of induction. As discussed, only the pMAL-c2x-malE/atpH transformants were able to produce the translated c_1 subunit product, which is in in essence synthesized as an extension of the more massive and soluble native MBP. Because *atpH* is only transcribed but not translated in the other transformants, it appears that stand-alone spinach chloroplast c_1 is targeted for degradation in *E. coli* immediately following translation – perhaps at the level of ribosomal peptide synthesis.

The signal recognition particle (SRP) interacts with the ribosome to assist in the transport of proteins as they are synthesized [70, 71]. Hypothetically, it is very possible that the SRP of *E. coli* does not recognize the N-terminal sequence of the chloroplast c-subunit when it is translated as a standalone protein, or with the leading 7 residues of the FLAG tag. Therefore, the SRP cannot direct the nascent

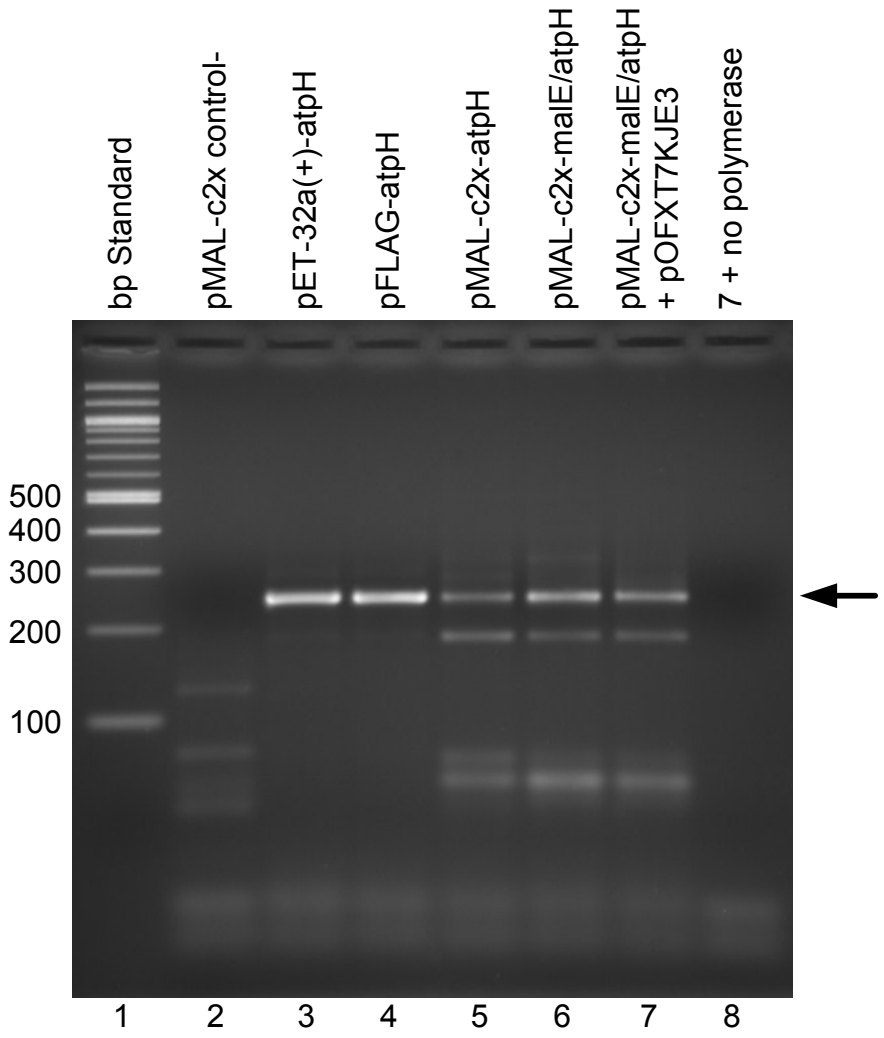

Figure 21. Reverse transcriptase PCR results on a 3% agarose gel. The presence of *atpH* mRNA transcripts in all *atpH* containing transformants is indicated, although stable translation is only observed with pMAL-c2x-malE/atpH. The amplified *atpH* cDNA is produced by reverse transcribing *atpH* mRNA transcripts, if present. The pMAL-c2x (no *atpH*) transformant is included as a negative control for the transcription of *atpH*. The sample in lane 8 was the same as lane 7 but without polymerase in the reaction for use a negative control for polymerase activity.

insoluble c_1 protein to the membrane, making it a quick target for degradation. On the other hand, the native *E. coli* MBP sequence on the N-terminus of MBP-c_1 would likely be recognized by SRP, enabling the nascent protein to probably be directed to the periplasm by the corresponding pathway. Or, this process may also occur similarly via the SecA/SecB mediated pathway [71, 72]. Thus, like a Trojan horse, the MBP is able to function as a clandestine means of disguising the small foreign hydrophobic c_1 subunit as a part of a native soluble protein that can be abundantly expressed in *E. coli* cells.

5.2. Purification of c_1

Two separate purification steps were employed, with a necessary protease cleavage step in between in order to successfully obtain purified c_1 subunit. The first purification step was for isolation of the fusion protein MBP-c_1, and the second purification step was for the isolation of the cleaved c_1 product.

5.2.1. MBP-c_1 can be purified from large scale cultures

The 50 kDa fusion protein MBP-c_1 was extracted and purified from large scale cultures of *E. coli* cells that were co-transformed with pMAL-c2x-malE/atpH and pOFXT7KJE3. The mass of cell pellet extracted from 1 L of culture is typically about 3 g. MBP-c_1 was effectively isolated from the cell lysate supernatant of the cell pellets by binding of the fusion protein to a column with amylose resin, followed by elution of the protein with the 10 mM maltose buffer. This was confirmed by comparing fractions collected during the preparation process of the

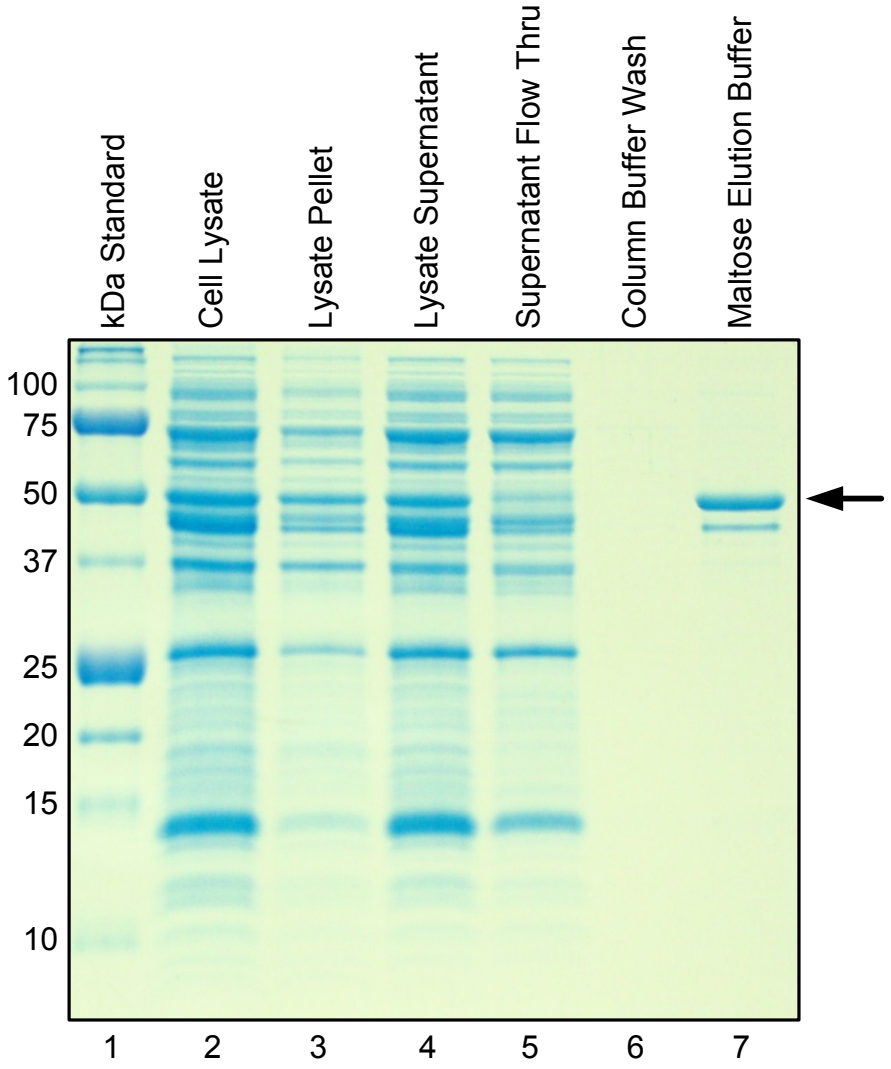

Figure 22. Polyacrylamide gel analysis of cell lysate samples from different steps of the preparation and purification process. Expression of the 50 kDa MBP-c_1 can be observed in the cell lysate supernatant in lane 4. The absence of this band in lane 5 indicates that it binds to the amylose resin column, as expected. And MBP-c_1 clearly elutes in the 10 mM maltose buffer in lane 7. The minor band that co-purifies is presumed to be the chaperone DnaJ.

lysed cell pellet on 12% polyacrylamide gels, which were stained with Coomassie Blue. An example of a resulting gel is shown in Figure 22. Expression of MBP-

c_1 is apparent in the soluble fraction, as well as a portion in the insoluble fraction. MBP-c_1 is absent in the flow through of the cell lysate collected from off the column. And MBP-c_1 is shown to elute in the 10 mM maltose wash fraction. The 41 kDa DnaJ chaperone protein also elutes as a minor co-purification product, perhaps bound to MBP-c_1, but this is later removed during final purification of the c_1 subunit. The amount of protein recovered in the maltose wash fraction originating from 1 L of cell culture is typically 10-12 mg, based on estimation with a modified Lowry assay (Section 3.1.15). Cells transformed with only pMAL-c2x-malE/atpH, and not the chaperone vector pOFXT7KJE3, typically produced about half the amount of purified protein. Therefore, chaperone co-expression was incorporated into the procedure as a helpful means of increasing expression yields.

5.2.2. Factor Xa protease cleaves c_1 from MBP

Experiments with Factor Xa protease show that it can effectively cleave c_1 from MBP in the presence of mild detergents. In preliminary experiments, it was observed that the efficiency of protease cleavage was only mildly influenced by variables such as incubation temperature, reaction time, and protease concentration. Immunoblots with samples cleaved under variations of these conditions are shown in Figure 23. A comparison of these immunoblots showed that protease concentration and incubation time were variables that had little effect on the specificity, and significant amount of the MBP-c_1 remained uncleaved regardless of the conditions. However, lower incubation temperature

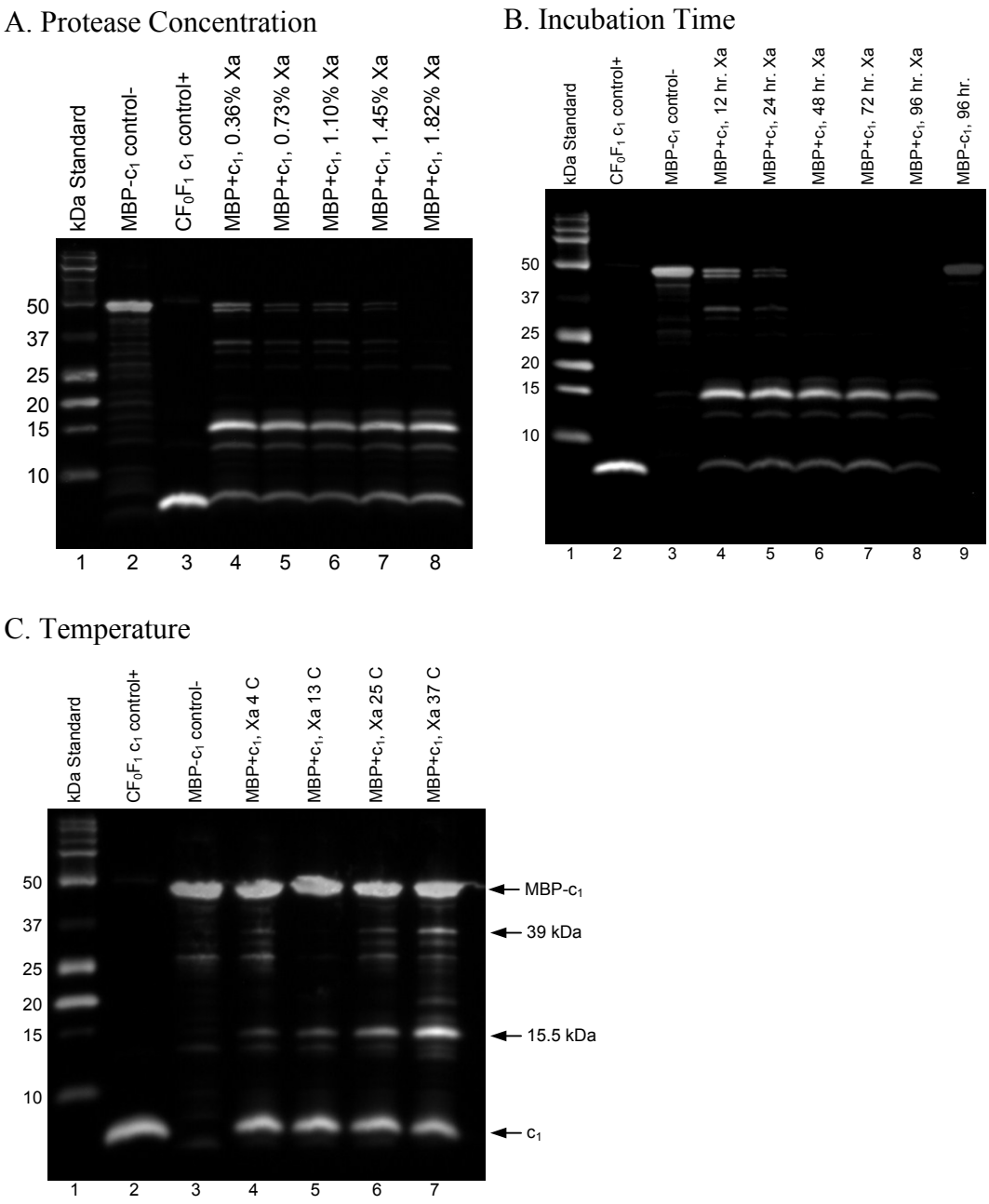

Figure 23. Immunoblots showing comparison of MBP-c_1 cleavage products with Factor Xa protease under variations of different conditions. Immunoblot **A** shows different concentrations of the protease in the cleavage reaction. Immunoblot **B** shows the cleavage product produced over a long period of time. Immunoblot **C** shows the effect of four different temperatures on cleavage product. All reactions used with these blots contained 0.01% SDS. The amount of cleaved 8 kDa c_1 did not vary much, but lower temperatures did appear to reduce secondary cleavage products (39 kDa, 15.5 kDa).

MBP-c_1 Amino Acid Sequence:

MKIEEGKLVIWINGDKGYNGLAEVGKKFEKDTGIKVTVEHPDK
LEEKFPQVAATGDGPDIIFWAHDR1FGGYAQSGLLAEITPDKAF
QDKLYPFTWDAVR2YNGKLIAYPIAVEALSLIYNKDLLPNPPKT
WEEIPALDKELKAKGKSALMFNLQEPYFTWPLIAADGGYAFKY
ENGKYDIKDVGVDNAGAKAGLTFLVDLIKNKHMNADTDYSIA
EAAFNKGETAMTINGPWAWSNIDTSKVNYGVTVLPTFKGQPSK
PFVGVLSAGINAASPNKELAKEFLENYLLTDEGLEAVNKDKPLG
AVALKSYEEELAKDPR3IAATMENAQKGEIMPNIPQMSAFWYAV
R4TAVINAASGR5QTVDEALKDAQTNSSSNNNNNNNNNNLGIEG
R6MNPLIAAASVIAAGLAVGLASIGPGVGQGTAAGQAVEGIAR7Q
PEAEGKIR8GTLLLSLAFMEALTIYGLVVALALLFANPFV

Possible Factor Xa Cleavage Fragments Containing c_1:

R1: 43 kDa
R2: 39 kDa
R3: 15.5 kDa
R4: 12 kDa
R5: 11 kDa
R6: 8 kDa

Figure 24. The amino acid sequence of MBP-c_1, with the c_1 residues highlighted in blue. All arginine residues are highlighted in red. Primary cleavage of 8 kDa c_1 from MBP by Factor Xa is expected to occur at the I-E-G-R site after the arginine (R6), the sixth in the sequence. Secondary cleavage at other Arg sites may also occur, resulting in larger fragments that would still give a signal for c_1 on an immunoblot. Because the c-subunit also contains two arginines (R7 and R8), other fragments that contain a portion of the c subunit are also possible.

did appear to reduce some of the secondary cleavage, and so 4°C was chosen as the optimized temperature for protease cleavage. Although Factor Xa has specificity for the recognition sequence I-E/D-G-R where cleavage occurs after Arg, other secondary cleavage sites that include Arg are often recognized as well

[57]. This is apparent in the immunoblots, where the lack of protease specificity results in a prominent 15 kDa contaminant. Figure 24 shows the MBP-c_1 sequence with the Arg residues highlighted, indicating possible secondary cleavage sites that contain c_1. This shows how a 15 kDa region fragment, among other fragments, may result from non-specific cleavage by the protease.

Variations in detergent type and concentration also were also tested, and these variables did appear to have an influence on the specificity of the protease cleavage. The immunoblot in Figure 25 shows a comparison of MBP-c_1 cleaved in the presence of various detergents at various concentrations. In general, less of the 15 kDa contaminant and more of the 8 kDa c_1 product was observed. The best results were with 0.1% or 0.01% n-β-dodecyl-D-maltoside (βDDM) in the reaction buffer, and so the medial concentration of 0.05% was chosen for all subsequent preparative purposes, in combination with a 24 hour incubation time period, 1.0% w/w Factor Xa, and the 4°C incubation temperature. Large scale preparations of MBP-c_1 were thus treated with the protease prior to purification of cleaved c_1 on the reversed phase column. The result of protease cleavage under these conditions is seen in the Figure 29.B immunoblot, on lane 4.

Unfortunately, none of the conditions that were tested were able to produce a cleavage yield of c_1 anywhere near 100%. A visual estimation of protease

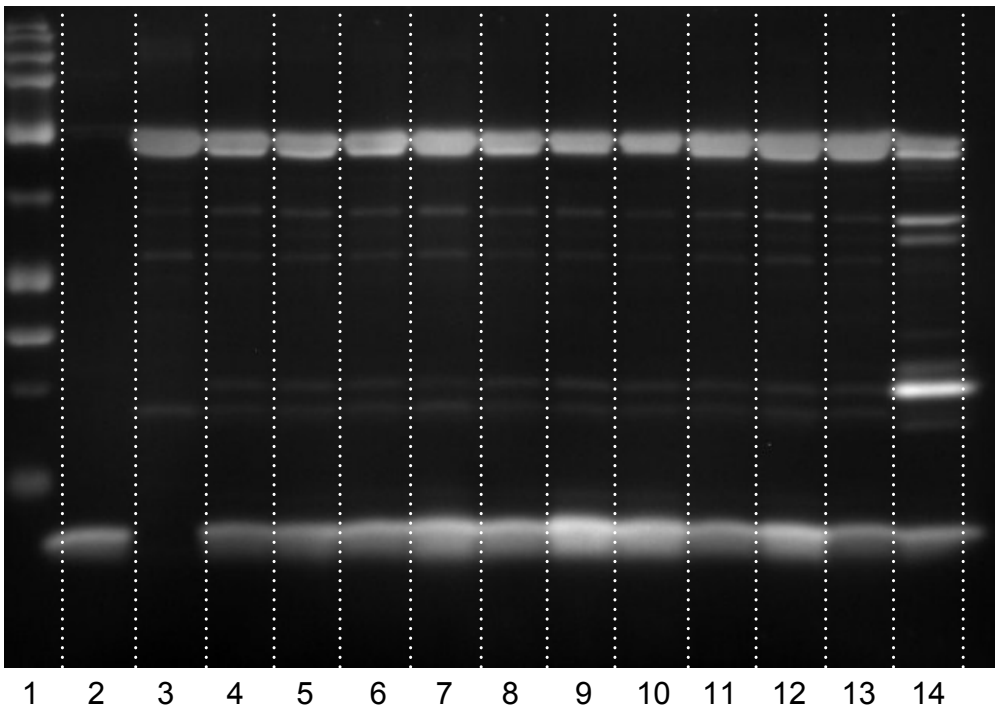

Figure 25. An immunoblot comparison of MBP-c_1 cleaved with Factor Xa protease in the presence of different detergents under a range of concentrations. The highest yield of cleaved 8 kDa c_1 and lowest amount of secondary cleavage product occurs at 0.01-0.10% n-β-dodecyl-D-maltoside (βDDM). Spinach chloroplast ATP synthase (CF_0F_1) is included in lane 2 as a positive control for c_1. A sample without Factor Xa protease is included in lane 3 as a negative control for protease cleavage. And for comparison, a sample with Factor Xa protease but no detergent is included in lane 4. Significant improvement was found in the use of Cholate, βOG, and βDDM over SDS (lane 14) which was used in previous experiments. Lines have been added for distinction.

cleaved c_1 product yield is closer to 20-30%. But it was interesting to note that the cleavage yield was slightly improved in the presence of detergents. The explanation for this is likely that the addition of detergent in low concentrations causes a slight disruption in the MBP-c_1 structure and thus makes the cleavage site more accessible without diminishing the activity of the protease. This balance is important because if the detergent is too harsh and/or concentrated, then it could conceivably denature the protease and render it inactive. The results with βDDM were chosen for large scale work, but the results with Na-cholate were also acceptable. β-octyl-D-glucopyranoside (βOG) is comparable as well, but does poorly in preventing aggregation. The results with sodium dodecyl sulfate (SDS) were poor, as a large amount of secondary cleavage product was evident on the immunoblot. Because the secondary cleavage products are presumably fragments of MBP fused to c_1, they would likely cause difficulties during the following steps of purification and reconstitution.

5.2.3. Reversed phase HPLC purifies cleaved c_1

Although rarely used for protein purification, reversed phase column high-pressure liquid chromatography (HPLC) was very effective in purifying the cleaved c_1 subunit. This method is not used with typical proteins because it tends to disrupt the secondary structure. This may be caused by the process of the protein unfolding as it binds to the hydrophobic column resin, or it may be caused by the use of organic solvents in the mobile phase – if not both [73]. Formerly

known as the proteolipid, the c-subunit is notoriously hydrophobic and thus unusually stable in the presence of organic solvents. And so although non-conventional for proteins, this method was applied successfully to the purification of c-subunit. The optimal organic solvent to use for reversed phase column elution was determined by comparing results with methanol, 2-propanol, and ethanol. In all trials, Eluent B was a 100% concentration of the corresponding organic solvent.

A comparison of purification schemes with the different organic solvents showed notable differences in when c_1 eluted, and how pure it was. Figure 26 shows the results when methanol was used as Eluent B. Also shown are the results from an experiment where methanol was used for Eluent B, and 0.05% βDDM was included in Eluent A. In both cases, c_1 elutes as a major peak once the gradient begins to level off at 100% methanol (Eluent B). The immunoblot showed that the c-subunit in that peak was free of secondary cleavage products. Although the yield is low, this is a viable means of purification. Inclusion of βDDM in Eluent A appeared to be unnecessary for elution of the protein; however it may be a worthwhile variable to continue testing as a possible means of reducing aggregation of protein on the column, which would enable more protein to be recovered in the eluted fraction.

Another test was executed with the less polar 2-propanol in Eluent B, and the results are shown in Figure 27. Under these conditions, c_1 eluted as a minor peak

Eluent A: 20 mM Tris-HCl pH 8.0

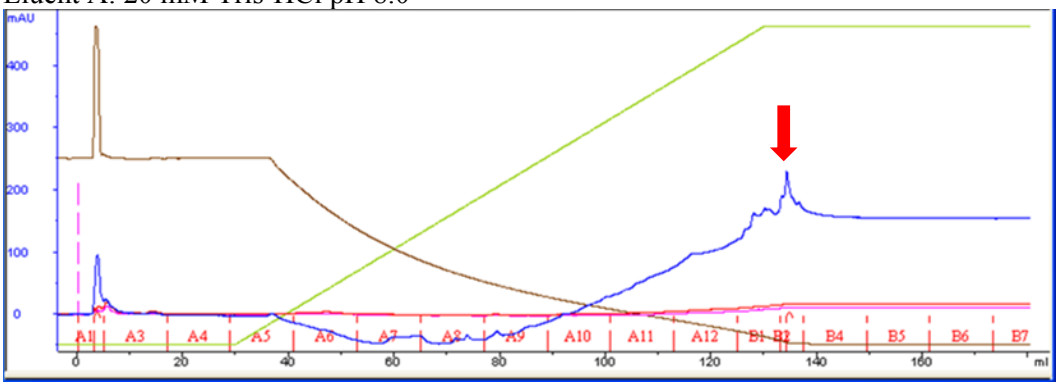

Eluent A: 20 mM Tris-HCl pH 8.0, 0.05% βDDM

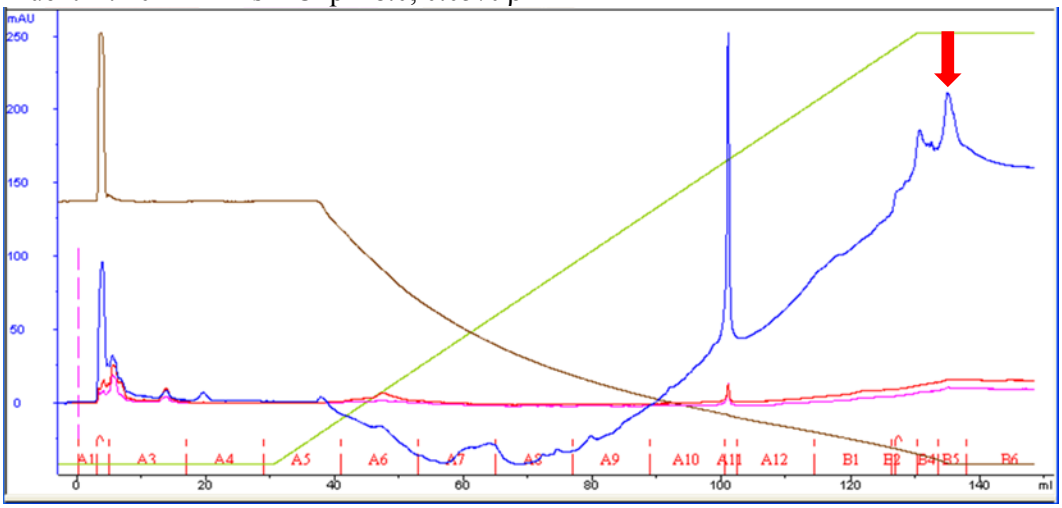

The blue line is A_{215}, the red is A_{257}, and the purple is A_{280}. The green line is concentration of Eluent B. The brown line is conductivity.

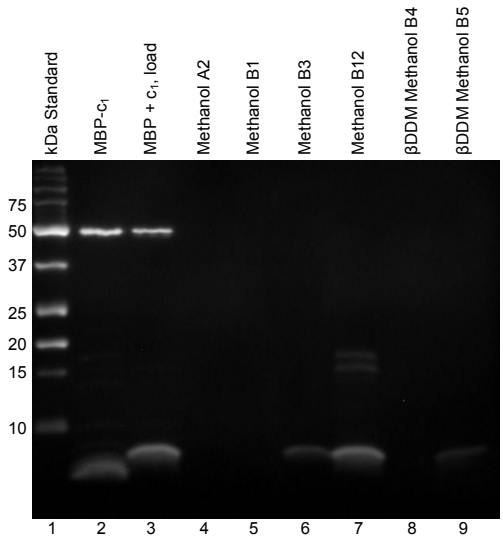

Figure 26. Reversed phase column purification of c_1 using methanol as Eluent B. The chromatogram below includes βDDM in Eluent A. In both cases, c_1 elutes as the final small peak (indicated by the red arrow) when Eluent B reaches 100% methanol. The immunoblot shows confirmation of c_1 in fraction B3 for the run without βDDM in Eluent A, and in fraction B5 for the run with βDDM in Eluent A. The fraction B12 shown on the immunoblot is from a waste collected during final column wash steps, and shows that some protein is lost as it tends to stick to the column.

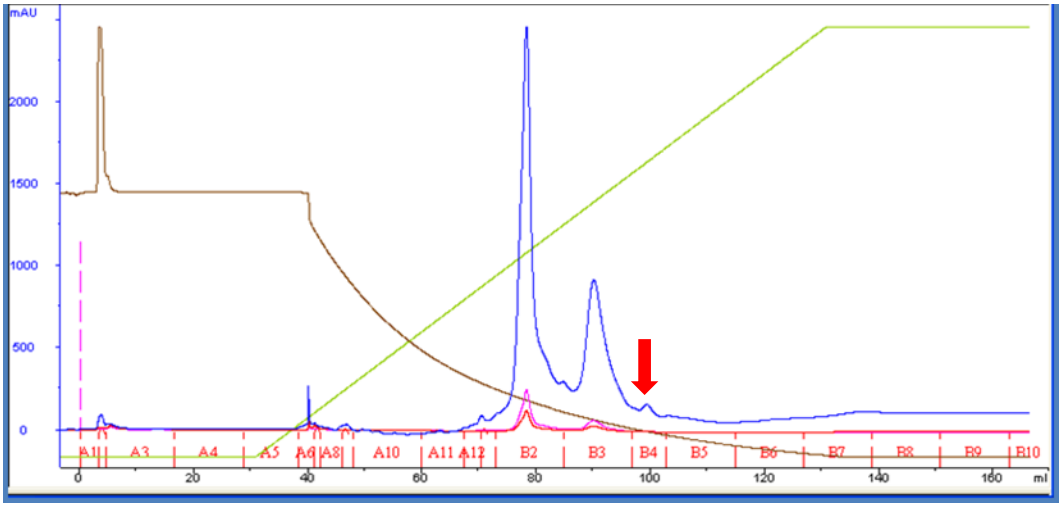

The blue line is A_{215}, the red is A_{257}, and the purple is A_{280}. The green line is concentration of Eluent B. The brown line is conductivity.

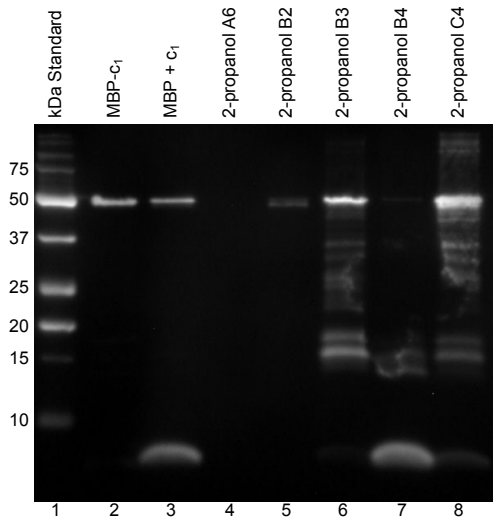

Figure 27. Reversed phase column purification of c_1 using 2-propanol as Eluent B. The c-subunit elutes at approximately 70% 2-propanol in Fraction B4 as indicated by the red arrow. This is confirmed by an analysis of the fractions on an immunoblot, shown left. Although most of the impurities are separated in the preceding peak, this blot shows that some secondary cleavage product is still present in the fraction B4, and so it is not very pure. Fraction C4 not shown on the chromatogram is from a later wash step, again showing proteins sticking to the column.

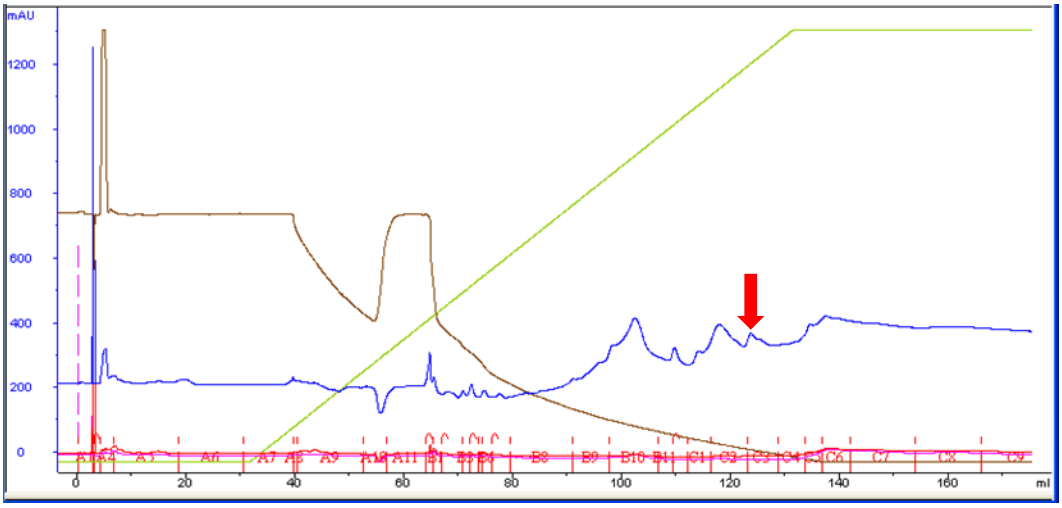

The blue line is A_{215}, the red is A_{257}, and the purple is A_{280}. The green line is concentration of Eluent B. The brown line is conductivity.

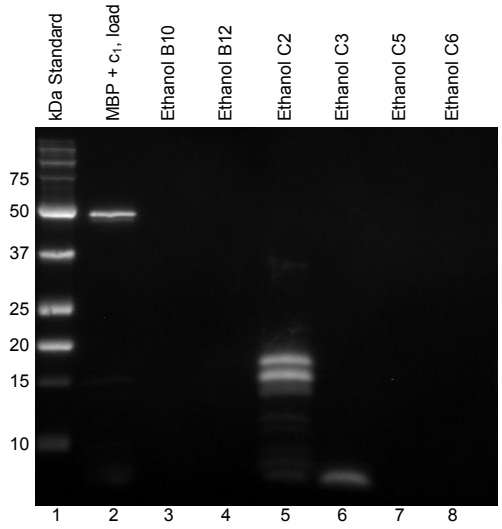

Figure 28. Reversed phase column purification of c_1 using ethanol as Eluent B. The c-subunit elutes at approximately 85% ethanol in Fraction C3 as indicated by the red arrow. This is confirmed by an analysis of the fractions on an immunoblot, shown left. The secondary cleavage products are all separated in the preceding peak, and fraction C3 highly pure.

when the gradient reached about 70% 2-propanol. However the fraction with c-subunit was shown to also contain a significant amount of secondary cleavage product. And so due to the lack of purity, 2-propanol was not used as eluent for c-subunit purification.

The most optimal results were obtained when ethanol was used in Eluent B, as shown in Figure 28. With ethanol, c_1 eluted when the gradient reached near 85% Eluent B. The amount of eluted protein was determined to be greater than when methanol was used, and the immunoblot shows that it was more pure than when 2-propanol is used. Although the c_1 containing peak does not appear to be very prominent on this chromatogram, it was much more pronounced on the large scale prep chromatograms (Figure 29.A).

These analytical RPC results led to the choice of ethanol for the Eluent B in the large scale preparative purification of c_1. The results of this purification procedure are shown in Figure 29, where approximately 19 mg of MBP+c_1 was loaded onto the column. The chromatogram shows that the absorbance peak that corresponds to the elution of the c_1 subunit in fractions E11 and E12 occurs when the Eluent B gradient approached 87% ethanol. The presence of c_1 in these fractions was confirmed by the immunoblot, and the purity of the confirmed c_1 product is clearly evident in lane 5 of the silver stained gel. The amount of c_1 product usually purified from a large scale preparative reversed phase column run was usually between 0.3 to 0.4 mg, when 15-20 mg of MBP+c_1 was loaded onto the column. Theoretically, 15-20 mg of MBP-c_1 could potentially yield 2.4-3.2 mg of cleaved and purified c_1. As noted, not all of c_1 is cleaved from MBP by the protease. And some c_1 is also lost during reversed phase HPLC purification as it remains bound to the column media, along with other proteins. This was

A. Chromatogram

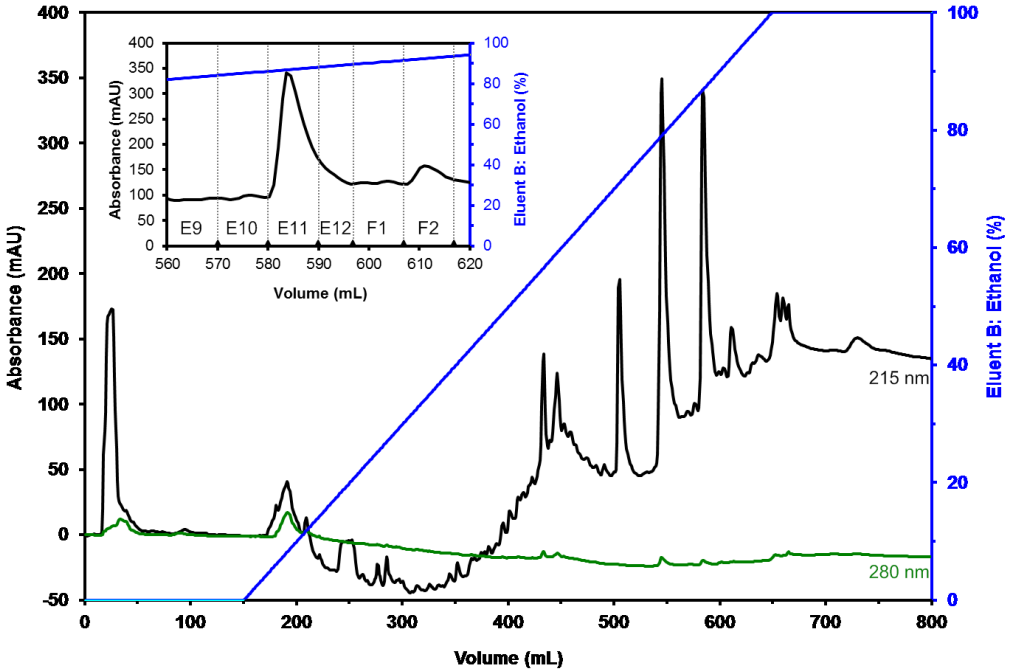

B. Immunoblot

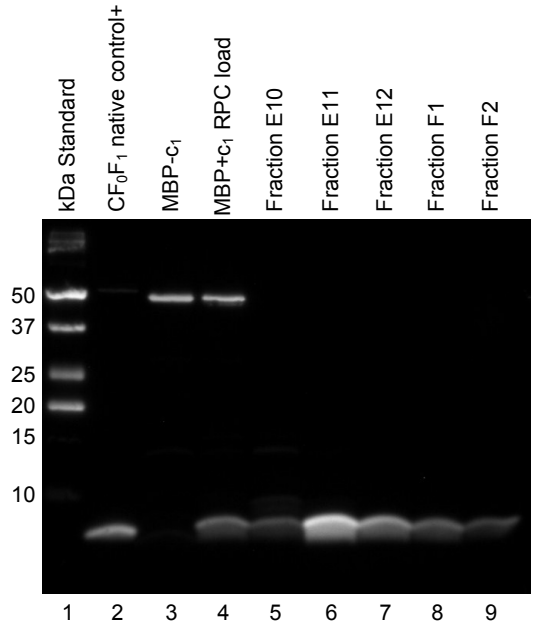

C. Silver Stained Gel

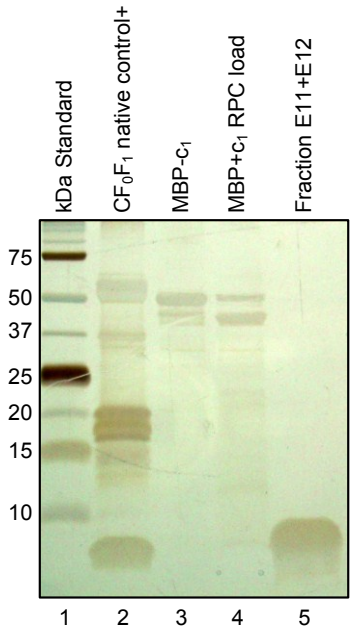

Figure 29. Reversed phase column HPLC purification of recombinant monomeric c_1 subunit. Elution of c_1 is observed at 87% Eluent B primarily in Fractions E11 and E12 (**A**). The c_1 subunit is identified on the immunoblot (**B**), and the purity of the 8 kDa protein is confirmed on the silver stained gel (**C**).

observed during wash steps carried out following use of the column. And so although the 12-13% yield of the final c_1 product is somewhat low, it is still a remarkable accomplishment for an eukaryotic membrane protein. But more importantly, the yield is sufficient for the intended applications.

As noted in Section 3.2.1, when 10 mM phosphate with pH 8.1 was used in place of 20 mM Tris-HCl with pH 8.0 in Eluent A, the c_1 peak emerged at 83% Eluent B. This indicates that the buffer used in Eluent A may also have some influence on how c_1 elutes, albeit far less than the influence of the organic solvent used. This observation was made during preparations for circular dichroism measurements (Section 3.2.1), where phosphate buffers are preferred in place of Tris buffers due to excessive absorbance of the amine groups in the low end UV spectrum.

5.3. Reconstitution of c_n-ring

Experiments with the purified recombinant c_1 subunit were directed toward attempts to reconstitute an oligomeric ring from the monomers by incorporation into liposomes. As demonstrated in previous reports, this approach has been used successfully for the reconstitution of an active *E. coli* F_0 channel [62, 74]. Reportedly, the approach was later applied successfully to the prokaryotic c-subunits of the bacterium *Propionigenium modestum* and *Ilyobacter tartaricus*, which were recombinantly expressed in *E. coli* [33]. Although it was expected that the recombinant chloroplast c_1 subunits would incorporate into the liposomes,

there was less certainty regarding whether they would likewise self-assemble to form rings in the process. And furthermore, if they did self-assemble, it was not known whether they would adopt the native c_{14} stoichiometry or a different oligomeric state. Given the possible outcomes, this phase of the project was fraught with uncertainty, but also some very interesting questions to be explored. The terminology c_{14} is used to distinguish the native ATP synthase c-ring extracted from spinach chloroplasts, from the recombinant version of the protein, which is designated as c_1 in its purified monomeric form or c_n in its reconstituted form.

5.3.1. Purified c_1 is highly alpha-helical

In order to evaluate the secondary structure of the purified recombinant c-subunit, circular dichroism (CD) spectroscopy was performed on the sample. The CD spectrum of the c_1 subunit in a sample collected from the reversed phase column is shown in Figure 30. The resulting curve shows the characteristic peaks associated with alpha-helical proteins [75], with two minima at 208.6 nm and 220.2 nm. Software analysis with CDSSTR produced a deconvoluted estimation of 85.5% alpha-helices, 6.0% beta-sheets, 3.9% turns, and 4.5% of residues in unordered conformations. The NRMSD value of the assignments is 0.052. Table 6 shows how this proportion of alpha-helices is consistent with the alpha-helical content as derived from NMR structures of monomeric c_1 subunits from *Bacillus* and *E. coli* (PDB ID: **1WU0**, **1A91**) [76], among other organisms. The c-subunit is typically characterized by two transmembrane alpha-helices connected by a

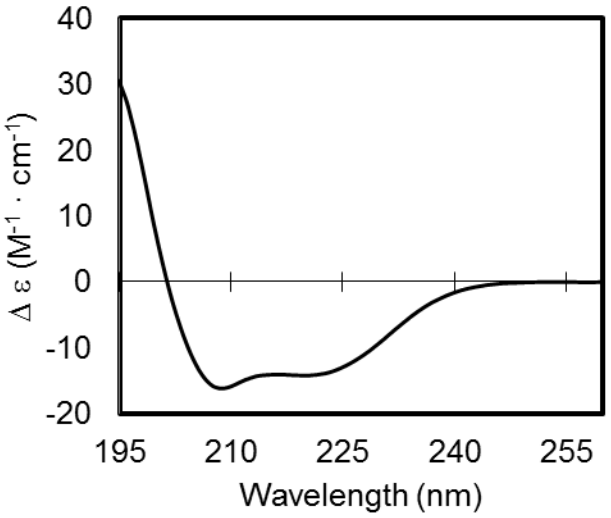

Figure 30. Molar Circular Dichroism (Δε) values plotted vs. the spectra 195-260 nm for the purified recombinant c_1 subunit. The resulting curve is indicative of a protein with high alpha-helical secondary structure.

c-subunit origin **Determination Method**	**α-helices (%)**
Recombinant *Spinacia oleracea* (Spinach) chloroplast **Circular Dichroism**	86
***Spinacia oleracea* (Spinach) chloroplast sequence** **Structure prediction, APPSPS2 algorithm**	83
Native *Spinacia oleracea* (Spinach) chloroplast **X-ray diffraction (PDB ID: 2W5J)**	73
Native *Arthrospira platensis* (Spirulina) thylakoid **X-ray diffraction (PDB ID: 2WIE)**	86
Recombinant *Bacillus sp.* **Solution NMR (PDB ID: 1WU0)**	81
Native *Escherichia coli* **Solution NMR (PDB ID: 1A91)**	88

Table 6. A comparison of estimated alpha-helical content in c-subunits from different sources, using different methods. The estimation of 86% for the recombinant spinach chloroplast c_1 is comparable to what has been estimated for other c-subunits.

A. *Spinacia oleracea* c_{14}

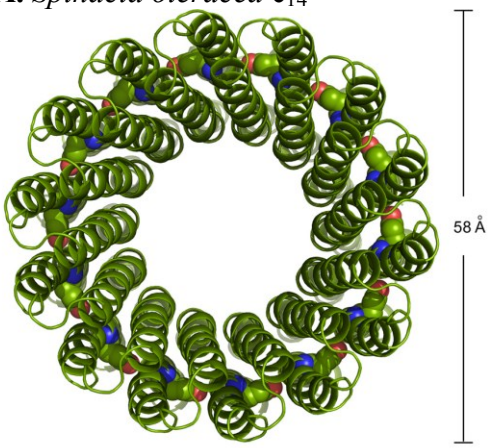

B. *Arthrospira platensis* c_{15}

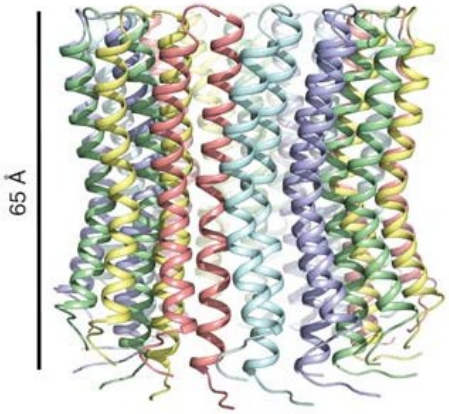

C. *Escherichia coli* c_1 of c_{10}

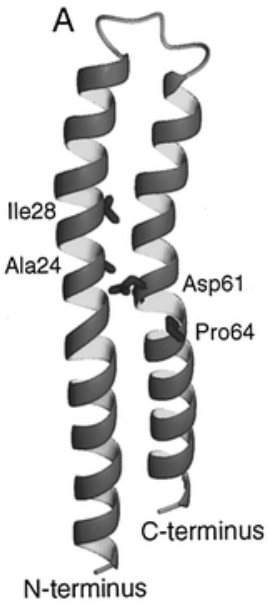

Figure 31. Structural models of the ATP synthase c-subunit and rings. An 'above'view is shown for the c_{14} ring from *S. oleracea* (**A**). A 'side' view is shown for the c_{15} ring from *A. platensis* (**B**). These two ring models are from x-ray crystal structures produced by Vollmar, et al. [77], and Pogoryelov et al.[78], respectively. The secondary structure is more recognizable when viewed as an individual subunit, as shown for the monomer of *E. coli* (**C**). This model is from an NMR solution structure produced by Girvin, et al. [76]. These models illustrate the high alpha-helical content that is generally inherent in the c-subunit.

small loop (Figure 31C). The CD derived alpha-helical estimation is also similar to what is predicted by secondary structure prediction software programs. The program APPSPS2 [79] predicts 82.7% alpha-helices based on the spinach chloroplast c-subunit amino acid sequence. The agreement of these CD results

with the structure prediction programs and the NMR structures thereby provides strong evidence that the purified recombinant c_1 subunit is correctly folded. Reconstitution of an oligomeric ring is not likely to occur unless the monomers are properly folded, so this positive result was prerequisite for the subsequent experiments.

5.3.2. Liposomes dissolve slowly in 2% βDDM

The mild detergent βDDM is able to slowly dissolve empty liposomes over an extended period of time at room temperature. The results of liposome dissolution with a 2% βDDM solution are shown in Figure 32. Absorbance at 600 nm was used to measure the amount of liposomes present, and this absorbance decreased exponentially over a period of 400 minutes until near the baseline. The plot shows that after about 200 minutes, most of the liposomes have dissolved. This profile is indicative of mild dissolution conditions that were desired for the purpose of gently extracting c_n from the liposome without disrupting the oligomeric state. It also shows that there is a convenient window of time after 200 minutes where experiments can be performed. Therefore, at least 200 minutes of incubation under these conditions was used for applications where the c-ring needed to be extracted from the proteoliposome for analysis. Other detergents can likewise produce a similar profile, but βDDM was chosen because it is used in other steps.

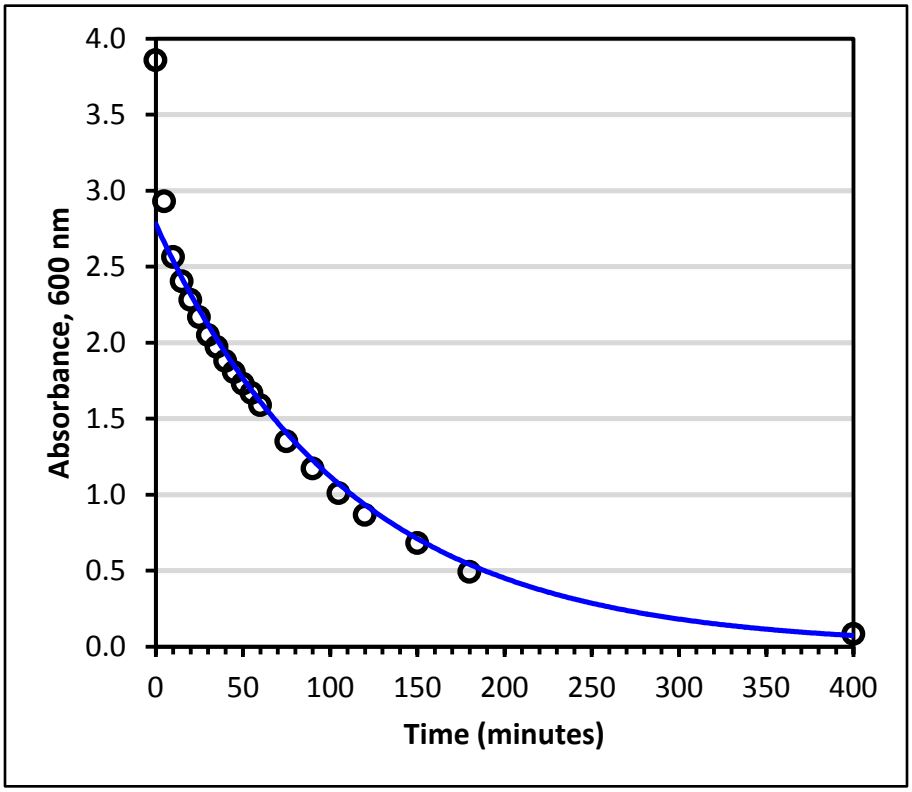

Figure 32. The dissolution of liposomes measured as 600 nm absorbance over a time course. A 2% βDDM detergent solution was used at room temperature. This plot shows that at least 200 minutes is required to dissolve most of the liposomes with 2% βDDM.

5.3.3. c_n and c_{14} gel filtration profiles are similar

A comparison of the gel filtration chromatography results for the reconstituted recombinant c_n and the native c_{14} samples shows a very strong correlation. In this experiment, the c_n proteoliposome that was reconstituted with recombinant c_1 monomers was mildly dissolved with 2% βDDM to remove phospholipids, and the sample was run on a gel filtration column. For a positive control, the native c_{14} ring was likewise reconstituted into proteoliposomes, dissolved, and run on the

gel filtration column. The experiment was carried out with a recombinant sample reconstituted in the presence of native pigments as well.

With the recombinant c_n sample that was reconstituted without pigments present, the protein elution peak on the gel filtration column is at 14.4 mL. The native c_{14} positive control sample also eluted with a peak at 14.4 mL. The chromatograms for both samples are shown in Figure 33, and it can be observed that both have nearly identical peak profiles.

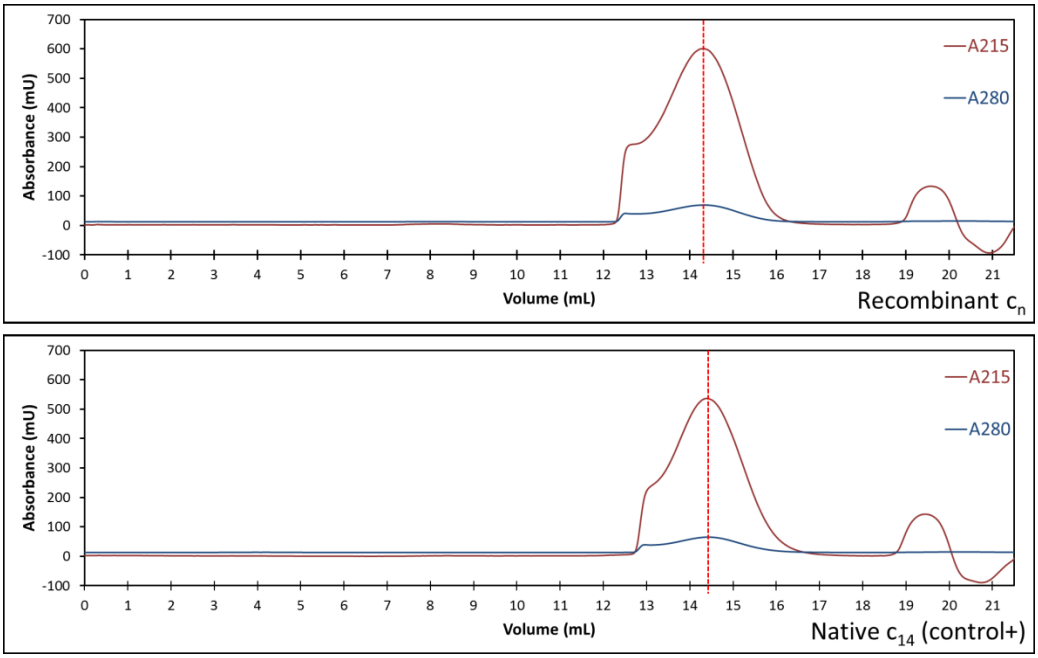

Figure 33. The gel filtration column chromatograms for the elution of dissolved proteoliposome samples. The recombinant c_n sample (above) appears to elute at the same time point (indicated by red-dashed line) and with a very similar profile as the native c_{14} positive control sample (below).

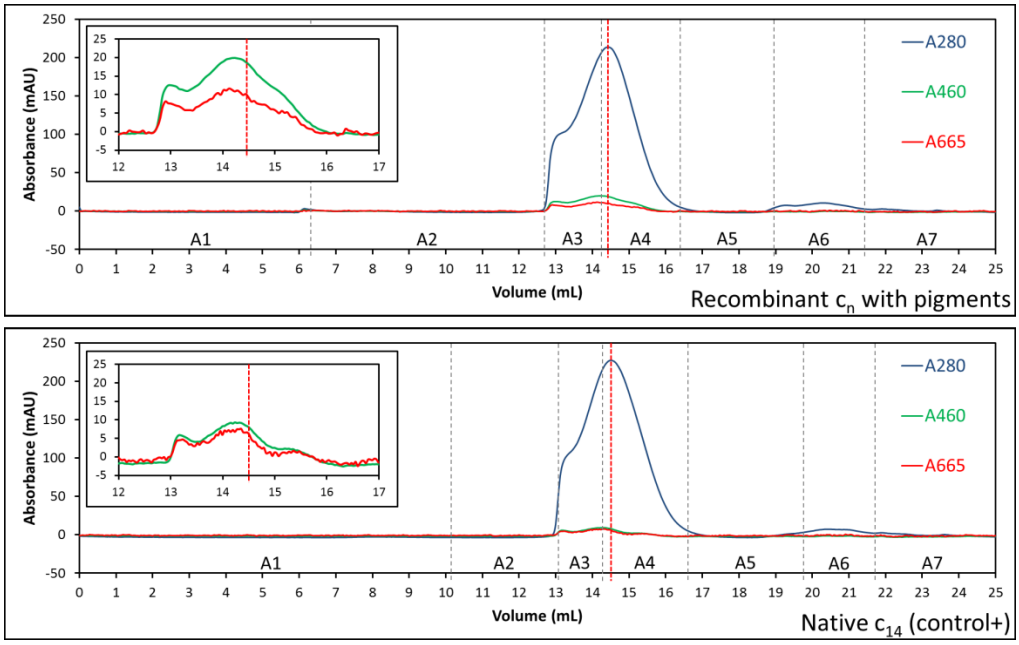

Figure 34. The gel filtration column chromatograms for the elution of dissolved proteoliposome samples. The recombinant c_n sample that was reconstituted into liposomes in the presence of pigments (above) appears to elute at nearly the same time point (indicated by red-dashed line) and with a very similar profile as the native c_{14} positive control sample (below). Fractions collected are indicated by dashed-gray lines. Absorbance is detected in both samples at 460 nm and 665 nm, indicating the association of chlorophyll-a and carotenes to the proteins in both samples. A detail of the pigment absorbance is shown on the left side of each chromatogram

The recombinant c_n sample that was reconstituted with the crude pigment extract included, showed similar elution behavior. Following dissolution of the proteoliposome, the recombinant c_n sample eluted with a peak at 14.4 mL. The native c_{14} sample eluted similarly with a peak at 14.5 mL. The comparison of chromatograms in Figure 34 shows elution peak profiles which are expectedly similar to what is shown in Figure 33, where the c_n sample was reconstituted without pigments. The same column was used, and the sample preparation and

column conditions were essentially identical to what was used with the other native c_{14} sample for comparison to the recombinant sample lacking pigments. There is very little variation in the peak elution time of reconstituted c_n (with or without pigment) and native c_{14}, and this result provides strong evidence for successful reconstitution of an oligomeric recombinant chloroplast c_n ring.

5.3.4. c_n and c_{14} native migration rates are comparable

The separation of proteins on native gels is influenced by charge, as well as size. The estimated charge of a monomeric c_1 subunit is -1.1, and thus the tetradecamer would have a theoretical charge of -15.4. And so although larger, the c_{14} oligomer appears to have a greater migratory potential toward the cathode than the monomer, based on preliminary observations with control samples.

Dissolved proteoliposomes of the c_n sample reconstituted from recombinant monomers appear to migrate on a native 4% polyacrylamide gel at the same rate as the positive control sample of native c_{14} subjected to the same treatment. This comparison is shown on the immunoblot in Figure 35. This result indicates that the recombinant sample is reconstituted into an oligomeric ring. The same result is observed in the samples after elution from the gel filtration column (Figure 36). However, the same samples analyzed on an SDS denaturing gel immunoblot are distinguished clearly by a difference in the stability of their oligomeric states (Figure 37). The denaturing gel shows that in the presence of SDS, a fraction of the native proteoliposome control sample remains in its oligomeric form and a

fraction is dissociated into the monomeric form. But, the recombinant sample appears entirely in monomeric form. And so although it is apparent that the recombinant ring is reconstituted in an oligomeric form, it is not as stable in SDS as its native homolog.

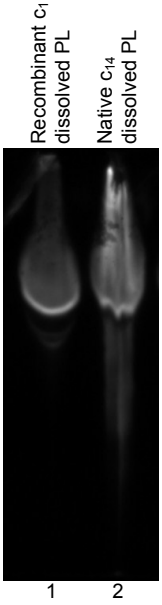

Figure 35. A native polyacrylamide gel immunoblot comparing the recombinant c_n liposome reconstitution (lane 1) with the native c_{14} liposome reconstitution (lane 2), as a positive control. Both samples were incubated in 2% βDDM to dissolve the liposome prior to loading onto a 4% polyacrylamide gel with 2% βDDM. The two samples exhibit an identical migration distance of the main band, providing strong evidence for a successful c_n ring reconstitution from the recombinant c_1 monomers. It is very possible that the recombinant ring has reconstituted with 14 subunits, given the identical migration distance as the native c_{14} sample.

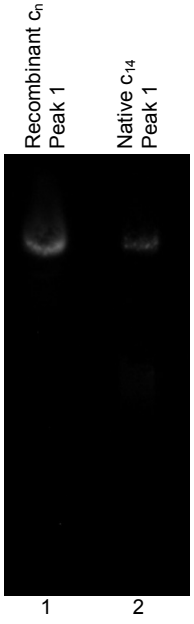

Figure 36. A native immunoblot prepared with reconstitution samples eluted from the gel filtration column. Lane 1 shows the recombinant c_n sample, and lane 2 shows the native c_{14} sample as a positive control. Both proteoliposome samples were dissolved in 2% βDDM, then run on the gel filtration column to compare retention times. This immunoblot confirms that the first peak contained c-subunit as expected, and provides strong evidence that the eluted c-subunit of both samples is of the same c_{14} stoichiometry.

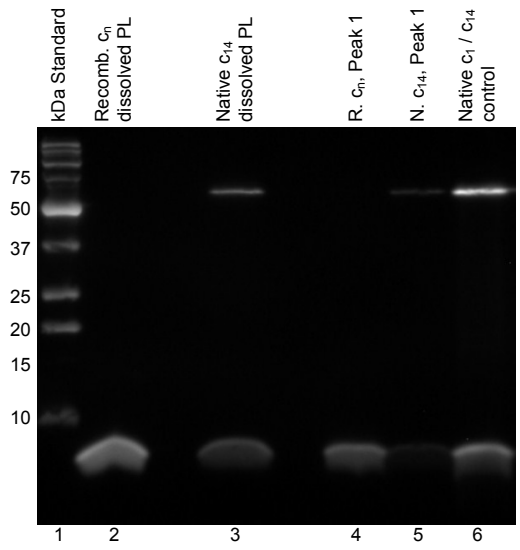

Figure 37. A denaturing SDS immunoblot with the recombinant c_1 reconstituted to form c_n in liposomes. A sample of native c_{14} likewise reconstituted into liposomes is included as a positive control for stable reconstitution. Lanes 2 and 3 show a comparison of the two proteoliposome samples after dissolution of the liposome. Lanes 4 and 5 show a comparison of the two proteoliposome samples after dissolution and elution through the gel filtration column. A native c_1 / c_{14} sample is included in lane 6 for use as a double control. Stable reconstitution is not observed in the recombinant (R.) sample.

5.3.5. Ring stability is not improved with pigments

As observed with the non-pigment treated sample, the recombinant sample reconstituted in the presence of native pigments migrated the same distance as the native c_{14} sample on the native gel (Figure 38). An interesting feature of the recombinant pigment sample is that in addition to the main band which migrates in accord with the native sample, there is at least one additional faint band nearby. This is also observed in the recombinant sample reconstituted without pigments, but it appears to be perhaps less pronounced. In the sample eluted from the gel filtration column, this aberrant minor band is observed to elute in the first half of the shouldered peak. It was hypothesized that analysis of the samples on an SDS denaturing gel would show evidence of a more stable reconstituted c-ring in the recombinant sample. Unfortunately, this result could not be observed according

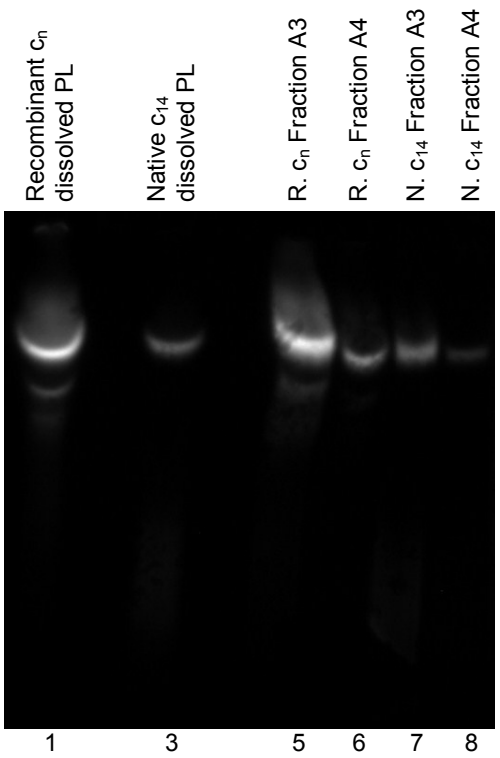

Figure 38. Native immunoblot with recombinant c_1 monomers reconstituted in liposomes in the presence of crude pigment extract to form c_n. As a positive control for a c_{14} state and natural pigment content, a proteoliposome sample with reconstituted native c_{14} is used. Lanes 1 and 3 contain samples of dissolved proteoliposomes (PL). Lanes 5-8 contain dissolved proteoliposome samples collected in fractions from the gel filtration column. As with the recombinant sample reconstituted without pigments, this blot shows that the recombinant and native samples migrate the same distance on the native polyacrylamide gel, indicating equal stoichiometries. The blot also confirms again that the c-subunit elutes in the first gel filtration column peak (fractions A3 and A4).

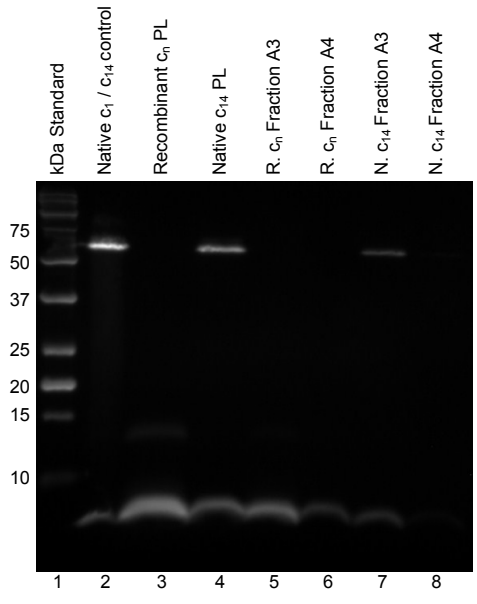

Figure 39. A denaturing SDS immunoblot with the recombinant c_1 reconstituted in the presence of crude pigment extracts to form c_n in liposomes. A sample of native c_{14} also reconstituted into liposomes is included as a positive control for stable reconstitution. Lanes 3 and 4 show a comparison of the two proteoliposome samples after dissolution of the liposome. Lanes 5-8 show a comparison of the two proteoliposome samples after dissolution and elution through the gel filtration column. A native c_1 / c_{14} sample is included in lane 2 for use as a double control. SDS-resistant ring reconstitution is not observed in the recombinant (R.) sample.

to the immunoblot shown in Figure 39. However, it was observed that another aberrant faint band with a molecular weight greater than the monomer appears running at about 14 kDa on the gel. This band may not necessarily reflect the size of the respective protein if it is in an oligomeric form and therefore not unfolded completely. Typically, c-subunit rings are approximately twice as large in molecular weight as they appear to run on SDS polyacrylamide gels [10], so this smaller band could indicate a trimer or tetramer. This aberrant band is not observed in the fraction of the cleaved c_1 subunit when purified on the reversed phase column (Figure 29.B), so it is not believed to be a secondary cleavage product. It seems that it must be a result of the liposome reconstitution with pigment.

5.3.6. Discussion of gel filtration and native gel results

The similarity between the gel filtration elution time and peak profile of the recombinant c_n sample and native c_{14} sample in these experiments provides some strong evidence that the c_n sample was indeed reconstituted into an oligomeric state. This evidence is corroborated by identical migration patterns observed on the native polyacrylamide gels. Although these methods cannot be used to directly visualize the stoichiometry of the oligomeric state, the c_n and c_{14} native gel results are identical enough that one could presume that the value of (n) in the recombinant c_n sample is the same as the native, where (n)=14. The argument could be made that perhaps the native c_{14} ring control sample has dissociated and

taken on a monomeric state, and this is why elution times and migration patterns are so similar. But the results with the denaturing SDS polyacrylamide gels show clearly that the native c_{14} extracted from proteoliposomes, purified on the gel filtration column, and run on the gel retains a significant fraction of its oligomeric c_{14} state.

Some possible explanations for the lesser stability in SDS may be related to other factors that are absent during recombinant expression, purification and reconstitution. The unique lipid membrane environment of chloroplasts could be a source of added stability. It is very possible that improved results could be seen using a native chloroplast lipid extract instead of the soybean lipid extract. Another possible explanation is that the stable assembly of the native ring could be mediated by a native chaperone protein, as found in the bacterium *P. modestum* [80]. In *P. modestum*, the *uncI* gene product was shown to be associated with ring formation, and this was demonstrated in vivo [80] and in vitro [81]. Using AFM, it has been observed with *P. modestum* that fewer complete rings are formed when the protein is produced recombinantly [34]. The authors of this report therefore hypothesized that the SDS-resistant stability of the c-ring is dependent upon the insertion of the final monomer into the ring. Presumably, the insertion of this final subunit is facilitated by a native chaperone such as the *uncI* gene product, and this final subunit acts as a keystone to stabilize the ring. Although a homologous gene is present in *E. coli* [80], it does not appear to be required in vitro for ring formation [82]. In the case of the

eukaryotic *S. cerevisiae*, several other proteins appear to have a similar chaperone role in F_0 assembly [80].

It is not known if an assembly chaperone is involved in the native chloroplast ATP synthase c-ring assembly. But this may be worth investigating, beginning with an analysis of the genome. If such a chaperone does exist, it may have some influence on the formation of a stable ring. If this is the case, then the most likely explanation for the instability of the recombinant c_n ring in SDS is that (n)=13, and a chaperone is required for insertion of the 'keystone' fourteenth c-subunit that would thereby confer SDS resistance. It may be difficult to discern c_{13} from c_{14} on a native gel, so the proposition that (n)=13 in this scenario is as likely as (n)=14 in a less stable complete ring.

5.3.7. Pigments associate with reconstituted c_n

The chromatograms in Figure 34 show that pigments co-purify with the c-subunit in the recombinant sample that was reconstituted in the presence of pigments. As expected, Figure 34 also shows that pigments are naturally present in the native sample purified on the gel filtration column following reconstitution and dissolution of the liposome. The absorbance scans shown in Figures 40 and 41 provide an illustrative comparison from which data was obtained to make a quantitative determination of absorbance values (Table 7) for the recombinant c_n and native c_{14}, respectively. The absorbance values at 280 nm indicate that both proteoliposome samples had similar amounts of protein, as intended. However, it

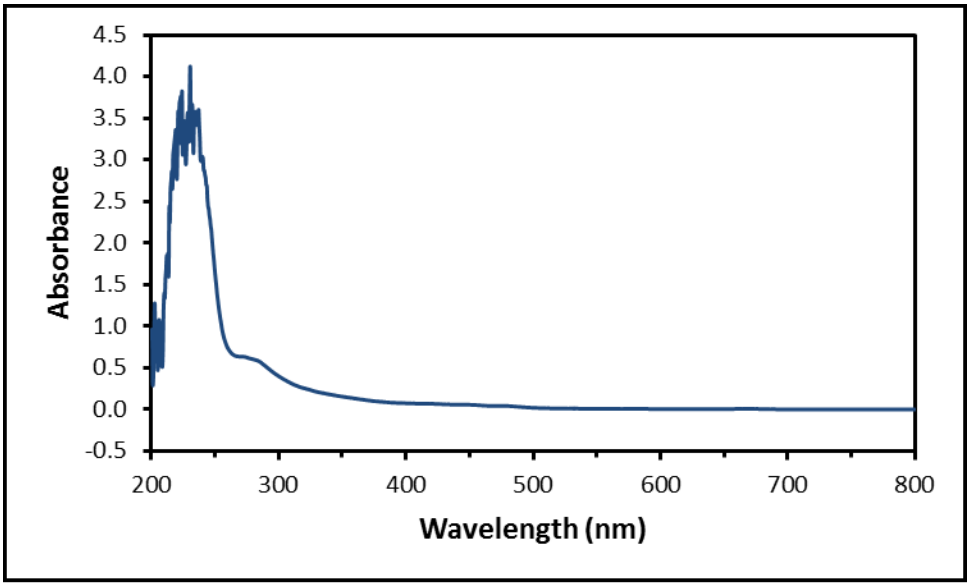

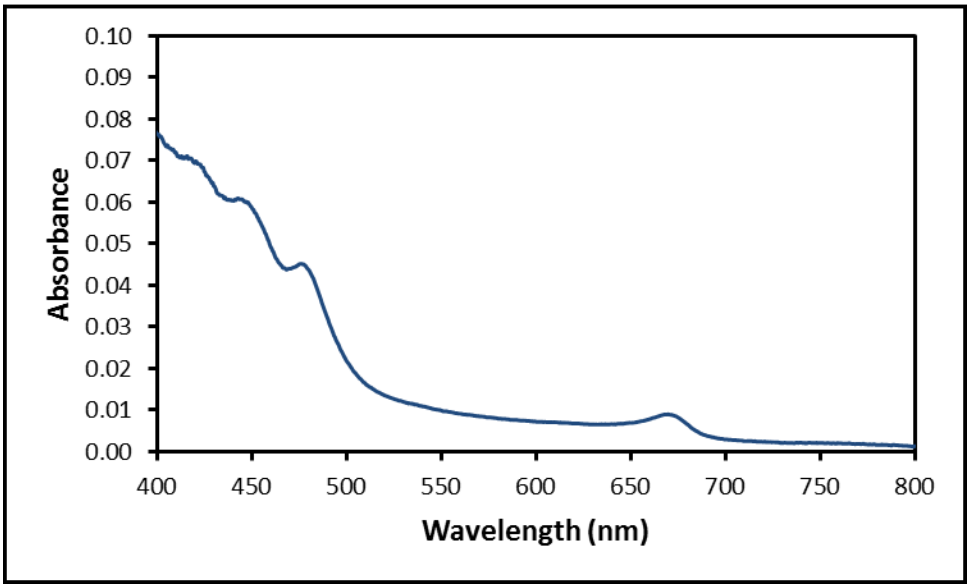

Figure 40. The absorbance scan for the pigment treated recombinant c_n extracted from the proteoliposome and collected in a gel filtration column HPLC fraction. The scan above is from 200 to 800 nm. The scan below is a more detailed look at the pigment absorbance range, from 400 to 800 nm.

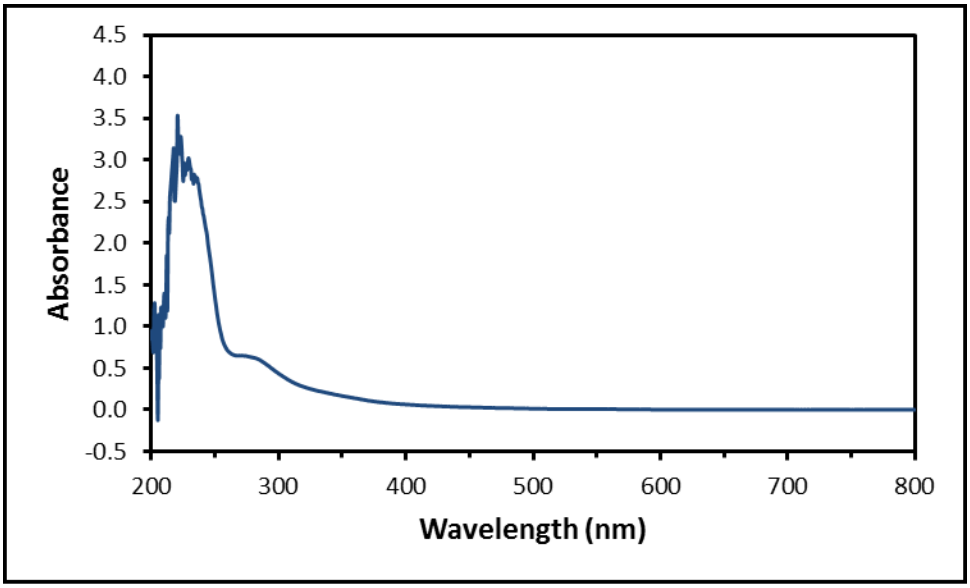

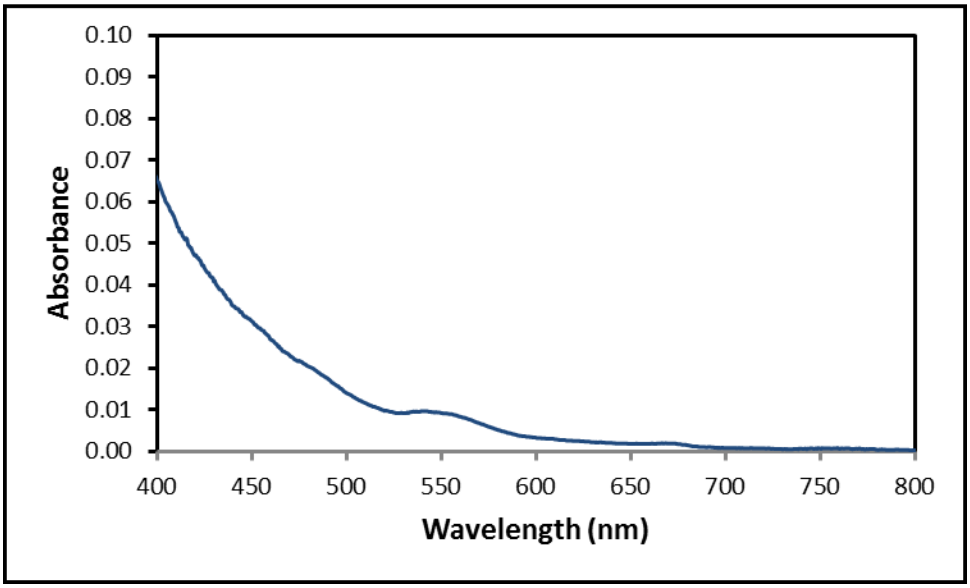

Figure 41. The absorbance scan for native c_{14} extracted from the proteoliposome and collected in a gel filtration column HPLC fraction. The scan above is from 200 to 800 nm. The scan below is a more detailed look at the pigment absorbance range, from 400 to 800 nm.

should be noted that these absorbance values cannot be directly correlated to protein concentration, as the presence of the associated pigments appears to contribute to absorbance at this wavelength. It is interesting to note that the amount of pigment in the recombinant sample is greater than the amount in the native sample. It is possible that in the process of purification, reconstitution, and extraction from liposomes, the native sample loses a fraction of its original pigment. Table 7 shows how the estimated molar amount of beta-carotene and chlorophyll-a in the two samples based on absorbance values reveals a high proportion of carotenoids in both samples. The amount of chlorophyll in the native sample is proportionally lower than the recombinant sample where pigments were added. It is possible that chlorophylls are more inclined to associate with the stromal opening of the ring, and incidentally are lost as the native sample was purified, reconstituted into liposomes, extracted, and separated on a gel filtration column. The electron density map derived from the crystal structure (Figure 7) seemed to provide some evidence that a chlorophyll is located at the stromal opening of the c_{14} ring, while the more linear carotenoids are able to align themselves in the center of the ring. Native spinach chloroplast c_{14} rings were reported to have a beta-carotene : chlorophyll-a ratio of approximately 2 [41].

Sample	A_{280}	A_{454} [β-carotene]	A_{665} [chlorophyll-a]	Molar Ratio β-car : Chl-a
Recomb. c_n	0.6046	0.0555 4.0×10^{-7} M	0.0086 1.1×10^{-7} M	3.5
Native c_{14}	0.6273	0.0297 2.1×10^{-7} M	0.0020 2.6×10^{-8} M	8.2

Table 7. Absorbance values from scans in Figures 40 and 41 for recombinant c_n and native c_{14} after reconstitution, extraction from liposomes, and examination on gel filtration column HPLC. Beta-carotene and chlorophyll-a concentrations are estimated based on absorbance values and extinction coefficients, and ratios are compared.

5.4. Optimization potential

The steps involved in producing the recombinant chloroplast c-subunit were developed in a systematic fashion based on the most favorable results. A summary of the possible routes that were explored during this process is illustrated in the flow diagram in Figure 42. Because the development of these reported methods and results has been primarily process driven, it is possible that some steps can be further improved to optimize product yield. Such can be an endless pursuit, however, and the ideal must often be compromised in favor of the practical. Nevertheless, for the sake of a broad perspective on the methods that were and were not tested, the following discussion is included.

Although not necessary, the co-expression of chaperone proteins DnaK, DnaJ, and GrpE greatly improves the yield of the MBP-c_1 fusion protein. Other available chaperone proteins such as GroES and GroEL have not been tested, but may similarly improve the yield of expressed protein [55]. The maltose binding

protein is imperative for the purpose of expression and highly efficient for the purpose of purification. It is possible that other large soluble fusion tags such as GST or SUMO could produce similar or improved results with regards to quantities of soluble expression and/or protease cleavage accessibility [28]. However, in regards to purification, the MBP-c_1 fusion protein is difficult to improve upon when used with the amylose resin. The BL21 derivative *E. coli* strain T7 Express *lysY*/I^q was used for the purposes of large scale expression, and as noted, similar results were observed with standard BL21(DE3) *E. coli* cells as well. Given the variety of BL21 derived *E. coli* cell lines that are currently available commercially [29], it is possible that slightly higher or lesser yields of expression can be obtained depending on the strain used. The growth conditions reported here are fairly standard, but it is also possible that expression yields can be further optimized by adjusting related variables such as growth medium composition, incubation temperature, or induction periods [26, 83]. Much work was done to find the optimal protease cleavage conditions, however as indicated by post-cleavage immunoassay and gel samples, a large amount of uncleaved protein remains. Variables such as Factor Xa protease concentration, detergent type and concentration, incubation time, and incubation temperature can possibly be combined in a slightly more effective manner to increase c_1 product yield. But a more likely improvement could result from extending the linker sequence between the MBP and c_1 in the design of the plasmid. A large clean peak on the reversed phase column was shown to correspond to purified c_1 product, however washing of the column revealed that a fraction of the loaded proteins tends to

stick to the column – as is often the case with reversed phase chromatography. Although the yield obtained with ethanol as the eluent was adequate and superior to results obtained with methanol or 2-propanol, there is certainly room for improvement. Further experimentation with other reversed phase column media, other solvents, and buffer additives such as trifluoroacetic acid (TFA) may be able to increase this yield.

It is possible that not all of the steps in the liposome reconstitution procedure are necessary. A variety of liposome reconstitution procedures can also be found in the literature, and many are less complex. It has even been reported that the *E. coli* c_{10} ring will self-assemble in the absence of liposomes, with only detergents present [82]. This has not yet been attempted experimentally with the spinach chloroplast c-subunit, but it is a valuable consideration. This provides some support for the idea that the reconstitution procedure could be greatly simplified. This should be explored, because many of the reconstitution steps appear to be superfluous and could possibly be detrimental to the overall yield.

Although some improvements in yield are possible, each step as reported has yielded reproducible results, and the quantity, quality, and purity of the final c_1 product obtained after purification is sufficient to provide a foundation for the intended experimental applications.

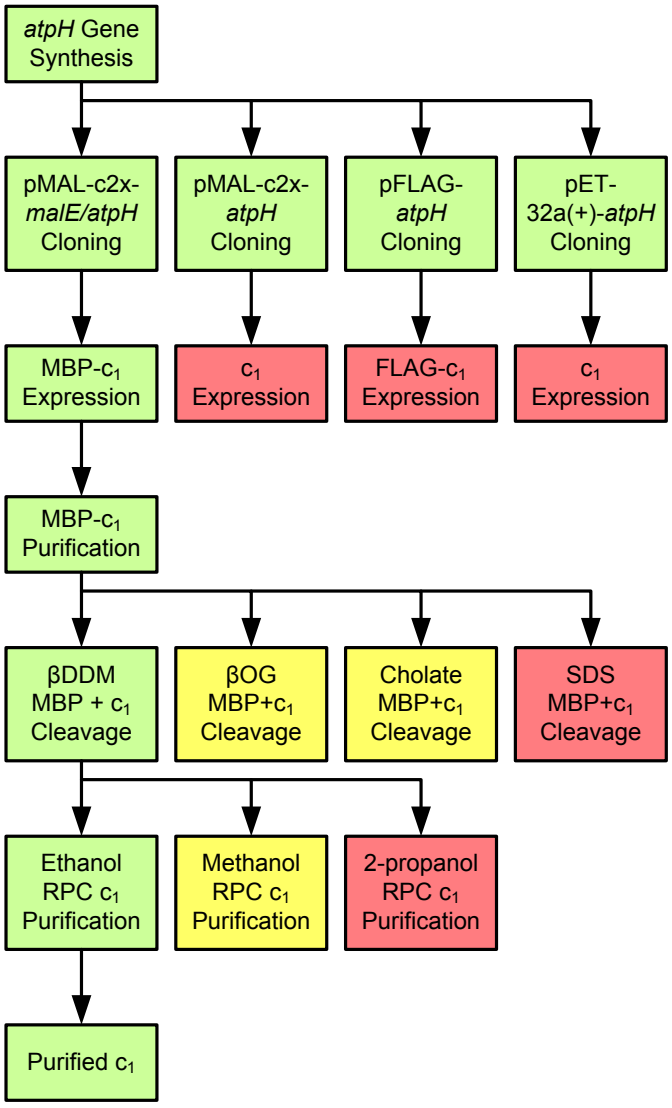

Figure 42. A summary of the optimized steps toward recombinant expression and purification of the chloroplast c-subunit. Some steps required a comparison of variable conditions in order to find the most viable route to the next step. Steps highlighted in green were most optimal, and incorporated into the process. Steps not incorporated into the process are highlighted in yellow or red. Yellow signifies that the technique was viable, but less optimal. And red signifies that the technique was not viable.

Chapter 6

FUTURE PLANS AND APPLICATIONS

6.1. AFM analysis of reconstituted c_n

The results of reconstituting the recombinant c-subunit into liposomes to induce formation of a c_n-ring appear to be promising, but not conclusive. The native immunoblots and gel filtration data appear to indicate that the recombinant sample has formed an oligomer with the same charge and molecular weight as the native c_{14} ring. However, in order to conclusively determine what the value of (n) is in the recombinant 'c_n' sample, other physical characterization techniques must be utilized. In recent decades, atomic force microscopy (AFM) techniques have been developed to the point of being able to characterize topographies of large membrane proteins with sub-nanometer resolution [84].

AFM techniques have been applied to different native c-subunit rings with great success. The technique has been used successfully with the *A. platensis* c_{15} [85], *I. tartaricus* c_{11} [86], and the *S. oleracea* c_{14} [11, 87]. The diameter of the rings is approximately 6 nm, which is near the limit of AFM capabilities. In each case, the rings are clearly observed arranged in a 2-dimensional array in a flat lipid bilayer, and the resolution is high enough to count the number of individual subunits. A remarkable example is included here in Figure 43 for the spinach c_{14} ring in work reported by Seelert, et al [87]. In each case, samples were measured in solution, using the contact mode of measurement.

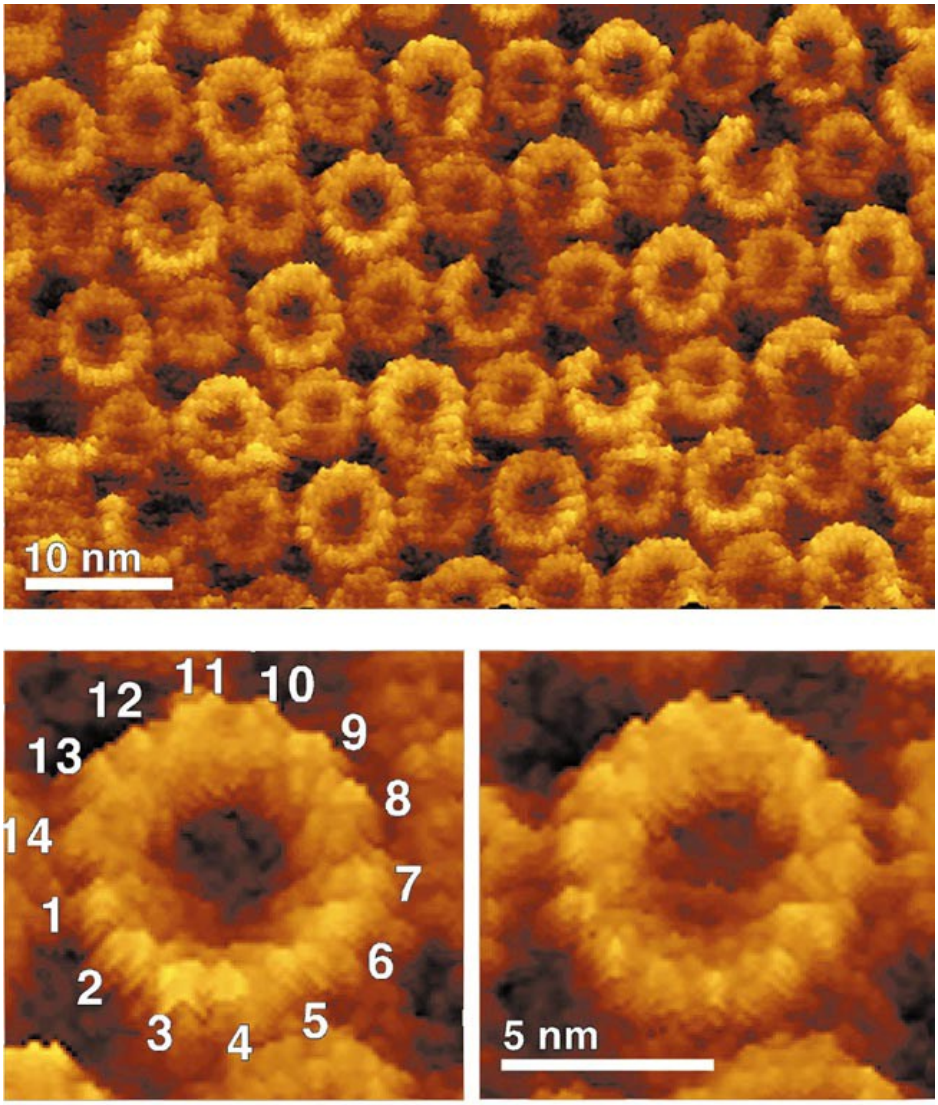

Figure 43. Atomic force microscopy images generated from 2-dimensional crystal arrays of the native spinach chloroplast ATP synthase c_{14} ring. These images have been produced by Seelert, et al. [87]. AFM resolution is sufficient to visualize the number of subunits in the ring, which is near 6 nm in diameter.

If the spinach recombinant c-subunit has successfully reconstituted into a ring in the liposomes, it may likewise reconstitute into lipid bilayer sheets in a similar 2-dimensional array as observed with the native samples in these examples.

Ongoing work with the recombinant c-subunit will be directed toward adapting these techniques for native AFM sample preparation in order to obtain similar high resolution images of the reconstituted recombinant chloroplast c_n ring. If the techniques work, and can be developed to produce comparable high-resolution images, the number of monomers in the recombinant ring can potentially be counted to determine if (n)=14 as observed in the native sample, or some other value.

6.2. Investigation of factors influencing stoichiometry

Once it has been established that the recombinant c-ring is reconstituted and the stoichiometry can be determined, access will be opened to an array of experiments that can be designed to investigate questions relating to stoichiometry. A recombinant expression system is of great value to this prospect because it allows complete control over all the major variables that are believed to be of influence in the assembly of the ring. This motive is currently driving a demand for this recombinant expression system [9].

As described, the early stages of experiments are underway to investigate how the presence or absence of pigment cofactors influences the assembly of a ring in liposomes. This will continue to be explored by testing different combinations of pigments at different ratios, while refining AFM imaging techniques. The native c_{14} ring should also be reconstituted into liposomes in the presence of pigments.

This would allow another comparison to be made to the recombinant sample, and may show a more similar ratio of pigments.

The amino acid sequence of the protein can be changed according to will by using site-directed mutagenesis techniques, or by completely re-synthesizing the *atpH* gene. This would enable further studies to be directed at investigating how amino acid sequence may affect ring stoichiometry. The sequence alignment shown in Figure 44 is a comparison of the *S. oleracea* c_{14} sequence to the *S. elongatus* c_{13}, *A. platensis* c_{15}, and *C. reinhardtii* putative c_{13}. Comparing these four sequences could reveal exactly which amino acid positions are key to the determination of the stoichiometry. These four c-subunits are all from the thylakoid membranes of photosynthetic organisms, so differences in stoichiometry are less likely to be influenced by variations in membrane composition or cofactors. This alignment shows a few locations where key mutations could lead to differences in stoichiometry. For instance, a common misalignment is found at Ala73. And it has been observed in other sequence alignments that the G-X-G-X-G-X-G-X segment (residues 23-30 in spinach) is well conserved among c-subunits, and the variations at any of the X positions may affect the stoichiometry [10]. There are two common mis-alignments in this region – Val26 and Thr30 on the spinach sequence. Nearby, a notable misalignment is also observed with the polar Ser21, which is a non-polar Ala in *S. elongatus* and *C. reinhardtii*. The structural comparison of the locations of these residues shown in Figure 45 indicates that this Ser21 is the most likely to have an influence because it extends directly

toward the adjacent subunit, whereas Ala73, Val26, and Thr30 do not. Furthermore, the multiple sequence alignment shown in Figure 5 reveals that position 21 is a small non-polar residue (Val, Ile, Ala or Gly) in all c_8-c_{13} ring sequences, but is replaced with the polar Ser in the larger *S. oleracea* c_{14} and *A. platensis* c_{15} rings. In the case of the *C. reinhardtii* and *S. elongatus* c_{13} sequence where residue 21 is Ala, a single nucleotide change could result in a Ser at that position, which could hypothetically be enough to shift the stoichiometry from c_{13} to c_{14} or c_{15}. Comparing the *S. oleracea* sequence to that of *C. reinhardtii* shows other key differences at Ala12, Gln34 and Leu57 on the *S. oleracea* sequence, which is Ser12, Tyr34 and Phe57 in *C. reinhardtii*, respectively. These are interesting differences because Try and Phe are conjugated ring structures bulkier than Gln and Leu. And Ser is polar, where Ala is not. Other differences in sequence can also be observed, but are less likely to be of consequence because they are either similar residues, or located on the N or C terminus. Amino acid changes at these positions may possibly work in combination to influence stoichiometry, making these excellent candidates for substitution experiments.

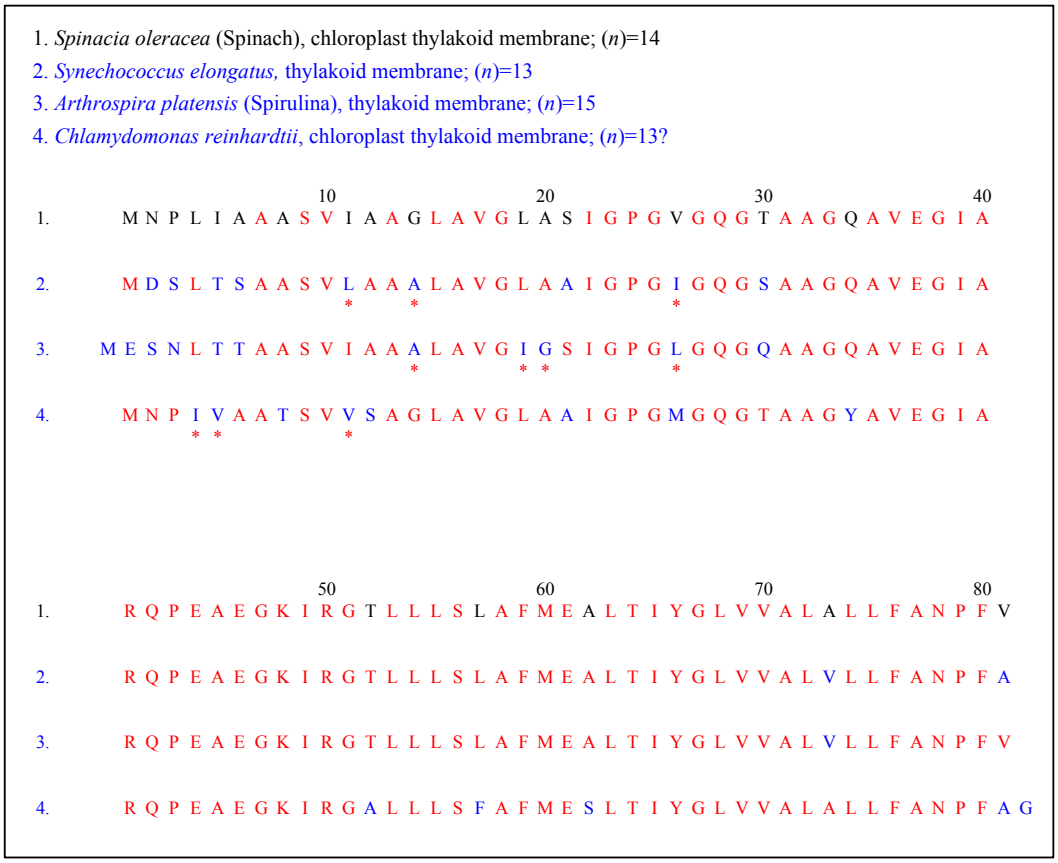

Figure 44. Alignment of the *S. oleracea* c_{14} sequence to the other three photosynthetic c subunit sequences. These sequences are highly similar, so slight differences in the sequence revealed by alignment are key hypothetical positions that determine the value of (*n*).

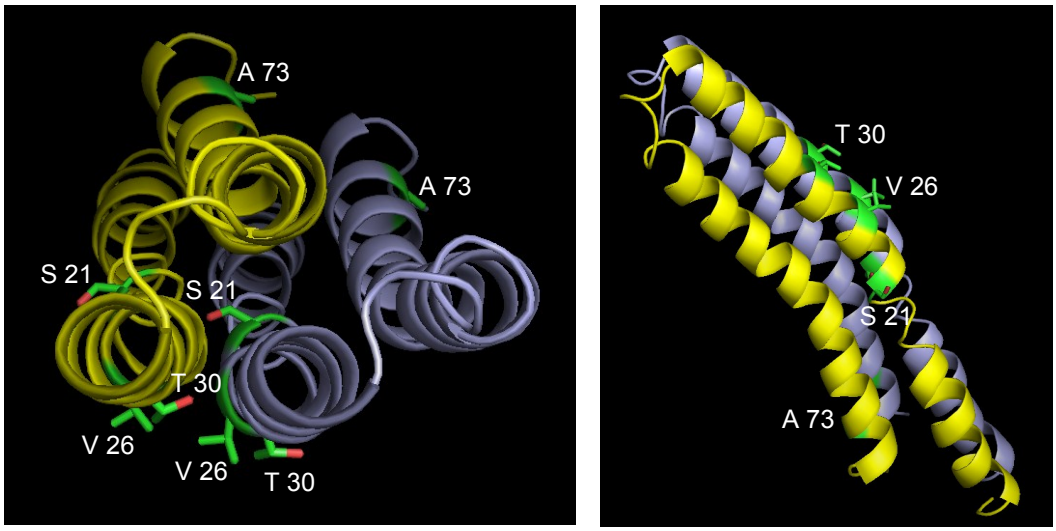

Figure 45. Structural arrangement of amino acids that may be influential in determining the stoichiometry of the spinach c_{14} ring. Two adjacent subunits are shown in these images, which were created using PyMol software (Schrödinger) with the protein data bank file (PDB ID: 2W5J) for the published *S. oleracea* c_{14} ring structure [77].

Another variable that can be investigated is the effect of the lipid membrane composition, which varies among organisms. Thylakoid membranes are typically composed of the following phospholipid proportions: 50% monogalactosyldiacyl-glycerol (MGDG), 30% digalactosyldiacyl-glycerol (DGDG), 5-12% sulfoquinovosyldiacyl-glycerol (SQDG), and 5-12% phosphatidyl-glycerol (PG). This proportion is conserved for most oxygenic photosynthetic organisms [88]. The lipid environment can easily be customized accordingly, or as otherwise desired during the reconstitution steps. This would be a worthwhile experiment to pursue, as it may have a stabilizing effect on the reconstituted ring. For instance, it has been reported that phospholipids from the thylakoid membrane are present in the structure of Photosystems II, where they act as cofactors to stabilize the

structure and influence the function [88]. And so it is not unreasonable to hypothesize that the lipid association may similarly have an effect on c-ring stoichiometry or stability.

In order to investigate the influence of adjacent subunits, particularly the γ-subunit and a-subunit, hybrid complexes can theoretically be reconstituted into liposomes and proton flux can be measured and correlated to ATP synthesis. *P. modestum* F_0 and *E. coli* F_1 hybrid complexes have been produced, and are reportedly active in ion transport and ATP synthesis [89]. Reconstitution of the complexes into liposomes and measurement of ion flow and ATP synthesis rates under the pressure of a gradient can be measured [90]. A comparison of these rates for different hybrid complexes can be used to determine whether or not the adjacent subunits have an influence on the coupling ratio, which would presumably be caused by a variance in (n).

Because each of these experimental scenarios takes place in vitro, they are not possible in a native system. And this is why having a recombinant expression system for the c-ring is prerequisite for researching the interesting questions related to stoichiometry. New knowledge gleaned from such research could be of significant relevance to broader scientific topics including cellular metabolism and bioenergetics. The rate of ATP synthesis is a direct function of the number of c-subunits in the ring, and this rate can be a direct means of regulating a long list of metabolic processes that are ATP dependent.

6.3. Expression and purification of other membrane proteins

There is currently much demand for new methods to recombinantly express membrane proteins in *E. coli*. This is motivated partly because membrane proteins are physiologically important and therefore often targets for therapeutic applications, and in part because they are inherently difficult to produce in amounts large enough for most studies [84, 91]. Given that the methods reported here proved effective for the spinach chloroplast c-subunit, it is likely that the methods can successfully be applied to other small hydrophobic membrane proteins as well, both eukaryotic and prokaryotic. Of particular interest are the c-subunits from other organisms which have not yet been characterized. The c-subunits found in other plant chloroplasts or in cyanobacteria are probably the most applicable to this system, given that they probably are the most homologous to the spinach c-subunit.

6.4. Determination of unknown stoichiometries

An understanding of how different factors influence ring stoichiometry can provide a reliable foundation for the determination of unknown stoichiometries in vitro. Only a handful of stoichiometries have been determined since the late 1990's because there are significant limitations in how much c-subunit can be extracted and purified in a native organism, and some organisms are not amenable to the established extraction and purification techniques. And so an alternative approach by means of recombinant expression, purification, reconstitution, and

AFM characterization would possibly be an option. Of course, the reliability of this proposed approach is contingent on the ability to develop and prove the process for c-rings of known stoichiometries first.

6.5. Crystallographic studies

The crystal structure for the spinach chloroplast c_{14} ring was published in 2009 with a resolution of 3.8 Å [77]. However, this structure was determined by using a symmetry-based computational model for phasing rather than direct experimental phase data. In the Fromme lab at Arizona State University, methods have been established for the crystallography of the spinach c_{14} ring as well, and diffraction has been detected to a resolution of up to 2.8 Å [41]. However, experimental phase data is lacking, which means that structure determination is unreliably dependent on known homologous c_n ring structures. A native spinach chloroplast c_{14} crystal is shown in Figure 46, as reported by Varco-Merth et al. [41]. In this image, the pigment association is apparent due to the typical yellow-green hue of the crystal.

An additional application of recombinant expression methods is the use of in vivo heavy atom labeling techniques which have been established for the purpose of determining the phases directly from the crystal diffraction using the multi-wavelength anomalous dispersion (MAD) technique [92]. Applying this technique with a recombinantly produced c_{14} ring would enable the determination of the experimental phases. In combination with the native diffraction data that

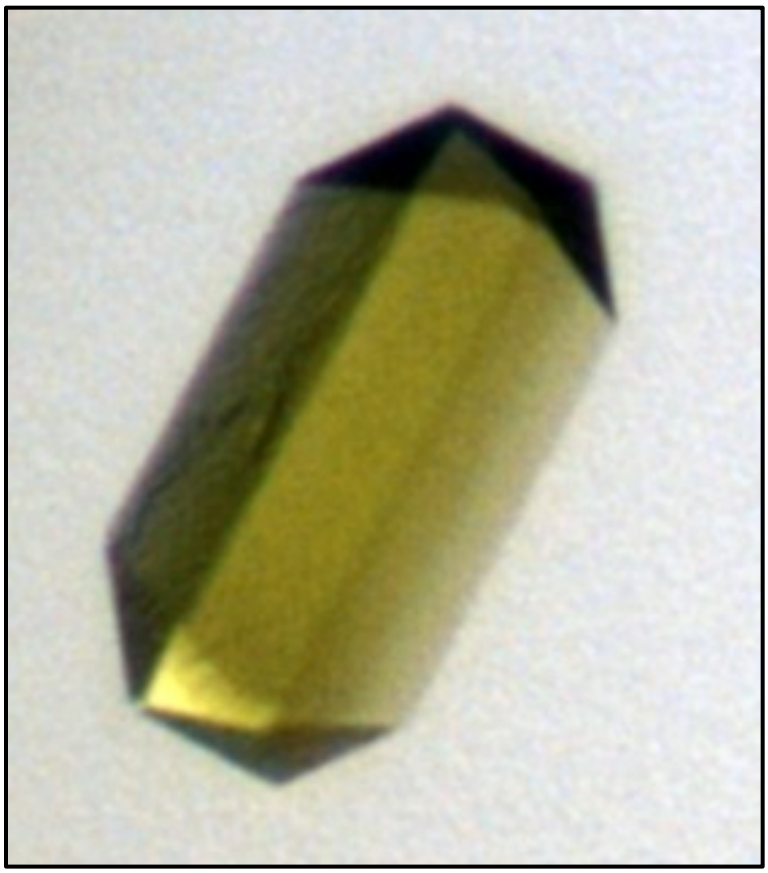

Figure 46. A crystal prepared from purified native spinach chloroplast ATP synthase c_{14} ring, as reported by Varco-Merth, et al. [41]. Similar crystal conditions could possibly be used for a recombinant c_{14} ring.

has heretofore been collected, the phase determination would likely result in an improved 2.8 Å structure of the c_{14} ring. Hypothetically, if this strategy can be proven with the determined c_{14} ring, it could potentially have application to other c-subunit rings to determine stoichiometry as well as atomic resolution 3-dimensional models.

6.6. Roadmap summary

As with the prior development of steps involved in expression, purification and reconstitution, the path toward understanding how ring stoichiometry is regulated will be influenced by several possible experimental outcomes. Developing a refined AFM technique is essential in order to conclusively determine the value of (n) in the recombinant spinach chloroplast c-ring. If (n) is a value other than 14, then further experimentation will lead to different reconstitution approaches, or the investigation of the involvement of a possible chaperone in the proteome of the spinach chloroplast. If (n) is 14, then reconstitution experiments can be directed toward improving the stability of the ring in SDS. Regardless of stability in SDS, the recombinant c_{14} ring may still be suitable for crystallographic studies. Also, based on the successful production of a c_{14} ring, additional plasmids could be designed to express c-subunits from other organisms, or mutations of *atpH* for the purpose of investigating the effect of amino acid substitutions at chosen positions. A roadmap of these possible routes toward understanding the structural influences of the c-ring is outlined in the flow diagram in Figure 47.

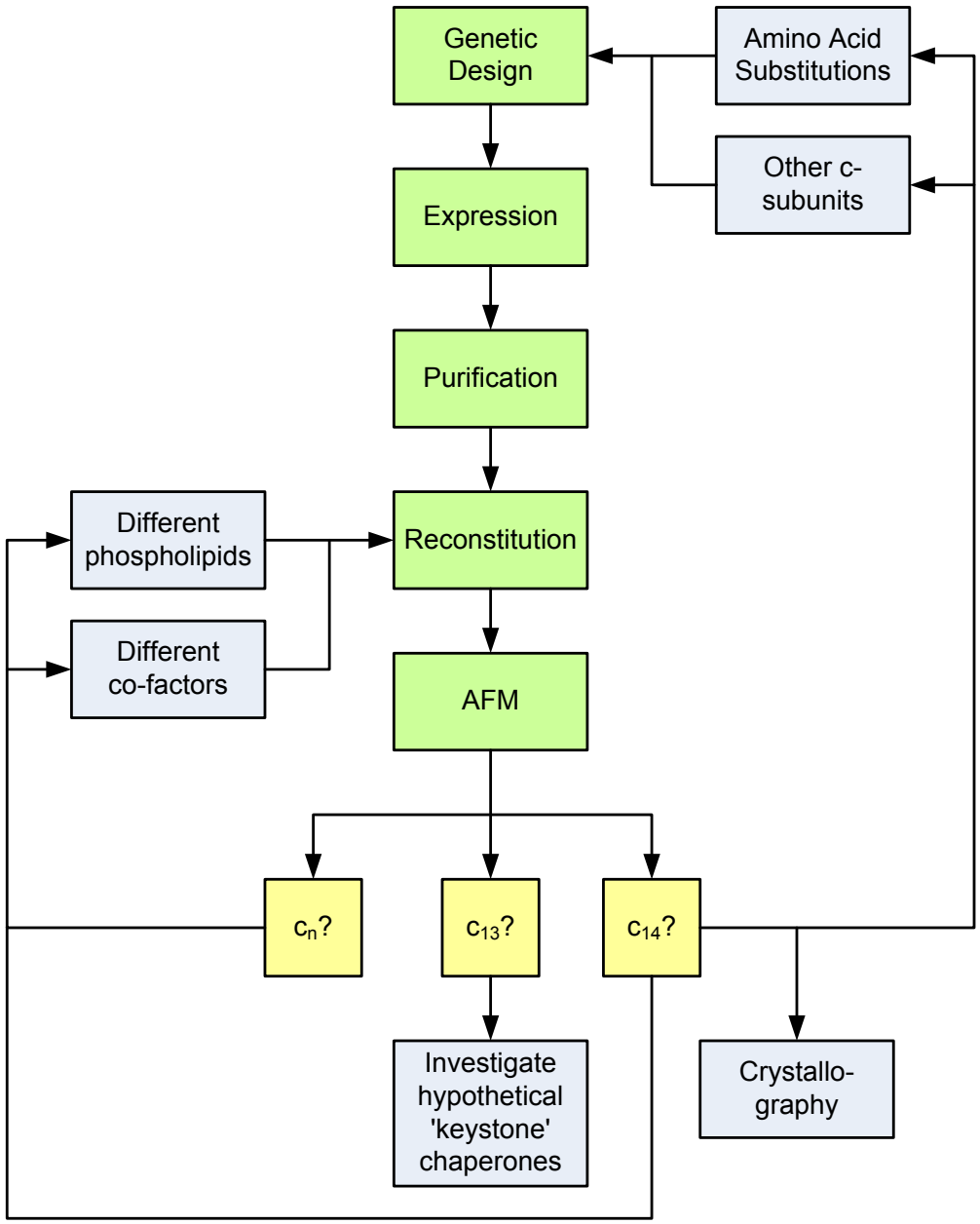

Figure 47. A roadmap flow diagram incorporating the future plans and applications for the recombinant c-ring, which could help define the factors that determine ring stoichiometry.

Chapter 7

CONCLUDING REMARKS

The combination of methods reported here has produced significant quantities of purified recombinant spinach chloroplast ATP synthase c_1 subunit. Approximately 0.4 mg of highly purified monomeric c-subunit can routinely be obtained from 2 L of cell culture – a volume that can easily be scaled up if needed. Most critical to achieving this result was the use of the maltose binding protein for expression and initial purification, the use of n-β-dodecyl-D-maltoside in the protease cleavage reaction, and the use of a reversed phase column in combination with ethanol as an eluent for final purification. Also important was the careful use of the analytical techniques described. Each step related to the expression and purification as reported has been repeated multiple times, and has been proven to yield very reproducible results. Results with reconstitution as described here are also reproducible. The objective of producing a stable c_{14} or c_n ring from the recombinantly expressed chloroplast monomer appears promising based on the reported results, but will require further experimentation and development of physical characterization methods.

The intention of the work described in this dissertation is to provide a foundation for experiments that can be designed to investigate the factors that determine ATP synthase c-ring stoichiometry. Such experimental investigations can be developed further from the various hypotheses proposed throughout this

dissertation. The experimental results will likely raise further important and interesting questions that will drive the perpetual scientific process forward, toward ultimately gaining a broader comprehension of metabolic regulation, as it relates to the ATP synthase.

REFERENCES

1. Fromme P (ed.): **Photosynthetic Protein Complexes**: Wiley-Blackwell; 2008.

2. Kaim G, Dimroth P: **ATP synthesis by F-type ATP synthase is obligatorily dependent on the transmembrane voltage**. *EMBO J* 1999, **18**(15):4118-4127.

3. Nakamoto RK, Scanlon JAB, Al-Shawi MK: **The rotary mechanism of the ATP synthase**. *Archives Biochem Biophys* 2008, **476**(1):43-50.

4. Fillingame RH, Angevine CM, Dmitriev OY: **Mechanics of coupling proton movements to c-ring rotation in ATP synthase**. *FEBS Lett* 2003, **555**(1):29-34.

5. Richter ML, Samra HS, He F, Giessel AJ, Kuczera KK: **Coupling proton movement to ATP synthesis in the chloroplast ATP synthase**. *J Bioenerg Biomembr* 2005, **37**(6):467-473.

6. Turina P, Samoray D, Graber P: **H^+/ATP ratio of proton transport-coupled ATP synthesis and hydrolysis catalysed by CF_0F_1 liposomes**. *EMBO J* 2003, **22**(3):418-426.

7. von Ballmoos C, Cook GM, Dimroth P: **Unique rotary ATP synthase and its biological diversity**. *Ann Rev Biophys* 2008, **37**:43-64.

8. Meier T, Polzer P, Diederichs K, Welte W, Dimroth P: **Structure of the rotor ring of F-type Na+-ATPase from *Ilyobacter tartaricus***. *Science* 2005, **308**(5722):659-662.

9. Tittingdorf J, Rexroth S, Schafer E, Schlichting R, Giersch C, Dencher NA, Seelert H: **The stoichiometry of the chloroplast ATP synthase oligomer III in *Chlamydomonas reinhardtii* is not affected by the metabolic state**. *Biochim Biophys Acta Biomembr* 2004, **1659**(1):92-99.

10. Pogoryelov D, Reichen C, Klyszejko AL, BrunisholZ R, Muller DJ, Dimroth P, Meier T: **The oligomeric state of c rings from cyanobacterial F-ATP synthases varies from 13 to 15**. *J Bacteriol* 2007, **189**(16):5895-5902.

11. Muller DJ, Dencher NA, Meier T, Dimroth P, Suda K, Stahlberg H, Engel A, Seelert H, Matthey U: **ATP synthase: constrained stoichiometry of the transmembrane rotor**. *FEBS Lett* 2001, **504**(3):219-222.

12. von Ballmoos C, Wiedenmann A, Dimroth P: **Essentials for ATP synthesis by F_1F_0 ATP synthases**. *Annu Rev Biochem* 2009, **78**:649-672.

13. Watt IN, Montgomery MG, Runswick MJ, Leslie AGW, Walker JE: **Bioenergetic cost of making an adenosine triphosphate molecule in animal mitochondria**. *Proc Natl Acad Sci USA* 2010, **107**(39):16823-16827.

14. Cross RL, Muller V: **The evolution of A-, F-, and V-type ATP synthases and ATPases: reversals in function and changes in the H^+/ATP coupling ratio**. *FEBS Lett* 2004, **576**(1-2):1-4.

15. Stock D, Leslie AGW, Walker JE: **Molecular architecture of the rotary motor in ATP synthase**. *Science* 1999, **286**(5445):1700-1705.

16. Jiang WP, Hermolin J, Fillingame RH: **The preferred stoichiometry of c subunits in the rotary motor sector of *Escherichia coli* ATP synthase is 10**. *Proc Natl Acad Sci USA* 2001, **98**(9):4966-4971.

17. Meier T, Matthey U, von Ballmoos C, Vonck J, von Nidda TK, Kuhlbrandt W, Dimroth P: **Evidence for structural integrity in the undecameric c-rings isolated from sodium ATP synthases**. *J Mol Biol* 2003, **325**(2):389-397.

18. Preiss L, Yildiz O, Hicks DB, Krulwich TA, Meier T: **A New Type of Proton Coordination in an F_1F_o-ATP Synthase Rotor Ring**. *PLoS Biol* 2010, **8**(8):10.

19. Seelert H, Dencher NA, Muller DJ: **Fourteen protomers compose the oligomer III of the proton-rotor in spinach chloroplast ATP synthase**. *J Mol Biol* 2003, **333**(2):337-344.

20. Pogoryelov D, Yu JS, Meier T, Vonck J, Dimroth P, Muller DJ: **The c(15) ring of the *Spirulina platensis* F-ATP synthase: F_1/F_0 symmetry mismatch is not obligatory**. *EMBO Rep* 2005, **6**(11):1040-1044.

21. Eddy SR: **Where did the BLOSUM62 alignment score matrix come from?** *Nat Biotechnol* 2004, **22**(8):1035-1036.

22. Cohen SN, Chang ACY: **Recircularization and autonomous replication of a sheared R-factor DNA segment in Escherichia coli transformants - (Plasmid transformation antibiotic resistance DNA)**. *Proceedings of the National Academy of Sciences of the United States of America* 1973, **70**(5):1293-1297.

23. Bergmans HEN, Vandie IM, Hoekstra WPM: **Transformation in *Escherichia coli* - Stages in the process**. *Journal of Bacteriology* 1981, **146**(2):564-570.

24. Weston A, Brown MGM, Perkins HR, Saunders JR, Humphreys GO: **Transformation of *Escherichia coli* with plasmid deoxyribonucelic-acid - Calcium-induced binding of deoxyribonucleic-acid to whole cells and to isolated membrane fractions**. *Journal of Bacteriology* 1981, **145**(2):780-787.

25. Dumon-Seignovert L, Cariot G, Vuillard L: **The toxicity of recombinant proteins in Escherichia coli: A comparison of overexpression in BL21(DE3), C41(DE3), and C43(DE3)**. *Protein Expression Purif* 2004, **37**(1):203-206.

26. Jana S, Deb JK: **Strategies for efficient production of heterologous proteins in *Escherichia coli***. *Appl Microbiol Biotechnol* 2005, **67**(3):289-298.

27. Neophytou I, Harvey R, Lawrence J, Marsh P, Panaretou B, Barlow D: **Eukaryotic integral membrane protein expression utilizing the Escherichia coli glycerol-conducting channel protein (GlpF)**. *App Microbiol Biotechnol* 2007, **77**(2):375-381.

28. Marblestone JG, Edavettal SC, Lim Y, Lim P, Zuo X, Butt TR: **Comparison of SUMO fusion technology with traditional gene fusion systems: Enhanced expression and solubility with SUMO**. *Protein Sci* 2006, **15**(1):182-189.

29. Miroux B, Walker JE: **Over-production of proteins in Escherichia coli: Mutant hosts that allow synthesis of some membrane proteins and globular proteins at high levels**. *J Mol Biol* 1996, **260**(3):289-298.

30. Schwarz D, Junge F, Durst F, Frolich N, Schneider B, Reckel S, Sobhanifar S, Dotsch V, Bernhard F: **Preparative scale expression of membrane proteins in Escherichia coli-based continuous exchange cell-free systems**. *Nat Protoc* 2007, **2**(11):2945-2957.

31. Ferreira GC, Pedersen PL: **Overexpression of higher eukaryotic membrane-proteins in bacteria - Novel Insights obtained with the liver mitochondrial proton phosphate symporter**. *J Biol Chem* 1992, **267**(8):5460-5466.

32. Burkovski A, Deckershebestreit G, Altendorf K: **Expression of subunit-III of the ATP synthase from spinach chloroplasts in *Escherichia coli***. *FEBS Lett* 1990, **271**(1-2):227-230.

33. Wehrle F, Appoldt Y, Kaim G, Dimroth P: **Reconstitution of F_0 of the sodium ion translocating ATP synthase of *Propionigenium modestum* from its heterologously expressed and purified subunits**. *Eur J Biochem* 2002, **269**(10):2567-2573.

34. Meier T, Yu JS, Raschle T, Henzen F, Dimroth P, Muller DJ: **Structural evidence for a constant c(11) ring stoichiometry in the sodium F-ATP synthase**. *FEBS J* 2005, **272**(21):5474-5483.

35. Ataullakhanov FI, Vitvitsky VM: **What determines the intracellular ATP concentration**. *Biosci Rep* 2002, **22**(5-6):501-511.

36. Dimroth P, von Ballmoos C, Meier T: **Catalytic and mechanical cycles in F-ATP synthases - Fourth in the cycles review series**. *EMBO Rep* 2006, **7**(3):276-282.

37. Birkenhager R, Greie JC, Altendorf K, Deckers-Hebestreit G: **F0 complex of the Escherichia coli ATP synthase - Not all monomers of the subunit c oligomer are involved in F1 interaction**. *Eur J Biochem* 1999, **264**(2):385-396.

38. Fillingame RH, Divall S, Skulachev V, Poole RK, Booth IR, Dimroth MJ, Padan E, Cook GM, Schafer G, Quivey RG *et al*: **Proton ATPases in bacteria: comparison to Escherichia coli F1F0 as the prototype**. In: *Bacterial Response to pH.* Edited by Chadwick D, Cardew G, vol. 221. Chichester: John Wiley & Sons Ltd; 1999: 218-234.

39. Ballhausen B, Altendorf K, Deckers-Hebestreit G: **Constant c(10) Ring Stoichiometry in the Escherichia coli ATP Synthase Analyzed by Cross-Linking**. *J Bacteriol* 2009, **191**(7):2400-2404.

40. Matthies D, Preiss L, Klyszejko AL, Muller DJ, Cook GM, Vonck J, Meier T: **The c13 Ring from a Thermoalkaliphilic ATP Synthase Reveals an Extended Diameter Due to a Special Structural Region**. *J Mol Biol* 2009, **388**(3):611-618.

41. Varco-Merth B, Fromme R, Wang MT, Fromme P: **Crystallization of the c(14)-rotor of the chloroplast ATP synthase reveals that it contains pigments**. *Biochim Biophys Acta Bioenerg* 2008, **1777**(7-8):605-612.

42. Winterma.Jf, Helmsing PJ, Polman BJJ, Vangisbe.J, Collard J: **Galactolipid transformations and photochemical activities of spinach chloroplasts**. *Biochim Biophys Acta* 1969, **189**(1):95-&.

43. Hudson GS, Mason JG, Holton TA, Koller B, Cox GB, Whitfeld PR, Bottomley W: **A gene cluster in the spinach and pea chloroplast genomes encoding one CF_1 and 3 CF_0 subunits of the H^+ ATP synthase complex and the ribosomal protein S2**. *J Mol Biol* 1987, **196**(2):283-298.

44. Schmitz-Linneweber C, Maier RM, Alcaraz JP, Cottet A, Herrmann RG, Mache R: **The plastid chromosome of spinach (*Spinacia oleracea*): complete nucleotide sequence and gene organization**. *Plant Mol Biol* 2001, **45**(3):307-315.

45. Kane JF: **Effects of rare codon clusters on high-level expression of heterologous proteins in *Escherichia coli***. *Curr Opin Biotechnol* 1995, **6**(5):494-500.

46. Welch M, Govindarajan S, Ness JE, Villalobos A, Gurney A, Minshull J, Gustafsson C: **Design parameters to control synthetic gene expression in *Escherichia coli***. *PLoS One* 2009, **4**(9).

47. Studier FW, Moffatt BA: **Use of bacteriophage T7 RNA-polymerase to direct selective high-level expression of cloned genes**. *J Mol Biol* 1986, **189**(1):113-130.

48. Studier FW, Rosenberg AH, Dunn JJ, Dubendorff JW: **Use of T7 RNA polymerase to direct expression of cloned genes**. *Methods Enzymol* 1990, **185**:60-89.

49. Deboer HA, Comstock LJ, Vasser M: **The tac promoter - a functional hybrid derived from the *trp* and *lac* promoters**. *PNAS-Biol Sci* 1983, **80**(1):21-25.

50. Kellermann OK, Ferenci T: **Maltose binding protein from *Escherichia coli***. *Methods Enzymol* 1982, **90**:459-463.

51. Kapust RB, Waugh DS: ***Escherichia coli* maltose-binding protein is uncommonly effective at promoting the solubility of polypeptides to which it is fused**. *Protein Sci* 1999, **8**(8):1668-1674.

52. Sorensen HP, Mortensen KK: **Soluble expression of recombinant proteins in the cytoplasm of Escherichia coli**. *Microbial Cell Factories* 2005, **4**.

53. Schumann W, Ferreira LCS: **Production of recombinant proteins in Escherichia coli**. *Genet Mol Biol* 2004, **27**(3):442-453.

54. Dower WJ, Miller JF, Ragsdale CW: **High efficiency transformation of Escherichia coli by high voltage electroporation**. *Nucleic Acids Res* 1988, **16**(13):6127-6145.

55. de Marco A, Deuerling E, Mogk A, Tomoyasu T, Bukau B: **Chaperone-based procedure to increase yields of soluble recombinant proteins produced in *E. coli***. *BMC Biotechnol* 2007, **7**.

56. Castanie HP, Berges H, Oreglia J, Prere MF, Fayet O: **A set of pBR322-compatible plasmids allowing the testing of chaperone-assisted folding of proteins overexpressed in *Escherichia coli***. *Anal Biochem* 1997, **254**(1):150-152.

57. Jenny RJ, Mann KG, Lundblad RL: **A critical review of the methods for cleavage of fusion proteins with thrombin and Factor Xa**. *Protein Expr Purif* 2003, **31**(1):1-11.

58. Greenfield NJ: **Using circular dichroism spectra to estimate protein secondary structure**. *Nat Protoc* 2006, **1**(6):2876-2890.

59. Johnson WC: **Analyzing protein circular dichroism spectra for accurate secondary structures**. *Proteins* 1999, **35**(3):307-312.

60. Sreerama N, Woody RW: **Estimation of protein secondary structure from circular dichroism spectra: Comparison of CONTIN, SELCON, and CDSSTR methods with an expanded reference set**. *Anal Biochem* 2000, **287**(2):252-260.

61. Sreerama N, Woody RW: **On the analysis of membrane protein circular dichroism spectra**. *Protein Sci* 2004, **13**(1):100-112.

62. Dmitriev OY, Altendorf K, Fillingame RH: **Reconstitution of the F_0 complex of *Escherichia coli* ATP synthase from isolated subunits**. *Eur J Biochem* 1995, **233**(2):478-483.

63. Cousins KR, Pierson KM: **A simplified method for the microscale extraction of pigments from spinach**. *J Chem Educ* 1998, **75**(10):1268-1269.

64. Porra RJ, Thompson WA, Kriedemann PE: **Determination of accurate extinction coefficients and simultaneous-equations for assaying chlorophyll-a and chlorophyll-b extracted with 4 different solvents - verification of the concentration of chlorophyll standards by atomic-absorbtion spectroscopy**. *Biochim Biophys Acta* 1989, **975**(3):384-394.

65. Eijckelhoff C, Dekker JP: **Determination of the pigment stoichiometry of the photochemical-reaction center of photosystem-II**. *Biochimi Biophys Acta, Bioenerg* 1995, **1231**(1):21-28.

66. Fromme P, Boekema EJ, Graber P: **Isolation and characterization of a supramolecular complex of subunit-III of the ATP synthase from chloroplasts**. *Z Naturforschl, C Biosci* 1987, **42**(11-12):1239-1245.

67. Wittig I, Karas M, Schagger H: **High resolution clear native electrophoresis for In-gel functional assays and fluorescence studies of membrane protein complexes**. *Mol Cell Proteom* 2007, **6**(7):1215-1225.

68. Schagger H: **Tricine-SDS-PAGE**. *Nat Protocol* 2006, **1**(1):16-22.

69. Markwell MAK, Haas SM, Bieber LL, Tolbert NE: **Modification of Lowry procedure to simplify protein determination in membrane and lipoprotein samples**. *Anal Biochem* 1978, **87**(1):206-210.

70. Egea PF, Stroud RM, Walter P: **Targeting proteins to membranes: structure of the signal recognition particle**. *Curr Opin Struct Biol* 2005, **15**(2):213-220.

71. Clerico EM, Maki JL, Gierasch LM: **Use of synthetic signal sequences to explore the protein export machinery**. *Biopolymers* 2008, **90**(3):307-319.

72. Neumann-Haefelin C, Schafer U, Muller W, Koch HG: **SRP-dependent co-translational targeting and SecA-dependent translocation analyzed as individual steps in the export of a bacterial protein**. *EMBO J* 2000, **19**(23):6419-6426.

73. Scopes RK: **Protein purification: principles and practice**: Springer; 1993.

74. Schneider E, Altendorf K: **All three subunits are required for the reconstitution of an active proton channel (F0) of *Escherichia coli* ATP synthase (F1F0)**. *Embo Journal* 1985, **4**(2):515-518.

75. Greenfield NJ: **Using circular dichroism spectra to estimate protein secondary structure**. *Nat Protoc* 2006, **1**(6):2876-2890.

76. Girvin ME, Rastogi VK, Abildgaard F, Markley JL, Fillingame RH: **Solution structure of the transmembrane H+-transporting subunit c of the F1F0 ATP synthase**. *Biochemistry* 1998, **37**(25):8817-8824.

77. Vollmar M, Schlieper D, Winn M, Buchner C, Groth G: **Structure of the c(14) rotor ring of the proton translocating chloroplast ATP synthase**. *J Biol Chem* 2009, **284**(27):18228-18235.

78. Pogoryelov D, Yildiz O, Faraldo-Gomez JD, Meier T: **High-resolution structure of the rotor ring of a proton-dependent ATP synthase**. *Nat Struct Mol Biol* 2009, **16**(10):1068-1073.

79. Raghava GPS: **A combination method for protein secondary structure prediction based on neural network and example based learning**. *CASP5* 2002, **A-132**.

80. Suzuki T, Ozaki Y, Sone N, Yoshida M: **Role of propionigenium modestum uncI gene in FOF1-ATP synthase: uncI is a molecular chaperon that assists c11-ring assembly**. *Biochim Biophys Acta Bioenerg* 2006:323-323.

81. Ozaki Y, Suzuki T, Kuruma Y, Ueda T, Yoshida M: **UncI protein can mediate ring-assembly of c-subunits of FoF1-ATP synthase in vitro**. *Biochem Biophys Res Commun* 2008, **367**(3):663-666.

82. Arechaga I, Jonathan P, Butler G, Walker JE: **Self-assembly of ATP synthase subunit c rings**. *FEBS Lett* 2002, **515**(1-3):189-193.

83. Studier FW: **Protein production by auto-induction in high-density shaking cultures**. *Protein Expression Purif* 2005, **41**(1):207-234.

84. Milhiet PE, Gubellini F, Berquand A, Dosset P, Rigaud JL, Le Grimellec C, Levy D: **High-resolution AFM of membrane proteins directly incorporated at high density in planar lipid bilayer**. *Biophys J* 2006, **91**(9):3268-3275.

85. Pogoryelov D, Yu JS, Meier T, Vonck J, Dimroth P, Muller DJ: **The c(15) ring of the Spirulina platensis F-ATP synthase: F-1/F-0 symmetry mismatch is not obligatory**. *EMBO Rep* 2005, **6**(11):1040-1044.

86. Stahlberg H, Muller DJ, Suda K, Fotiadis D, Engel A, Meier T, Matthey U, Dimroth P: **Bacterial Na+-ATP synthase has an undecameric rotor**. *EMBO Rep* 2001, **2**(3):229-233.

87. Seelert H, Poetsch A, Dencher NA, Engel A, Stahlberg H, Muller DJ: **Structural biology - Proton-powered turbine of a plant motor**. *Nature* 2000, **405**(6785):418-419.

88. Loll B, Kern J, Saenger W, Zouni A, Biesiadka J: **Lipids in photosystem II: Interactions with protein and cofactors**. *Biochim Biophys Acta Bioenerg* 2007, **1767**(6):509-519.

89. Kaim G, Dimroth P: **A double mutation in subunit-c of the Na+ specific F1F0-ATPase of Propionigenium modestum results in a switch from Na+ to H+ coupled ATP synthesis in the Escherichia coli host cell**. *J Mol Biol* 1995, **253**(5):726-738.

90. Grotjohann I, Graber P: **The H+-ATPase from chloroplasts: effect of different reconstitution procedures on ATP synthesis activity and on phosphate dependence of ATP synthesis**. *Biochim Biophys Acta Bioenerg* 2002, **1556**(2-3):208-216.

91. Sahdev S, Khattar SK, Saini KS: **Production of active eukaryotic proteins through bacterial expression systems: a review of the existing biotechnology strategies**. *Mol Cell Biochem* 2008, **307**(1-2):249-264.

92. Strub MP, Hoh F, Sanchez JF, Strub JM, Bock A, Aumelas A, Dumas C: **Selenomethionine and selenocysteine double labeling strategy for crystallographic phasing**. *Structure* 2003, **11**(11):1359-1367.

APPENDIX A

COMMERCIAL BUFFER COMPOSITION

T4 Polynucleotide Kinase Buffer A (Fermentas, EK0031)

500 mM Tris-HCl (pH 7.6 at 25°C)

100 mM $MgCl_2$

50 mM DTT

1 mM spermidine

DNA Ligase Reaction Buffer, 5X (Invitrogen, 15224-017)

250 mM Tris-HCl (pH 7.6)

50 mM MgCl2

5 mM ATP

5 mM DTT

25% (w/v) polyethylene glycol-8000

Phusion High Fidelity Polymerase Buffer, 5X (New England Biolabs, F-530S)

Proprietary mixture containing 7.5 mM $MgCl_2$

Thermoscript Reverse Transcriptase Buffer, 5X (Invitrogen, 12236-014)

250 mM Tris acetate, pH 8.4

375 mM potassium acetate

40 mM magnesium acetate

APPENDIX B

WIZARD SV GEL AND PCR CLEAN-UP KIT

PROMEGA, A9281

PRODUCT INSTRUCTIONS

The following pages are taken from the product instruction manual for the Promega Wizard SV Gel and PCR Clean-Up kit. This kit was used for the extraction and purification of DNA fragments from agarose gels. In summary, agarose gel fragments containing the desired DNA band were excised and dissolved in Membrane Binding Solution by heating. The dissolved DNA is bound to a silica membrane in the SV Mini-column by centrifugation. DNA binds to this substrate in the presence of chaotropic salts, which are present in the Membrane Binding Solution. DNA remains bound in the presence of ethanol and salts in the Membrane Wash Solution which is used to wash non-binding compounds. The DNA fragments are then is eluted from the column by washing water through the silica membrane by a final centrifugation step. Steps 4B and 5A from the following pages were used. The final page includes a list and contents of the buffers included in this kit.

From: Promega™ Corporation

Promega

4.B. Dissolving the Gel Slice

1. Load and run the gel using an established protocol. DNA can be extracted from standard or low-melt agarose gels run with either TAE or TBE buffer.
2. Weigh a 1.5ml microcentrifuge tube for each DNA fragment to be isolated and record the weight.
3. Visualize and photograph the DNA using a long-wavelength UV lamp and an intercalating dye such as ethidium bromide. To reduce nicking, irradiate the gel for the absolute minimum time possible (1–4). Excise the DNA fragment of interest in a minimal volume of agarose using a clean scalpel or razor blade. Transfer the gel slice to the weighed microcentrifuge tube and record the weight. Subtract the weight of the empty tube from the total weight to obtain the weight of the gel slice (see Notes 1–3 below).

   Note: The gel slice may be stored at 4°C or at –20°C for up to one week in a tightly closed tube under nuclease-free conditions before purification.
4. Add Membrane Binding Solution at a ratio of 10µl of solution per 10mg of agarose gel slice.
5. Vortex the mixture (see Note 4) and incubate at 50–65°C for 10 minutes or until the gel slice is completely dissolved. Vortex the tube every few minutes to increase the rate of agarose gel melting. Centrifuge the tube briefly at room temperature to ensure the contents are at the bottom of the tube. Once the agarose gel is melted, the gel will not resolidify at room temperature.
6. To purify the DNA using a microcentrifuge, proceed to Section V.A. To purify the DNA using a vacuum manifold, proceed to Section V.B.

Notes:

1. Recovery from 1% high-melting-point agarose is comparable to that from 1–2% low-melting-point agarose. High-melting-point agarose concentrations of up to 3% have been tested. Gel slices with higher agarose concentrations (2–3%) may require a longer time to melt completely than a 1% agarose gel slice and may show reduced yields.
2. The maximum capacity of the column is 350mg of gel mass dissolved in 350µl of Membrane Binding Solution per column pass. For gel slices >350mg, continue to pass additional sample through the SV Minicolumn until all of the sample has been processed. The maximal amount of agarose that can be processed through a single column is approximately 3.5g (10 × 350mg) total.
3. The maximum binding capacity of the column is approximately 40µg per column, and as little as 10ng has been successfully purified.
4. DNA fragments that are larger than 5kb should be mixed gently to prevent shearing. Do not vortex if DNA fragment is larger than 5kb; mix by inversion.

Promega Corporation · 2800 Woods Hollow Road · Madison, WI 53711-5399 USA
Toll Free in USA 800-356-9526 · Phone 608-274-4330 · Fax 608-277-2516 · www.promega.com
Printed in USA. Part# TB308
Revised 12/10

From: Promega™ Corporation

Promega

4.C. Processing PCR Amplification Products

1. Amplify target of choice using standard amplification conditions.
2. Add an equal volume of Membrane Binding Solution to the PCR amplification (see Notes 1–4 below).
3. To purify the DNA using a microcentrifuge, proceed to Section 5.A.
   To purify the DNA using a vacuum manifold, proceed to Section 5.B.

Notes:

1. The maximal capacity of a single SV Minicolumn is approximately 1ml of PCR amplification added to 1ml Membrane Binding Solution (2ml total). For PCR volumes >350µl, continue to pass the sample through the column until all of the sample has been processed.
2. The maximum binding capacity is approximately 40µg per column, and as little as 10ng has been successfully purified.
3. Mineral oil does not interfere with purification.
4. For amplification reactions that do not produce a single product or where amplification has been inefficient and there is highly visible primer dimer, gel purification of the band of interest is recommended. Alternatively, an 80% ethanol wash solution can be substituted for the supplied Membrane Wash Solution to reduce primer-dimer carryover.

5. DNA Purification

Prepare the gel slice or PCR product as described in Section 4. Use either the centrifugation procedure (Section 5.A) or the vacuum procedure (Section 5.B) to recover the DNA from the dissolved gel slice or PCR amplification. After the procedure is completed, the DNA may be used in downstream applications.

5.A. DNA Purification by Centrifugation

1. Place one SV Minicolumn in a Collection Tube for each dissolved gel slice or PCR amplification.
2. Transfer the dissolved gel mixture or prepared PCR product to the SV Minicolumn assembly and incubate for 1 minute at room temperature.
3. Centrifuge the SV Minicolumn assembly in a microcentrifuge at 16,000 × *g* (14,000rpm) for 1 minute. Remove the SV Minicolumn from the Spin Column assembly and discard the liquid in the Collection Tube. Return the SV Minicolumn to the Collection Tube.

Note: Failure to spin at 16,000 × *g* (14,000rpm) can result in reduced yield.

From: Promega™ Corporation

4. Wash the column by adding 700µl of Membrane Wash Solution, previously diluted with 95% ethanol (see Section 4.A), to the SV Minicolumn. Centrifuge the SV Minicolumn assembly for 1 minute at 16,000 × *g* (14,000rpm). Empty the Collection Tube as before and place the SV Minicolumn back in the Collection Tube. Repeat the wash with 500µl of Membrane Wash Solution and centrifuge the SV Minicolumn assembly for 5 minutes at 16,000 × *g*.

5. Remove the SV Minicolumn assembly from the centrifuge, being careful not to wet the bottom of the column with the flowthrough. Empty the Collection Tube and recentrifuge the column assembly for 1 minute with the microcentrifuge lid open (or off) to allow evaporation of any residual ethanol.

6. Carefully transfer the SV Minicolumn to a clean 1.5ml microcentrifuge tube. Apply 50µl of Nuclease-Free Water directly to the center of the column without touching the membrane with the pipette tip. Incubate at room temperature for 1 minute. Centrifuge for 1 minute at 16,000 × *g* (14,000rpm).

7. Discard the SV Minicolumn and store the microcentrifuge tube containing the eluted DNA at 4°C or –20°C.

Note: The volume of the eluted DNA will be approximately 42–47µl. If the DNA needs to be further concentrated, perform an ethanol precipitation. Alternatively, the DNA may be eluted in as little as 15µl of Nuclease-Free Water without significant reduction in yield. If using an elution volume of 15µl, verify that the membrane is completely covered with Nuclease-Free Water before centrifugation. Elution volumes less than 15µl are not recommended (see Table 3).

5.B. DNA Purification by Vacuum

1. Attach one Vacuum Adapter with a Luer-Lok® fitting to one port of the manifold (e.g., Vac-Man® or Vac-Man® Jr. Laboratory Vacuum Manifold) for each dissolved gel slice or PCR amplification. Insert SV Minicolumn into the Vacuum Adapter until it fits snugly in place.

2. Transfer the dissolved gel mixture or PCR amplification to the SV Minicolumn and incubate for 1 minute at room temperature. Apply a vacuum to pull the liquid completely through the SV Minicolumn.

   Note: The minimum vacuum pressure is 15 inches of mercury. See the table below for comparison of inches of Hg to other pressure measurements.

1 Inch Hg	15 Inches Hg
3.386kPa	50.8kPa
25.4Torr	381Torr
0.0334atm	0.501atm
0.491psi	7.37psi
2.54cm Hg	38.1cm Hg
33.86mbar	508mbar

From: Promega™ Corporation

7. References

1. Zimmermann, M., Veeck, J. and Wolf, K. (1998) Minimizing the exposure to UV light when extracting DNA from agarose gels. *BioTechniques* **25**, 586.
2. Hengen, P. (1997) Methods and reagents. Protecting vector DNA from UV light. *Trends Biochem. Sci.* **22**, 182–3.
3. Grundemann, D. and Schomig, E. (1996) Protection of DNA during preparative agarose gel electrophoresis against damage induced by ultraviolet light. *BioTechniques* **21**, 898–903.
4. Cariello, N.F. *et al.* (1988) DNA damage produced by ethidium bromide staining and exposure to ultraviolet light. *Nucl. Acids Res.* **16**, 4157.

8. Appendix

8.A. Composition of Buffers and Solutions

Membrane Wash Solution
(after ethanol addition)
10mM potassium acetate (pH 5.0)
80% ethanol
16.7µM EDTA (pH 8.0)

To prepare this solution, add 95% ethanol to the supplied Membrane Wash Solution (concentrated) as described in Table 2 in Section IV.A.

Membrane Binding Solution
4.5M guanidine isothiocyanate
0.5M potassium acetate (pH 5.0)

1X TE buffer
10mM Tris-HCl (pH 7.5)
1mM EDTA (pH 8.0)

1X TBE buffer
89mM Tris base
89mM boric acid
2mM EDTA (pH 8.0)

1X TAE buffer
40mM Tris base
5mM sodium acetate
1mM EDTA (pH 8.0)

Promega Corporation · 2800 Woods Hollow Road · Madison, WI 53711-5399 USA
Toll Free in USA 800-356-9526 · Phone 608-274-4330 · Fax 608-277-2516 · www.promega.com
Printed in USA.
Revised 12/10
Part# TB308

APPENDIX C

PHUSION HIGH-FIDELITY DNA POLYMERASE

NEW ENGLAND BIOLABS, F-530S

PRODUCT INSTRUCTIONS

The Phusion DNA Polymerase is highy-fidelity, meaning that the rate of random mutations in DNA copies generated is very low. As with other polymerase chain reactions, the use of this polymerase requires the inclusion of a buffer, forward and reverse primers for the target sequence, dNTP's, and template DNA. DMSO was not included in any reactions reported in this dissertation. The 5X HF Buffer that was used contains 7.5 mM $MgCl_2$ as noted, but likely contains other propriety compounds that are not disclosed. Recommended cycling conditions were followed according to the size of the DNA fragment that was being amplified.

From: New England BioLabs®

FINNZYMES

Phusion™

High-Fidelity DNA Polymerase

Product codes: F-530S, 100 U
F-530L, 500 U

NEW ENGLAND BioLabs Inc. Distributed by New England Biolabs, Inc.

Stable for one year from the assay date. Store at -20°C.

1. Introduction

Finnzymes' Phusion™ High-Fidelity DNA Polymerase offers extreme performance for all PCR applications. Incorporating an exciting new technology, Phusion DNA Polymerase brings together a novel *Pyrococcus*-like enzyme with a processivity-enhancing domain. The Phusion DNA Polymerase generates long templates with an accuracy and speed previously unattainable with a single enzyme, even on the most difficult templates. The extreme fidelity makes Phusion DNA Polymerase a superior choice for cloning. Using a *lacI*-based method modified from previous studies[1], the error rate of Phusion DNA Polymerase in Phusion HF Buffer is determined to be 4.4 x 10^{-7}, which is approximately 50-fold lower than that of *Thermus aquaticus* DNA polymerase, and 6-fold lower than that of *Pyrococcus furiosus* DNA polymerase.

Phusion DNA Polymerase possesses the following activities: 5´→3´ DNA polymerase activity and 3´→5´ exonuclease activity. It generates blunt ends in the amplification products. The polymerase is suitable also for amplification of long amplicons such as 7.5 kb genomic and 20 kb λ DNA used in Finnzymes' quality control assays.

Phusion™ DNA Polymerase is unlike other enzymes. Please read the Quick Guide to modify your protocol for optimal results!

Quick Guide:

- Use Phusion DNA Polymerase at 0.5-1.0 U per 50 µl reaction volume. Do not exceed 2 U/50 µl. (See 4.1)
- Use 15-30 s/kb for extension. Do not exceed 1 min/kb. (See 6.4)
- Use 98°C for denaturation. (See 6.1 & 6.2)
- Anneal at Tm+3°C (> 20nt) or use 2-step protocol. (See 6.3)
- Use 200 µM of each dNTP. Do not use dUTP. (See 4.3)
- Note: Phusion DNA Polymerase produces blunt end DNA products.

2. Package Information

F-530S	**100 U (2 U/µl)** Material provided: Phusion™ DNA Polymerase 100 U (50 µl), 5x Phusion™ HF Buffer (2 x 1.5ml), 5x Phusion™ GC Buffer (1.5 ml), DMSO (500 µl) and 50 mM $MgCl_2$-solution (1.5ml).
F-530L	**500 U (2 U/µl)** Material provided: Phusion™ DNA Polymerase 500 U (250 µl), 5x Phusion™ HF Buffer (6 x 1.5ml), 5x Phusion™ GC Buffer (2 x 1.5ml), DMSO (500 µl) and 50mM $MgCl_2$- solution (2 x1.5ml).

3. Guidelines for Using Phusion™ DNA Polymerase

Phusion DNA Polymerase (2U/µl) is provided with 5x Phusion HF Buffer and 5x Phusion GC Buffer. Both buffers contain 1.5 mM $MgCl_2$ at final reaction concentrations. Separate tubes of DMSO and 50 mM $MgCl_2$ solutions are provided for further optimization.

3.1 Basic reaction conditions for PCR amplifications

Carefully mix and centrifuge all tubes before opening to improve recovery. PCR reactions should be set up on ice. Prepare a master mix for the appropriate number of samples to be amplified. Phusion DNA Polymerase should be pipetted carefully and gently as the high glycerol content (50 %) in the storage buffer may otherwise lead to pipetting errors. It is critical that the Phusion DNA Polymerase is the last component added to the PCR mixture, since the enzyme exhibits 3´→5´ exonuclease activity that can degrade primers in the absence of dNTPs.

Table 1. Pipetting instructions (in order).

Component	Volume / 50 µl reaction	Volume / 20 µl reaction	Final conc.
H_2O	add to 50 µl	add to 20 µl	
5x Phusion HF Buffer*	10 µl	4 µl	1x
10 mM dNTPs	1 µl	0.4 µl	200 µM each
primer A**	x µl	x µl	0.5 µM
primer B**	x µl	x µl	0.5 µM
template DNA	x µl	x µl	
(DMSO***, optional)	(1.5 µl)	(0.6 µl)	(3 %)
Phusion DNA Polymerase	0.5 µl	0.2 µl	0.02U/µl

* Optionally 5x Phusion GC Buffer can be used, see section 4.2. for details.

** The recommendation for final primer concentration is 0.5 µM, but it can be varied in a range of 0.2-1.0 µM if needed.

*** Addition of DMSO is recommended for GC-rich amplicons. DMSO is not recommended for amplicons with very low GC % or amplicons that are >2Okb.

From: New England BioLabs®

4. Notes about Reaction Components

4.1 Enzyme

The optimal amount of enzyme depends on the amount of template and the length of the PCR product. Usually 1 unit of Phusion DNA Polymerase per 50 µl reaction volume gives good results, but optimal amounts could range from 0.5–2 units per 50 µl reaction depending on amplicon length and difficulty. **Do not exceed 2 U/50 µl (0.04 U/µl), especially for amplicons that are > 5kb.**

When cloning fragments amplified with Phusion DNA Polymerase, blunt end cloning is recommended. If TA cloning is required, it can be performed by adding A overhangs to the blunt PCR product with e.g. DyNAzyme™ II DNA Polymerase (F-501). However, before adding the overhangs it is very important to remove all the Phusion DNA Polymerase by purifying the PCR product carefully, as any remaining Phusion DNA Polymerase will degrade the A overhangs creating blunt ends again. A detailed protocol for TA cloning of Phusion PCR products can be found on Finnzymes' website (www.finnzymes.com).

4.2 Buffers

Two buffers are provided with the enzyme: 5x Phusion HF Buffer (F-518) and 5x Phusion GC Buffer (F-519). The error rate of Phusion DNA Polymerase in HF Buffer (4.4×10^{-7}) is lower than that in GC Buffer (9.5×10^{-7}). Therefore, the HF Buffer should be used as the default buffer for high-fidelity amplification. However, GC Buffer can improve the performance of Phusion DNA Polymerase on some difficult or long templates, i.e. GC-rich templates or those with complex secondary structures. Use of GC Buffer is recommended for those cases where amplification with HF Buffer has failed. For applications such as microarray or DHPLC, where the DNA templates need to be free of detergents, detergent-free reaction buffers (F-520, F-521) are available for Phusion DNA Polymerase.

4.3 Mg^{2+} concentration and dNTP concentration

Concentration of Mg^{2+} is critical since Phusion DNA Polymerase is a magnesium dependent enzyme. Excessive Mg^{2+} stabilizes the DNA double strand and prevents complete denaturation of DNA. Excess Mg^{2+} can also stabilize spurious annealing of primer to incorrect template sites and decrease specificity. Conversely, inadequate Mg^{2+} could lead to lower product yield. The optimal Mg^{2+} concentration will also depend on the dNTP concentration, the specific template DNA and the sample buffer composition. In general, the optimal Mg^{2+} concentration is 0.5 to 1 mM over the total dNTP concentration for standard PCR. If the primers and/or template contain chelators such as EDTA or EGTA, the apparent Mg^{2+} optimum may be shifted to higher concentrations. If further optimization is needed, increase Mg^{2+} concentration in 0.2 mM steps.

High quality dNTPs (e.g. F-560) should be used for optimal performance with Phusion DNA Polymerase. Use of dUTP and other dUTP-derivatives or analogues is not recommended. Due to the increased processivity of Phusion DNA Polymerase there is no advantage of increasing dNTP concentrations. For optimal results always use 200 µM of each dNTP.

4.4 Template

General guidelines are: 1 pg - 10 ng / 50 µl reaction with low complexity DNA (e.g. plasmid, lambda or BAC DNA); 50-250 ng/50 µl reaction with high complexity genomic DNA. If cDNA synthesis reaction mixture is used as a source of template, the volume of the template should not exceed 10 % of the final PCR reaction volume.

4.5 PCR additives

The recommended reaction conditions for GC-rich templates include 3 % DMSO as a PCR additive, which aids in the denaturing of templates with high GC contents. For further optimization DMSO should be varied in 2 % increments. In some cases DMSO may also be required for supercoiled plasmids to relax for denaturation. Other PCR additives such as formamide, glycerol, and betaine are also compatible with Phusion DNA Polymerase.

If high DMSO concentration is used, the annealing temperature must be lowered, as DMSO decreases the melting point of the primers. It has been reported that 10 % DMSO decreases the annealing temperature by 5.5-6.0°C[2].

5. Cycling Conditions

Due to the novel nature of Phusion DNA Polymerase, optimal reaction conditions may differ from standard enzyme protocols. Phusion DNA Polymerase tends to work better at elevated denaturation and annealing temperatures due to higher salt concentrations in its buffer. Please pay special attention to the conditions listed below when running your reactions. Following the guidelines will ensure optimal enzyme performance.

Table 2. Cycling instructions.

	2-step protocol		3-step protocol		
Cycle step	**Temp.**	**Time**	**Temp.**	**Time**	**Cycles**
Initial denaturation	98°C	30 s	98°C	30 s	1
Denaturation Annealing (see 6.3) Extension (see 6.4)	98°C - 72°C	5-10 s - 15-30 s / 1 kb	98°C X°C 72°C	5-10 s 10-30 s 15-30 s / 1 kb	25-35
Final extension	72°C 4°C	5-10 min hold	72°C 4°C	5-10 min hold	1

6. Notes about Cycling Conditions

6.1 Initial denaturation

Denaturation should be done at 98°C (calculated sample temperature). Due to the high thermostability of Phusion DNA Polymerase even higher than 98°C denaturation temperatures can be used. We recommend 30 seconds initial denaturation at 98°C for most templates. Some templates may require longer initial denaturation and the length of the initial denaturation time can be extended up to 3 minutes.

6.2 Denaturation

Keep the denaturation as short as possible. Usually 5-10 seconds at 98°C is enough for most templates. **Note:** The denaturation time and temperature may vary depending on the ramp rate and temperature control mode of the cycler.

From: New England BioLabs®

6.3 Primer annealing

The Phusion DNA Polymerase has the ability to stabilize primer-template hybridization. As a basic rule, for primers > 20nt, anneal for 10 – 30 seconds at a Tm +3°C of the lower Tm primer. The Tm's should be calculated with the nearest-neighbor method[3] as results from primer Tm calculations can vary significantly depending on the method used. For primers ≤ 20nt, use an annealing temperature equal to the Tm of the lower Tm primer. If necessary, use a temperature gradient to find the optimal annealing temperature for each template-primer pair combination. The annealing gradient should extend up to the extension temperature (two-step PCR). Two-step cycling without annealing step is also recommended for high Tm primer pairs. Instructions for Tm calculation and a link to a calculator using the nearest-neighbor method can be found on Finnzymes' website (www.finnzymes.com).

6.4 Extension

The extension should be performed at 72°C. Extension time depends on amplicon length and complexity. For low complexity DNA (e.g. plasmid, lambda or BAC DNA) use extension time 15 seconds per 1kb. For high complexity genomic DNA 30 seconds per 1kb is recommended. For some cDNA templates, the extension time can be increased up to 40 seconds per 1 kb to obtain optimal results.

7. Troubleshooting

No product at all or low yield

- Repeat and make sure that there are no pipetting errors.
- Use fresh high quality dNTPs. Do not use dNTP mix that contains dUTP.
- Use more template, sample concentration may be too low.
- Template DNA may be damaged. Use carefully purified template.
- Lengthen extension time.
- Increase the number of cycles.
- Optimize annealing temperature.
- Optimize enzyme concentration.
- Titrate DMSO (2-8 %) in the reaction (see section 4.5).
- Denaturation temperature may be too low. Optimal denaturation temperature for most templates is 98°C or higher.
- Denaturation time may be too long or too short. Optimize the denaturation time.
- Check the condition of the primers.
- Check primer design.
- Try using the alternative GC Buffer (see section 4.2).

Non-specific products - High molecular weight smears

- Reduce enzyme concentration (see section 4.1).
- Shorten extension time (see section 6.4).
- Reduce the total number of cycles.
- Increase annealing temperature or try 2-step protocol (see section 6.3)
- Vary denaturation temperature (see section 6.2).
- Optimize Mg^{2+}-concentration.
- Lower primer concentration.

Non-specific products - Low molecular weight discrete bands

- Raise annealing temperature (see section 6.3).
- Shorten extension time (see section 6.4).
- Lower enzyme concentration.
- Optimize Mg^{2+}-concentration.
- Titrate template amount.
- Lower primer concentration.
- Design new primers.

8. Component Specifications

8.1 Phusion™ High-Fidelity DNA Polymerase (F-530)

Thermostable Phusion DNA Polymerase is purified from an *E.coli* strain expressing the cloned Phusion DNA Polymerase gene. Phusion DNA Polymerase possesses the following activities: 5´→3´ DNA polymerase activity and 3´→5´ exonuclease activity. Phusion DNA Polymerase is purified free of contaminating endo- and exonucleases.

Storage buffer: 20 mM Tris-HCl (pH 7.4 at 25°C), 0.1 mM EDTA, 1 mM DTT, 100 mM KCl, stabilizers, 200 µg/ml BSA and 50 % glycerol.

Unit definition: One unit is defined as the amount of enzyme that will incorporate 10 nmoles of dNTPs into acid-insoluble form at 74°C in 30 minutes under the stated assay conditions.

Unit assay conditions: Incubation buffer: 25 mM TAPS-HCl, pH 9.3 (at 25°C), 50 mM KCl, 2 mM $MgCl_2$, 1 mM β-mercaptoethanol, 100 µM dCTP, 200 µM each dATP, dGTP, dTTP.

Incubation procedure: 20 µg activated calf thymus DNA and 0.5 µCi [α-^{32}P] dCTP are incubated with 0.1 units of DNA polymerase in 50 µl incubation buffer at 74°C for 10 minutes. The amount of incorporated dNTPs is determined by trichloroacetic acid precipitation.

DNA amplification assay: Performance in PCR is tested in amplification of 7.5 kb genomic DNA and 20 kb λ DNA.

Exonuclease activity: Incubation of 10 U for 4 hours at 72°C in 50 µl assay buffer with 1 µg sonicated ^{3}H ssDNA ($2x10^5$ cpm/µg) released < 1% of radioactivity.

Endonuclease assay: No endonuclease activity is observed after incubation of 10 U of DNA polymerase with 1 µg of λ DNA in assay buffer at 72°C for 4 hours.

Caution: Repeated freezing and thawing of the buffer can result in the precipitation or accumulation of $MgCl_2$ in insoluble form. For consistent results heat the buffer to 90°C for 10 min and vortex prior to use if needed or store refrigerated.

8.2 5x Phusion™ HF Buffer (F-518)

The 5x Phusion HF Buffer contains 7.5 mM $MgCl_2$, which provides 1.5 mM $MgCl_2$ in final reaction conditions.

8.3 5x Phusion™ GC Buffer (F-519)

The 5x Phusion GC Buffer contains 7.5 mM $MgCl_2$, which provides 1.5 mM $MgCl_2$ in final reaction conditions.

From: New England BioLabs®

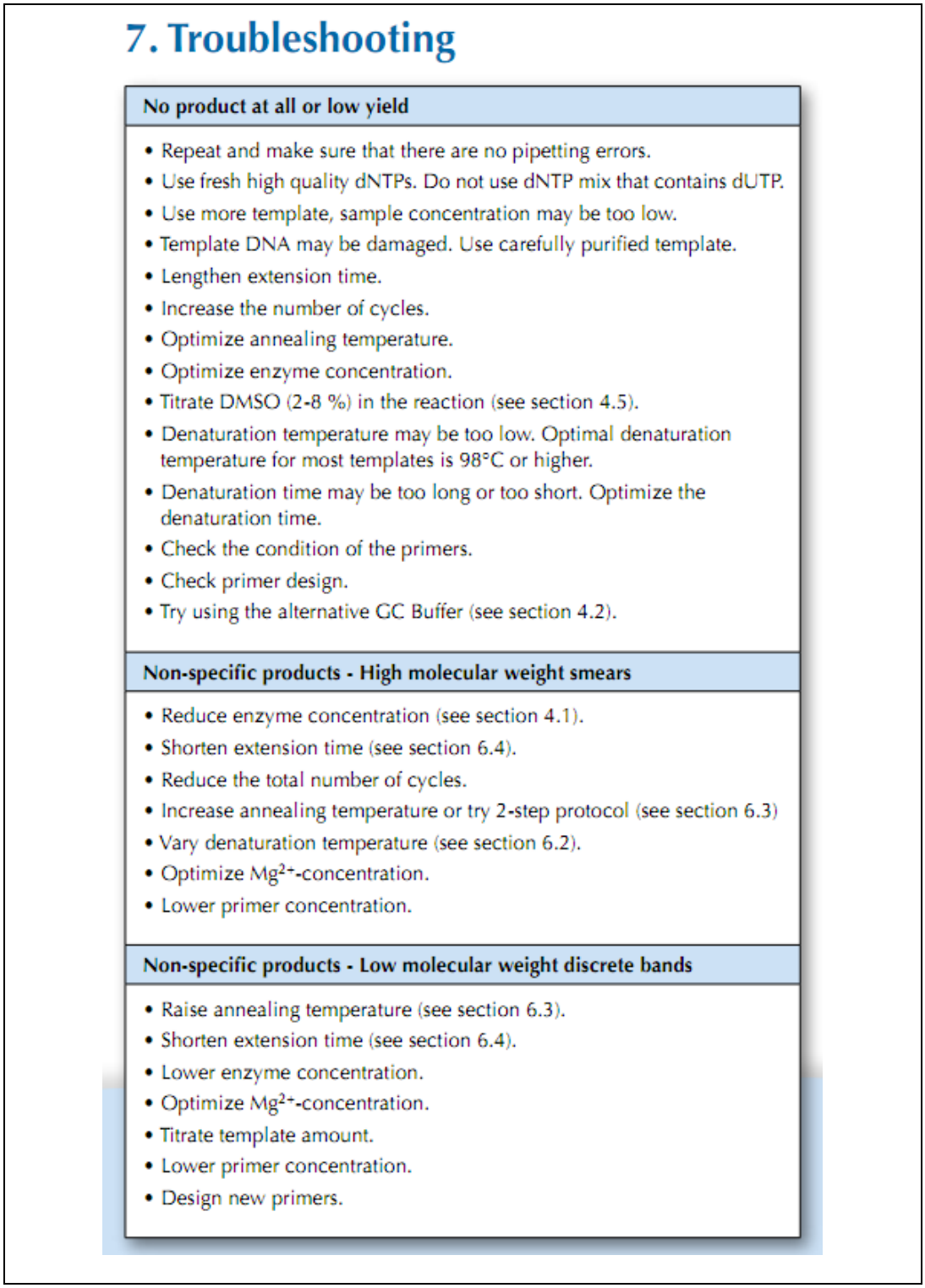

7. Troubleshooting

No product at all or low yield

- Repeat and make sure that there are no pipetting errors.
- Use fresh high quality dNTPs. Do not use dNTP mix that contains dUTP.
- Use more template, sample concentration may be too low.
- Template DNA may be damaged. Use carefully purified template.
- Lengthen extension time.
- Increase the number of cycles.
- Optimize annealing temperature.
- Optimize enzyme concentration.
- Titrate DMSO (2-8 %) in the reaction (see section 4.5).
- Denaturation temperature may be too low. Optimal denaturation temperature for most templates is 98°C or higher.
- Denaturation time may be too long or too short. Optimize the denaturation time.
- Check the condition of the primers.
- Check primer design.
- Try using the alternative GC Buffer (see section 4.2).

Non-specific products - High molecular weight smears

- Reduce enzyme concentration (see section 4.1).
- Shorten extension time (see section 6.4).
- Reduce the total number of cycles.
- Increase annealing temperature or try 2-step protocol (see section 6.3)
- Vary denaturation temperature (see section 6.2).
- Optimize Mg^{2+}-concentration.
- Lower primer concentration.

Non-specific products - Low molecular weight discrete bands

- Raise annealing temperature (see section 6.3).
- Shorten extension time (see section 6.4).
- Lower enzyme concentration.
- Optimize Mg^{2+}-concentration.
- Titrate template amount.
- Lower primer concentration.
- Design new primers.

From: New England BioLabs®

8.4 50 mM $MgCl_2$ Solution (F-510MG)

Both Phusion Buffers supply 1.5 mM $MgCl_2$ at final reaction conditions. If higher $MgCl_2$ concentrations are desired, use 50 mM $MgCl_2$ solution to increase the $MgCl_2$ titer. Using the following equation you can calculate the volume of 50 mM $MgCl_2$ needed to attain the final $MgCl_2$ concentration: [desired mM Mg] – [1.5 mM] = µl to add to a 50 µl reaction.

For example to increase the $MgCl_2$ concentration to 2.0 mM, add 0.5 µl of the 50 mM $MgCl_2$ solution. Because the PCR reactions can be quite sensitive to changes in the $MgCl_2$ concentration, it is recommended that the 50 mM $MgCl_2$ stock solution is diluted 1:5 (to 10 mM) to minimize pipetting errors.

9. References

1. Frey & Suppmann (1995) *Biochemica* 34-35.
2. Chester & Marshak (1993) *Analytical Biochemistry* 209, 284-290.
3. Breslauer *et al.*, (1986) *PNAS* 83, 3746-3750.

Storage and shipping

Phusion DNA Polymerase is shipped on gel ice. Upon arrival, store the components at -20°C. The Phusion DNA Polymerase is stable for one year from the assay date when stored and handled properly.

Warranty

Finnzymes Oy warrants that its products will meet the specifications stated on the technical data section of the data sheets, and Finnzymes Oy agrees to replace the products free of charge if the products do not conform to the specifications. Notice for replacement must be given within 60 days of receipt. In consideration of the above commitments by Finnzymes Oy, the buyer agrees to and accepts the following conditions:

1. That this warranty is in lieu of all other warranties, express or implied;
2. That **ALL WARRANTIES OF MERCHANT ABILITY OR OF FITNESS FOR A PARTICULAR PURPOSE ARE HEREBY EXCLUDED AND WAIVED;**
3. That the buyer's sole remedy shall be to obtain replacement of the product free of charge from Finnzymes Oy; and
4. That this remedy is in lieu of all other remedies or claims for damages, consequential or otherwise, which the buyer may have against Finnzymes Oy.

Exclusive terms of sale

Finnzymes Oy does not agree to and is not bound by any other terms or conditions, unless those terms and conditions have been expressly agreed to in writing by a duly authorised officer of Finnzymes Oy. Prices are subject to change without notice.

Recommended guidelines for safe use of the products

Finnzymes Oy recommends that the buyer and other persons using the products follow the N.I.H. guidelines published in the Federal Register, Volume 41, No. 131, July 7, 1976, and any amendments thereto. Finnzymes Oy disclaims any and all responsibility for any injury or damage which may be caused by the failure of the buyer or any other person to follow said guidelines.

Research use only

Since these products are intended for research purposes by qualified persons, the Environmental Protection Agency does not require us to supply Premanufacturing Notice.

Notice to user

The information presented here is accurate and reliable to the best of our knowledge and belief, but is not guaranteed to be so. Nothing herein is to be construed as recommending any practice or any product in violation of any patent or in violation of any law or regulation. It is the user's responsibility to determine for himself or herself the suitability of any material and/or procedure for a specific purpose and to adopt such safety precautions as may be necessary.

Phusion™ DNA Polymerases Notice to Purchaser: Limited license.

The purchase price of this product includes a limited, non-transferable license under U.S. and foreign patents (5,500,363 and 5,352,778) owned by New England Biolabs, Inc. to use this product. No other license under these patents is conveyed expressly or by implication to the purchaser by the purchase of this product. The purchase price of this product includes a limited, non-transferable license under U.S. and foreign patents owned by BIO-RAD Laboratories, Inc., to use this product. No other license under these patents is conveyed expressly or by implication to the purchaser by the purchase of this product.

The quality system of Finnzymes Oy is certified according to standard SFS-EN ISO9001:2000.

Phusion is a trademark of Finnzymes Oy.

Version 1.5, June 2007

To Place an Order

For technical support or to place an order, please contact New England Biolabs, Inc. or the appropriate NEB subsidiary/distributor:

United States (NEB, Inc.)	800-632-5227
Canada (NEB, Ltd.)	800-387-1095
China (NEB Beijing, Ltd.)	010-82378265
Germany (NEB GmbH)	0800/246 5227
Japan (NEB Japan, Inc.)	03 5669 6191
United Kingdom (NEB UK, Ltd.)	0800 318486

Distributed by
New England Biolabs, Inc.
www.neb.com

NEW ENGLAND BioLabs Inc.
the leader in enzyme technology

FINNZYMES
TOOLS FOR MOLECULAR BIOLOGY

FINNZYMES OY
Kaitaranta 16 A, 02150 Espoo, Finland
Tel. +358 9 584 121
Fax +358 9 5841 2200
fz@finnzymes.fi, www.finnzymes.com

APPENDIX D

ELECTROMAX DH10B *E. COLI* CELLS

INVITROGEN, 12033-015

PRODUCT INSTRUCTIONS

DH10B E. coli cells are commonly used for transformation with newly ligated plasmids. They have very high transformation efficiency, which is essential because when ligating two linear pieces of DNA together such as an open plasmid and a gene insert, one can expect an extremely low probability (efficiency) of success. These cells are electrocompetent, which means that cellular pores can be induced to expand upon exposure to a brief electrical shock. Following the shock, some cells will survive, and of those that survived, a few will have taken up the plasmid DNA. These cells are not used for protein expression, but rather for amplification of plasmid DNA by growing small cultures of the cells, then extracting the plasmid DNA. This approach is preferable to PCR for large plasmid DNA sequences because it utilizes a natural in vivo process, which is less prone to genetic mutations than the in vitro PCR.

From: Invitrogen™

invitrogen

ElectroMAX™ DH10B™ T1 Phage Resistant Cells

Cat. No. 12033-015

Size: 0.5 ml
Store at -80°C
(Do not store in liquid nitrogen)

Description

ElectroMAX™ DH10B™ T1 Phage Resistant Cells confer resistance to the T1 and T5 lytic bacteriophages (1). These cells can only be transformed by electroporation and are **not** transformed by "heat shock" (2, 3). The *mcr*A genotypic marker and the *mcr*BC, *mrr* deletion make this strain suitable for cloning DNA that contains methylcytosine and methyladenine (4, 5, 6). DH10B™ T1 Phage Resistant Cells allow efficient cloning of both prokaryotic and eukaryotic genomic DNA and efficient plasmid rescue from eukaryotic genomes (7). These cells are suitable for construction of gene banks or for generation of cDNA libraries using plasmid-derived vectors. The ϕ80*lac*ZΔM15 marker provides α-complementation of the β-galactosidase gene allowing blue/white screening on agar plates containing X-gal or Bluo-gal.

Component	Amount
DH10B™ T1 Phage Resistant Cells	5 x 100 µl
pUC19 DNA (10 pg/µl)	50 µl
S.O.C. Medium	2 x 6 ml

Genotype

F⁻ *mcr*A Δ(*mrr-hsd*RMS-*mcr*BC) ϕ80*lac*Z ΔM15 Δ*lac*X74 *rec*A1 *end*A1 *ara*D139 Δ(*ara, leu*)7697 *gal*U *gal*K λ⁻ *rps*L *nup*G *ton*A

Quality Control

ElectroMAX™ DH10B™ T1 Phage Resistant Cells are tested for transformation efficiency using the protocol on the next page and the following electroporator conditions: 2.0 kV, 200 Ω, 25 µF. Transformation efficiency should be >1.0×10^{10} transformants/µg of pUC19 DNA.

Part No. 12033015.pps Rev. Date: 5 Oct 2005

From: Invitrogen™

Transformation Procedure

pUC19 control DNA (10 pg/µl) is provided to determine transformation efficiency. Use sample DNA that is free of phenol, ethanol, salts, protein, and detergents to obtain maximum transformation efficiency.

1. Add DNA to microcentrifuge tubes.
   A. To determine transformation efficiency, add 1 µl of the pUC19 control DNA to a microcentrifuge tube.
   B. For ligation reactions, precipitate the sample DNA with ethanol and resuspend in TE Buffer (10 mM Tris HCl, pH 7.5; 1 mM EDTA). The concentration of resuspended DNA should not exceed 100 ng/µl. Add 1 µl of the DNA to a microcentrifuge tube (see Note 1).
2. Thaw ElectroMAX™ DH10B™ T1 Phage Resistant Cells on wet ice.
3. When cells are thawed, mix cells by tapping gently. Add 20 µl of cells to each chilled microcentrifuge tube containing DNA.
4. Refreeze any unused cells in a dry ice/ethanol bath for 5 minutes before returning them to the -80°C freezer. Do not use liquid nitrogen. Although the cells are refreezable, subsequent freeze-thaw cycles will decrease transformation efficiency.
5. Pipette the cell/DNA mixture into a chilled 0.1 cm cuvette and electroporate. If you are using the BTX® ECM® 630 or Bio-Rad GenePulser® II electroporator, we recommend using the following electroporation conditions: 2.0 kV, 200 Ω, 25 µF (see Note 2).
6. Add 1 ml of S.O.C. medium to the cells in the cuvette and transfer the solution to a 15 ml snap-cap tube (*e.g.* Falcon™ tube).
7. Shake at 225 rpm (37°C) for 1 hour.
8. Dilute cells transformed with pUC19 control DNA 1:100 with S.O.C. medium. Spread 50 µl of the dilution on prewarmed LB plates containing 100 µg/ml ampicillin.

From: Invitrogen™

9. Dilute sample reactions as necessary and spread 100-200 µl on selective plates.
10. Incubate plates overnight at 37°C.

Growth of Transformants for Plasmid Preparations

Grow ElectroMAX™ DH10B™ T1 Phage Resistant Cells which have been transformed with a pUC-based plasmid overnight at 37°C in Terrific Broth (TB) (8). A 100 ml culture in a 500 ml baffled shake flask will yield approximately 1 mg of pUC19 DNA.

Notes

1. Transformation efficiencies will be 10- to 100-fold lower for ligation mixtures and cDNA than for intact control plasmids such as pUC19. **Salts and buffers severely inhibit electroporation.** Ligation reactions can be diluted 5-fold, and 1 µl added to 20 µl of cells. For optimal results, precipitate ligation mixtures with ethanol prior to transformation. Use 1 to 2 µl of resuspended DNA per 20 µl reaction. Adding undiluted ligation mixtures or a too large volume of DNA decreases transformation efficiency and increases the risk of arcing.
2. If you are using an electroporator other than a BTX® ECM® 630 or BioRad GenePulser® II electroporator, you may need to vary the electroporation conditions to achieve optimal transformation efficiency.

Calculating transformation efficiency (CFU/µg)

$$\frac{\text{CFU on control plate}}{\text{pg pUC19 DNA}} \times \frac{1 \times 10^6 \text{ pg}}{\mu\text{g}} \times \frac{\text{volume of transformants}}{\text{volume plated}} \times \text{dilution factor}$$

For example, if 10 pg of pUC19 yields 50 colonies when 50 µl of a 1:100 dilution is plated, then:

$$\text{CFU}/\mu\text{g} = \frac{50 \text{ CFU}}{10 \text{ pg}} \times \frac{1 \times 10^6 \text{ pg}}{\mu\text{g}} \times \frac{1 \text{ ml}}{0.05 \text{ ml plated}} \times 10^2 = 1.0 \times 10^{10}$$

From: Invitrogen™

References

1. Killmann, H., Benz, R., and Braun, V. (1996) *J. Bacteriol. 178*, 6313.
2. Calvin, N. M., and Hanawalt, P. C. (1988) *J. Bacteriol. 170*, 2796.
3. Dower, William J., et al. (1988) *Nucl. Acids Research 16*, 6127.
4. Raleigh, E. A. (1988) *Nucl. Acids Research 16*, 1523.
5. Woodcock, D. M., et al. (1989) *Nucl. Acids Research 17*, 3469.
6. Blumenthal, R. M. (1989) *Focus® 11:3*, 41.
7. Grant, S., et al. (1990) *Proc. Nat. Acad. Sci. USA 87*, 4645.
8. Tartof, K. D. and Hobbs, C. A., (1987) *Focus® 9:2*, 12.

APPENDIX E

QIAPREP SPIN MINIPREP KIT

QIAGEN, 27104

PRODUCT INSTRUCTIONS

The QIAprep Spin Miniprep kit is very useful for extracting plasmid DNA from *E. coli* cells such as strain DH10B. It does not appear to work as well as the Promega Wizard SV Kit (Appendix B) for gel extraction of DNA, however. But it functions on a similar principle. *E. coli* cells are lysed in the presence of the alkaline Buffers P1 and P2. Then in the presence of high salt concentration contained in Buffer N3, plasmid DNA (less than 10 kb) in the cell lysate supernatant binds to the silica membrane in the QIAprep Spin Column. Buffer PB is used in a final wash step to remove salts. And DNA is eluted by centrifugal washing with water in the critical pH range of 7.0 to 8.5. The exact composition of the buffers used is not disclosed by the manufacturer. The following pages from the manual contain the steps that were followed for the extraction of plasmid DNA from DH10B cells.

From: Qiagen™

QIAprep Spin

Protocol: Plasmid DNA Purification Using the QIAprep Spin Miniprep Kit and a Microcentrifuge

This protocol is designed for purification of up to 20 µg of high-copy plasmid DNA from 1–5 ml overnight cultures of *E. coli* in LB (Luria-Bertani) medium. For purification of low-copy plasmids and cosmids, large plasmids (>10 kb), and DNA prepared using other methods, refer to the recommendations on page 44.

Please read "Important Notes" on pages 15–21 before starting.

Note: All protocol steps should be carried out at room temperature.

Procedure

1. **Resuspend pelleted bacterial cells in 250 µl Buffer P1 and transfer to a microcentrifuge tube.**

   Ensure that RNase A has been added to Buffer P1. No cell clumps should be visible after resuspension of the pellet.

   If LyseBlue reagent has been added to Buffer P1, vigorously shake the buffer bottle to ensure LyseBlue particles are completely dissolved. The bacteria should be resuspended completely by vortexing or pipetting up and down until no cell clumps remain.

2. **Add 250 µl Buffer P2 and mix thoroughly by inverting the tube 4–6 times.**

   Mix gently by inverting the tube. Do not vortex, as this will result in shearing of genomic DNA. If necessary, continue inverting the tube until the solution becomes viscous and slightly clear. Do not allow the lysis reaction to proceed for more than 5 min.

   If LyseBlue has been added to Buffer P1 the cell suspension will turn blue after addition of Buffer P2. Mixing should result in a homogeneously colored suspension. If the suspension contains localized colorless regions or if brownish cell clumps are still visible, continue mixing the solution until a homogeneously colored suspension is achieved.

3. **Add 350 µl Buffer N3 and mix immediately and thoroughly by inverting the tube 4–6 times.**

   To avoid localized precipitation, mix the solution thoroughly, immediately after addition of Buffer N3. Large culture volumes (e.g. ≥ 5 ml) may require inverting up to 10 times. The solution should become cloudy.

   If LyseBlue reagent has been used, the suspension should be mixed until all trace of blue has gone and the suspension is colorless. A homogeneous colorless suspension indicates that the SDS has been effectively precipitated.

4. **Centrifuge for 10 min at 13,000 rpm (~17,900 x *g*) in a table-top microcentrifuge.**

   A compact white pellet will form.

From: Qiagen™

5. **Apply the supernatants from step 4 to the QIAprep spin column by decanting or pipetting.**
6. **Centrifuge for 30–60 s. Discard the flow-through.**
7. **Recommended: Wash the QIAprep spin column by adding 0.5 ml Buffer PB and centrifuging for 30–60 s. Discard the flow-through.**

   This step is necessary to remove trace nuclease activity when using *endA*+ strains such as the JM series, HB101 and its derivatives, or any wild-type strain, which have high levels of nuclease activity or high carbohydrate content. Host strains such as XL-1 Blue and DH5α™ do not require this additional wash step.
8. **Wash QIAprep spin column by adding 0.75 ml Buffer PE and centrifuging for 30–60 s.**
9. **Discard the flow-through, and centrifuge for an additional 1 min to remove residual wash buffer.**

   Important: Residual wash buffer will not be completely removed unless the flow-through is discarded before this additional centrifugation. Residual ethanol from Buffer PE may inhibit subsequent enzymatic reactions.
10. **Place the QIAprep column in a clean 1.5 ml microcentrifuge tube. To elute DNA, add 50 µl Buffer EB (10 mM Tris·Cl, pH 8.5) or water to the center of each QIAprep spin column, let stand for 1 min, and centrifuge for 1 min.**

Protocol: Plasmid DNA Purification Using the QIAprep Spin Miniprep Kit and 5 ml Collection Tubes

The QIAprep Spin Miniprep procedure can be performed using 5 ml centrifuge tubes (e.g., Greiner, cat. no. 115101 or 115261) as collection tubes to decrease handling. The standard protocol on pages 22–23 should be followed with the following modifications:

Step 4: Place a QIAprep spin column in a 5 ml centrifuge tube instead of a 2 ml collection tube.

Step 6: Centrifuge at 3000 x *g* for 1 min using a suitable rotor (e.g., Beckman® GS-6KR centrifuge at ~4000 rpm). (The flow-through does not need to be discarded.)

Steps 7 and 8: For washing steps, centrifugation should be performed at 3000 x *g* for 1 min. (The flow-through does not need to be discarded.)

Step 9: Transfer the QIAprep spin column to a microcentrifuge tube. Centrifuge at maximum speed for 1 min. Continue with step 10 of the protocol.

APPENDIX F

RESTRICTION ENDONUCLEASES

HINDIII, NEW ENGLAND BIOLABS

NDEI, NEW ENGLAND BIOLABS

SACII, NEW ENGLAND BIOLABS

XHOI, NEW ENGLAND BIOLABS, R0146

XMNI, NEW ENGLAND BIOLABS

PRODUCT INSTRUCTIONS

Restriction endonucleases are used to cleave DNA strands at defined points where a particular 6-10 bp sequence is recognized by a corresponding endonuclease. This is useful for inserting a gene into a plasmid, or as a means to verify the insertion of a gene into a plasmid based on the expected plasmid sequence. Restriction endonuclease reactions were typically prepared with a 1X concentration of buffer which corresponds favorably to the particular endonuclease(s), about 1 to 10 units of the endonuclease, and less than 1 µg of DNA. Reactions are usually prepared in 10 to 50 µL volumes and incubated at 37°C for 1-2 hours. Selections from the product instructions for different enzymes used are shown below, including the contents of the various reaction buffers.

From: New England BioLabs®

HindIII

Recognition Site:

Source:
A *E. coli* strain that carries the HindIII gene from *Haemophilus influenzae* Rd (ATCC 51907).

Enzyme Properties

Activity in NEBuffers:
NEBuffer 1: 50%
NEBuffer 2: 100%
NEBuffer 3: 10%
NEBuffer 4: 50%

When using a buffer other than the optimal (supplied) NEBuffer, it may be necessary to add more enzyme to achieve complete digestion.

Reaction & Storage Conditions

Reaction Conditions:

1X NEBuffer 2

Incubate at 37°C.

1X NEBuffer 2:

10 mM Tris-HCl

50 mM NaCl

10 mM $MgCl_2$

1 mM Dithiothreitol

pH 7.9 @ 25°C

From: New England BioLabs®

NdeI

Recognition Site:

Source:
A *E. coli* strain that carries the NdeI gene from *Neisseria denitrificans* (NRCC 31009).

Enzyme Properties

Activity in NEBuffers:
NEBuffer 1: 75%
NEBuffer 2: 100%
NEBuffer 3: 75%
NEBuffer 4: 100%

When using a buffer other than the optimal (supplied) NEBuffer, it may be necessary to add more enzyme to achieve complete digestion.

Reaction & Storage Conditions

Reaction Conditions:

1X NEBuffer 4

Incubate at 37°C.

1X NEBuffer 4:

20 mM Tris-acetate

50 mM potassium acetate

10 mM Magnesium Acetate

1 mM Dithiothreitol

pH 7.9 @ 25°C

From: New England BioLabs®

SacII

Recognition Site:

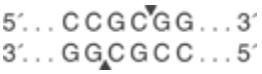

Source:
A *Streptomyces lividans* strain that carries the SacII gene from *Streptomyces achromogenes*(ATCC 12767).

Enzyme Properties

Activity in NEBuffers:
NEBuffer 1: 25%
NEBuffer 2: 75%
NEBuffer 3: 10%
NEBuffer 4: 100%

When using a buffer other than the optimal (supplied) NEBuffer, it may be necessary to add more enzyme to achieve complete digestion.

Reaction & Storage Conditions

Reaction Conditions:

1X NEBuffer 4

Incubate at 37°C.

1X NEBuffer 4:

20 mM Tris-acetate

50 mM potassium acetate

10 mM Magnesium Acetate

1 mM Dithiothreitol

pH 7.9 @ 25°C

From: New England BioLabs®

XhoI

Recognition Site:

Source:
A *E. coli* strain that carries the XhoI gene from *Xanthomonas holcicola* (ATCC 13461).

Reagents Supplied:
NEBuffer 4 (10X)
BSA (100X)

Enzyme Properties

Activity in NEBuffers:
NEBuffer 1: 75%
NEBuffer 2: 100%
NEBuffer 3: 100%
NEBuffer 4: 100%

When using a buffer other than the optimal (supplied) NEBuffer, it may be necessary to add more enzyme to achieve complete digestion.

Reaction & Storage Conditions

Reaction Conditions:

1X NEBuffer 4

Supplemented with 100 µg/ml Bovine Serum Albumin

Incubate at 37°C.

1X NEBuffer 4:

20 mM Tris-acetate

50 mM potassium acetate

10 mM Magnesium Acetate

1 mM Dithiothreitol

pH 7.9 @ 25°C

From: New England BioLabs®

XmnI

Recognition Site:

5′...GAANN▼NNTTC...3′
3′...CTTNN▲NNAAG...5′

Source:
A *E.coli* strain that carries the XmnI gene from *Xanthomonas manihotis* 7AS1 (ATCC 49764).

Reagents Supplied:
NEBuffer 4 (10X)
BSA (100X)

Enzyme Properties

Activity in NEBuffers:
NEBuffer 1: 100%
NEBuffer 2: 100%
NEBuffer 3: 50%
NEBuffer 4: 100%

When using a buffer other than the optimal (supplied) NEBuffer, it may be necessary to add more enzyme to achieve complete digestion.

Reaction & Storage Conditions

Reaction Conditions:

1X NEBuffer 4

Supplemented with 100 µg/ml Bovine Serum Albumin

Incubate at 37°C.

1X NEBuffer 4:

20 mM Tris-acetate

50 mM potassium acetate

10 mM Magnesium Acetate

1 mM Dithiothreitol

pH 7.9 @ 25°C

APPENDIX G

T7 EXPRESS *lysY/I*^{q} COMPETENT *E. COLI* CELLS

NEW ENGLAND BIOLABS, C3013H

PRODUCT INSTRUCTIONS

The principle of transformation for T7 Express lysY/Iq *E. coli* cells is the same as for the DH10B cells (Appendix D). The process, however, is different. Whereas DH10B cells are electrocompetent, T7 Express cells are chemically competent. This means that the T7 cells take up plasmid DNA following heat shock, rather than electrical shock. The application is also different. T7 Express cells are genetically engineered for protein expression, particular for proteins that can be toxic. The following product information is available, and product instructions were followed for transformations of this *E. coli* strain.

From: New England BioLabs®

T7 Express *lysY/I^q* Competent *E. coli* (High Efficiency)

- Transformation efficiency: 0.6-1 x 10^9 cfu/µg pUC19 DNA
- Enhanced BL21 derivative
- B Strain
- T7 RNA Polymerase in the *lac* operon - no λ prophage
- Tight control of expression by *lacI^q* allows potentially toxic genes to be cloned
- Control of T7 RNA Polymerase by lysozyme allows toxic genes to be expressed
- Lys Y is a variant of T7 lysozyme lacking any amidase activity, thus cells are less susceptible to lysis during induction
- Maintenance of lysozyme/*lacI^q* plasmid does not require antibiotic selection
- Deficient in proteases Lon and OmpT
- Resistant to phage T1 *(fhuA2)*
- Does not restrict methylated DNA (McrA$^-$, McrBC$^-$, EcoBr$^-$m$^-$, Mrr$^-$)

Description:

Chemically competent *E. coli* cells suitable for high efficiency transformation and protein expression.

Reagents Supplied:

C3013H:

20 x 0.05 ml/tube of chemically competent T7 Express *lysY/I^q* Competent *E. coli* cells (**Store at -80°C**)

20 ml of SOC Outgrowth Medium (**Store at room temperature**)

0.025 ml of 50 pg/µl pUC19 Control DNA (**Store at -20°C**)

Genotype: MiniF *lysY, lacI^q*(Cam^R) **/** *fhuA2 lacZ::T7 gene1 [lon] ompT gal sulA11 R(mcr-73::miniTn10--Tet^S)2 [dcm] R(zgb-210::Tn10--Tet^S) endA1 Δ(mcrC-mrr)114::IS10*

Transformation Protocol Variables:

Thawing: Cells are best thawed on ice and DNA added as soon as the last bit of ice in the tube disappears. Cells can also be thawed by hand, but warming above 0°C will decrease the transformation efficiency.

Incubation of DNA with Cells on Ice: For maximum transformation efficiency, cells and DNA should be incubated together on ice for 30 minutes. Expect a 2-fold loss in transformation efficiency for every 10 minutes you shorten this step.

Heat Shock: Both the temperature and the timing of the heat shock step are important and specific to the transformation volume and vessel. Using the transformation tube provided, 10 seconds at 42°C is optimal.

Outgrowth: Outgrowth at 37°C for 1 hour is best for cell recovery and for expression of antibiotic resistance. Expect a 2-fold loss in transformation efficiency for every 15 minutes you shorten this step. SOC gives 2-fold higher transformation efficiency than LB medium; and incubation with shaking or rotating the tube gives 2-fold higher transformation efficiency than incubation without shaking.

Plating: Selection plates can be used warm or cold, wet or dry without significantly affecting the transformation efficiency. However, warm, dry plates are easier to spread and allow for the most rapid colony formation.

From: New England BioLabs®

High Efficiency Transformation Protocol (C3013)

Overview

For C3013H, perform steps 1-7 in the tube provided.

Protocol

For C3013H: Thaw a tube of T7 Express *lysY/I*^{q} Competent *E. coli* cells on ice for 10 minutes.
For C3013I: Thaw a tube of T7 Express *lysY/I*^{q} Competent *E. coli* cells on ice until the last ice crystals disappear. Mix gently and carefully pipette 50 µl of cells into a transformation tube on ice.
Add 1-5 µl containing 1 pg-100 ng of plasmid DNA to the cell mixture. Carefully flick the tube 4-5 times to mix cells and DNA. **Do not vortex.**
Place the mixture on ice for 30 minutes. Do not mix.
Heat shock at exactly 42°C for exactly 10 seconds. Do not mix.
Place on ice for 5 minutes. Do not mix.
Pipette 950 µl of room temperature SOC into the mixture.
Place at 37°C for 60 minutes. Shake vigorously (250 rpm) or rotate.
Warm selection plates to 37°C.
Mix the cells thoroughly by flicking the tube and inverting, then perform several 10-fold serial dilutions in SOC.
Spread 50-100 µl of each dilution onto a selection plate and incubate overnight at 37°C.
Alternatively, incubate at 30°C for 24-36 hours or at 25°C for 48 hours.

APPENDIX H

RIBOPURE-BACTERIA KIT

AMBION, AM1925

PRODUCT INSTRUCTIONS

The Ribo-Pure-Bacteria kit is used to extract and purify total RNA from bacterial cell lystates. Great care is taken in this procedure to avoid RNAse contaminations. The process of RNA purification is similar to that of DNA purification with the Wizard SV kit or QiaPrep Miniprep kit (Appendices B and E). Pages from the product instruction manual are included below. The procedure for RNA extraction as used in this dissertation is described in the included pages. The contents of the included buffers is not disclosed.

From: Ambion®

I. Introduction

IMPORTANT

Before using this product, read and understand the "Safety Information" in the appendix in this document.

A. Background

RiboPure™-Bacteria is a rapid RNA isolation kit which combines disruption of bacterial cell walls with Zirconia Beads, phenol extraction of the lysate, and glass-fiber filter purification of the RNA. It can be used to isolate total RNA from a variety of gram-negative and gram-positive bacteria. RiboPure-Bacteria was extensively tested with *E. coli*, *Pseudomonas aeruginosa*, *Staphylococcus aureus*, *Bacillus subtilis*, *Campylobacter fetus*, and *Rhodobacter sphaeroides*, however, the kit will work with almost any gram-negative or gram-positive bacterial species.

The RiboPure-Bacteria method disrupts bacterial cell walls by beating cells mixed with RNAwiz and 0.1 mm Zirconia Beads on a vortex adapter (e.g. P/N AM10024) for 10 min. The lysate is then mixed with chloroform and centrifuged to form three distinct phases. The upper aqueous phase contains RNA, the semi-solid interphase contains DNA, and the lower organic phase contains mostly proteins, polysaccharides, fatty acids and other cellular debris. The RNA is then diluted with ethanol and bound to a silica filter. The RNA bound to the filter is washed to remove contaminants, and eluted in a low ionic strength solution. The kit also includes Ambion DNA-*free*™ reagents for the optional post-elution removal of contaminating genomic DNA, and for the subsequent removal of the DNase I and divalent cations in the buffer using our exclusive DNase Inactivation Reagent.

The entire RNA isolation procedure requires approximately 1 hr, starting with fresh, snap-frozen, or RNA*later*® treated cells. The optional DNA removal step requires ~30 min of additional time. The resulting RNA is of superb quality, free of DNA and proteins, and suitable for use in Northern blotting, RT-PCR, mRNA enrichment, and microarray analysis. As with all glass fiber filter purification methods, 5S ribosomal RNAs and tRNAs are not quantitatively recovered using the RiboPure-Bacteria Kit.

From: Ambion®

B. Amount of Starting Material

The RiboPure-Bacteria procedure is designed for small scale RNA isolation from bacterial cells. The chart below lists the maximum recommended number of cells of various species to use in the procedure. Typically these are the number of cells present in 1–10 mL of logarithmic phase cultures in a rich medium such as LB or BHI.

For organisms not on the list start with 0.5–1 x 10^9 cells.

	Maximum amount starting material	Expected RNA yield
Escherichia coli	1 x 10^8 cells	90 µg
Bacillus subtilis	5 x 10^8 cells	60 µg
Pseudomonas aeruginosa	1 x 10^{10} cells	90 µg
Staphylococcus aureus	1 x 10^8 cells	40 µg

C. Cell Disruption and Initial RNA Purification

NOTE

All centrifugation steps should be done at an RCF of ~13,000–16,000 X g. This is typically near the maximum speed setting on a microfuge.

1. Dispense 250 µL Zirconia Beads into a 0.5 mL screw cap tube for each sample

For each sample, pour ~250 µL of ice-cold Zirconia Beads into a 0.5 mL screw cap tube (supplied with the kit) using the picture below to estimate the volume of beads.

Figure 2. Estimating Volume of Zirconia Beads.

2. Collect cells by centrifugation

a. Collect the cells from a bacterial culture or from an RNA*later* suspension by centrifugation for 30–60 sec.

b. Thoroughly remove the supernatant from the pellet, and discard the supernatant.

3. Resuspend cells in 350 µL RNAwiz

Add 350 µL RNAwiz to the cell pellet and resuspend by vortexing vigorously for 10–15 sec.

From: Ambion®

4. Add cells in RNAwiz to Zirconia Beads

Transfer the cells in RNAwiz from step C.3 on page 6 to a tube containing 250 µL Zirconia Beads. Securely fasten the lid.

5. Beat cells 10 min on vortex mixer with a vortex adapter

Position the sample tubes horizontally on the vortex adapter with the tube caps towards the center. Turn the vortex mixer on at maximum speed, and beat 10 min.

The bacterial cells should be lysed after this treatment.

6. Pellet Zirconia Beads 5 min at 4°C

a. Centrifuge for 5 min at 4°C.

b. Transfer the bacterial lysate to a fresh 1.5 mL Tube (supplied with the kit) and discard the Zirconia Beads. Estimate the lysate volume while transferring the lysate; typically 200–250 µL of lysate is recovered at this step.

7. Add 0.2 volumes chloroform, mix well, and incubate 10 min at room temp

Add 0.2 volumes chloroform to the lysate from step 6.b above. Shake vigorously for 30 sec, then incubate 10 min at room temp.

Adding the chloroform and incubating at room temp will allow the aqueous and organic phases to be separated by centrifugation.

8. Spin 5 min at 4°C to separate the phases and transfer aqueous phase to a fresh tube

a. Centrifuge for 5 min at 4°C.

b. Transfer the aqueous phase (top), containing the partially purified RNA, to a fresh 1.5 mL Tube. Estimate the lysate volume while transferring the lysate; typically 200–250 µL of aqueous phase is recovered at this step.

D. Final RNA Purification

NOTE

Perform all centrifugation steps at ~13,000–16,000 X g. Alternatively, for steps 2–4 below, the solutions can be drawn through the Filter Cartridges with vacuum pressure if desired. Simply place the Filter Cartridges into sterile 5 mL syringe barrels mounted on a vacuum manifold.

- Inspect Wash Solution 1 to see if a precipitate formed after storage at 4°C. If so, warm the solution to 37°C to dissolve the precipitate.
- Place 50–100 µL Elution Solution per sample into an RNase-free tube and preheat it in a heat block set to 95–100°C.

1. Add 0.5 volume 100% ethanol to each sample

Add 0.5 volumes of 100% ethanol to the aqueous phase recovered in step C.8.b on page 7 and mix thoroughly.

From: Ambion®

RiboPure™-Bacteria Kit

2. Pass sample through a Filter Cartridge

a. Place a Filter Cartridge into a 2 mL Collection Tube for each sample.

IMPORTANT

Briefly inspect the Filter Cartridges before use. Occasionally, the glass fiber filters may become dislodged during shipping. If this is the case, gently push the filter down to the bottom of the cartridge using the wide end of a RNase-free pipette tip.

b. Transfer the sample to the Filter Cartridge, close the lid, and centrifuge for ~1 min or until all the liquid is through the filter.

c. Discard the flow-through and return the Filter Cartridge to the same Collection Tube.

NOTE

The RNA is now bound to the filter in the Filter Cartridge.

3. Wash filter with 700 µL Wash Solution 1

a. Wash the filter by adding 700 µL Wash Solution 1 to the Filter Cartridge, and centrifuge for ~1 min or until all of the liquid is through the filter.

b. Discard the flow-through and return the Filter Cartridge to the same Collection Tube.

4. Wash filter with 2 x 500 µL Wash Solution 2/3

a. Wash the filter by adding 500 µL Wash Solution 2/3 to the Filter Cartridge, and centrifuge for ~1 min or until all of the liquid is through the filter.

b. Discard the flow-through and return the Filter Cartridge to the same Collection Tube.

c. Repeat with a second 500 µL aliquot of Wash Solution 2/3.

5. Centrifuge to remove excess wash solution from the filter

a. Spin the Filter Cartridge for 1 min to remove excess wash. (This step should be done using a centrifuge, not vacuum pressure.)

b. Transfer the Filter Cartridge to a fresh 2 mL Collection Tube.

6. Elute RNA with 25–50 µL preheated Elution Solution

a. Elute RNA by applying 25–50 µL Elution Solution, preheated to 95–100°C, to the center of the filter.

b. Centrifuge for 1 min.

c. Repeating the elution step with a second 25–50 µL aliquot of preheated Elution Solution will maximize total RNA yields.

From: Ambion®

E. (optional) DNase I Treatment

The DNase I treatment describe below will remove trace amounts of genomic DNA from the eluted RNA.

1. Add 10X DNase Buffer and DNase 1 to the RNA

Add the following to the RNA and mix gently but thoroughly:

Amount	Component
1/9th volume	10X DNase Buffer
4 µL	DNase 1 (2 U/µL)

2. Incubate 30 min at 37°C

Incubate 30 min at 37°C so that the DNase 1 can digest the genomic DNA.

3. Add DNase Inactivation Reagent and mix well

NOTE

The DNase Inactivation Reagent may become difficult to pipette after multiple uses. If this happens, add Elution Solution equal to ~10–20% of the bed volume of the remaining reagent and vortex thoroughly to recreate a pipettable slurry.

a. Add a volume of DNase Inactivation Reagent equal to 20% of the volume of RNA treated to each sample.
For example if 100 µL of RNA is treated with DNase, add 20 µL of DNase Inactivation Reagent.

Vortex the DNase Inactivation Reagent tube vigorously to ensure it is completely resuspended. the To pipette the reagent, insert the pipet tip well below the surface and observe the material in the tip to ensure that it is mostly white, without a significant amount of clear fluid. If treating multiple samples, re-vortex the reagent as needed.

b. Vortex the tube of RNA after adding the DNase Inactivation Reagent to mix well.

4. Leave at room temp for 2 min

Store at room temp for 2 min flicking the tube once or twice during this period to resuspend the DNase Inactivation Reagent.

5. Pellet the DNase Inactivation Reagent and transfer the RNA to a new tube

Centrifuge the sample for ~1 min at maximum speed to pellet the DNase Inactivation Reagent, then transfer the RNA solution to a new RNase-free tube (not supplied with the kit).

From: Ambion®

III. Assessing RNA Yield and Quality

A. UV Absorbance

The concentration and purity of RNA can be determined by diluting an aliquot of the preparation (usually a 1:100 to 1:200 dilution) in TE (10 mM Tris-HCl pH 8, 1 mM EDTA) and reading the absorbance in a spectrophotometer at 260 nm and 280 nm. Be sure to zero the spectrophotometer with the TE used for sample dilution.

Concentration

An A_{260} of 1 is equivalent to 40 µg RNA/mL.

The concentration (µg/mL) of RNA is therefore calculated as follows:

A_{260} x dilution factor x 40 µg/mL

Following is a typical example:

RNA is eluted in 40 µL
6 µL of the prep is diluted 1:50 into 294 µL of TE
A_{260}=0.42
RNA concentration = 0.42 x 50 x 40 µg/mL = 840 µg/mL or 0.84 µg/µL

Since there are 34 µL of the prep left after using 6 µL to measure the concentration, the total amount of remaining RNA is:

34 µL x 0.84 µg/µL = 28.56 µg

Be aware that any contaminating DNA in the RNA prep will lead to an overestimation of yield, since all nucleic acids absorb at 260 nm.

Purity

The ratio of A_{260} to A_{280} values is a measure of RNA purity, and it should fall in the range of 1.8 to 2.1. Even if an RNA prep has an A_{260}:A_{280} ratio outside this range, it may function well in common applications such as Northern blotting, RT-PCR, and RNase protection assays.

B. Denaturing Agarose Gel Electrophoresis

Ambion NorthernMax® reagents for Northern blotting include everything needed for denaturing agarose gel electrophoresis. These products are optimized for ease of use, safety, and low background, and they include detailed instructions for use.

An alternative to using the NorthernMax reagents is to use the procedure described below for electrophoresis in a formaldehyde denaturing agarose gel. This procedure is modified from "Current Protocols in Molecular Biology", Section 4.9 (Ausubel et al., eds.). It is more difficult and time-consuming than the NorthernMax method, but it gives similar results.